ISSN 2521-6317

Volume 8
Number 1
2024

Journal of Baku Engineering University

ADVANCES in CHEMISTRY and CHEMICAL ENGINEERING

Journal is published twice a year
Number - 1. June, Number - 2. December

An International Journal

http://journal.beu.edu.az

Contact address

Journal of Baku Engineering University
AZ0101, Khirdalan city, Hasan Aliyev str. 120, Absheron, Baku, Azerbaijan
Tel: *00 994 12 - 349 99 95* ***Fax:*** *00 994 12 349-99-90/91*
e-mail: *chemstrybiology@beu.edu.az,* *journal@beu.edu.az*
web: *http://journal.beu.edu.az*
facebook: *Journal Of Baku Engineering University*

ISSN 2521-6317

ISSN 2521-6317

Journal of Baku Engineering University

ADVANCES IN CHEMISTRY AND CHEMICAL ENGINEERING

Baku - AZERBAIJAN

JOURNAL OF BAKU ENGINEERING UNIVERSITY
ADVANCES IN CHEMISTRY AND CHEMICAL ENGINEERING
2024. Volume 8, Number 1

CONTENTS

JOURNAL OF BAKU ENGINEERING UNIVERSITY-ADVANCES IN CHEMISTRY AND CHEMICAL ENGINEERING
2024. Volume 8, Number 1 ***Pages 3-12***

UOT: 631.52:576.3
https://doi.org/10.30546/2521-6317.2024.205

MOLECULAR SIMULATION OF GEMINI-LIKE SURFACTANT BASED ON PROPOXYLATED ETHYL PIPERAZINE AND STEARIC ACID

Elgun E. HASANOV[1,2*], Ravan A. RAHIMOV[1,2]

[1]*Department of Chemical Engineering,*
Baku Engineering University, Hasan Aliyev str. 120,
Baku, Absheron, AZ0101, Azerbaijan
[2]*Institute of Petrochemical Processes of the Ministry of Science and Education of Azerbaijan,*
Hojaly ave. 30, AZ 1025, Baku, Azerbaijan

ARTICLE INFO

Article history:
Received 2024-08-11
Received in revised form:2024-09-20
Accepted:2024-10-15
Available online

Keywords:
Gemini-like;
Molecular simulation;
Ethyl piperazine;
DPD;
Stearic acid

ABSTRACT

Molecular simulation of a gemini-like surfactant 1-(propane-2-olyl)-4-ethylpiperazine-1,4-di-ium di-octadecanoate is performed applying Dissipative Particle Dynamics (DPD) methodology. Coarse graining of the surfactant and water molecules is done employing a well-established approach. The Flory-Huggins chi parameters were used for DPD parametrization. DPD simulation successfully predicts aggregation behavior of the surfactant solutions. Radial Distribution Function (RDF) curves of the gemini-like surfactant at varying concentrations are analyzed to determine orderly arrangements of molecules within solution. Existence of a second RDF peak at intermolecular distance range is related to the formation of aggregates. RDF curves approach to zero at higher distances due to very low concentration of molecules outside the aggregates. Critical Micelle Concentration (CMC) is calculated from DPD simulation outcomes and compared to the experimentally determined CMC value. Fluctuation of theoretically calculated CMCs at different concentrations is small and within acceptable limits. Even though the average theoretical CMC is greater than the experimental CMC value, both are in the same order of magnitude.

* Corresponding author.
E-mail addresses: ehasanov1@beu.edu.az (Elgun E. Hasanov).

1. Introduction

Surface-active compounds or surfactants are crucial components of various chemical products ranging from detergents to industrial drilling fluids. Due to their wide range of applications in science and technology and important place in day-to-day life of humans, surfactants and surface activity phenomena have been subject to in-depth scientific research. Computational chemistry is one of the most modern research methods being applied to investigate surface-active compounds. A suitable computational scheme for modelling and studying medium to large molecular systems including surfactant systems is Molecular Mechanics methods [1]. One of the most widely applied coarse-grained Molecular Mechanics tools standing out for its effectiveness and efficiency in modelling the behavior of surface-active compounds is called Dissipative Particle Dynamics (DPD) [2].

Recently several studies dedicated to DPD molecular simulations of various surfactant systems have been conducted. Vishnyakov et al. [3] applied DPD methodology for studying micellization behavior of non-ionic surfactants C_8E_8 (octaethylene glycol monooctyl ether $nC_8H_{17}(OCH_2CH_2)_8OH$), DDAO (dodecyldimethylamineoxide $nC_{12}H_{25}NO(CH_3)_2$) and MEGA-10 (N-decanoyl-N-methyl-D-glucamine $nC_9H_{19}(NCH_3)$ $(HCOH)_4CH_2OH$). They used a new approach of calculating DPD soft repulsion parameters utilizing infinite dilution activity coefficient data of the reference compounds. The authors confirmed that theoretically calculated CMC values from DPD simulations are closely matching the experimental CMC values of the investigated non-ionic surfactants. Gong et al. [4] used DPD simulation to investigate aggregation properties of quaternary ammonium surfactant hexyldimethyloctylammonium bromide (C_6C_8Br) in aqueous environment. They used angle evolution data extracted from DPD simulation to determine the configuration of C_6C_8Br molecules at different concentrations. It was established that as the surfactant concentration increases, the interior angle between alkyl chains of the surfactant becomes larger, thus the molecular configuration approaches a straight line. The authors related the experimental evidence of breakage of vesicle structure at higher concentrations to the formation of rigid linear structure of the C_6C_8Br molecules as revealed by DPD simulations. Goodarzi and Zendehboudi [5] employed DPD methodology to predict the interfacial behavior of water-oil emulsion in the presence of an inorganic salt and non-ionic surfactant hexaethyleneglycol monododecyl ether. They determined that increasing water/oil ratio in the simulation box resulted in interfacial tension to drop. Radius of gyration of surfactant molecules at the oil-water interface increased upon increasing the system temperature, indicating stretching of the molecules at the interface and thus reduction of interfacial tension. When an inorganic salt was introduced to the system, the interfacial tension initially dropped considerably due to the released ions shielding the repulsion between the surfactant headgroups at the interface. However, raising the salt concentration further did not result any visible change in interfacial tension, since the surfactant molecules saturated the interface. The authors verified the results deduced from the DPD simulation with previous experimental and theoretical works.

In this work we used DPD simulation to investigate micellization properties of a gemini-like surfactant 1-(propane-2-olyl)-4-ethylpiperazine-1,4-di-ium di-octadecanoate (C_{18}-EPPO-C_{18}) constructed from propoxylated ethyl piperazine and stearic acid. Theoretically evaluated parameters related to surfactant-water system were analyzed to determine the connection

between the molecular simulation and experimental properties of the surfactant. Synthesis and experimental measurements related to C_{18}-EPPO-C_{18} was done in one of our previous works [6].

2. Simulation Methods

2.1 DPD Theory

In DPD computation process Newton's classical laws of motion equations are solved for mesomolecular particles called beads to determine their final position and momenta and as a result to display the equilibrated configuration of the system [7] [8].

In molecular simulations the forces acting on a bead particle are categorized into non-bonded interaction forces and bonded interaction forces. The total sum of the forces due to non-bonded interactions is expressed via Eq. (1) below:

$$F_i = \sum_{i \neq j \neq k} F_{ij}^C + F_{ij}^D + F_{ij}^R + F_{ij}^E \quad (1)$$

Where F_{ij}^C is the conservative force, F_{ij}^D is the dissipative force, F_{ij}^R is the random force, and F_{ij}^E is the electrostatic force.

The conservative force F_{ij}^C expresses the repulsive interactions between two different bead particles. It simulates the specific chemical and physical characteristics of the molecules. For the current work the soft harmonic form of conservative force as expressed by Eq. (2) was used:

$$F_{ij}^C = \begin{cases} a_{ij}\left(1 - \frac{r_{ij}}{r_C}\right) & r_{ij} < r_C \\ 0 & r_{ij} \geq r_C \end{cases} \quad (2)$$

Where a_{ij} is called the interaction parameter between bead i and bead j, r_C is called the cut-off radius and r_{ij} expresses the distance between bead i and bead j.

The dissipative force F_{ij}^D expresses the frictional forces between the beads and is directly proportional to the approaching velocity of two beads. The dissipative force F_{ij}^D is expressed by Eq. (3) below:

$$F_{ij}^D = -\gamma_{ij}\omega^D(r_{ij})(v_{ij}) \quad (3)$$

Where γ_{ij} is called the friction coefficient and $\gamma_{ij} = \gamma_{ji} > 0$. $v_{ij} = v_i - v_j$ is difference between the velocities of two bead particles. ω^D is called distance dependent weight function and is calculated by Eq. (4) below:

$$\omega^D = \begin{cases} \left(1 - \frac{r_{ij}}{r_C}\right)^2 & r_{ij} < r_C \\ 0 & r_{ij} \geq r_C \end{cases} \quad (4)$$

The random force F_{ij}^R is included to simulate the effect of random motion of the beads in the liquid phase. It was calculated using the Eq. (5) below:

$$F_{ij}^R = \sigma_{ij}\omega^R(r_{ij})\xi_{ij}\frac{1}{\sqrt{\Delta t}} \quad (5)$$

Where σ_{ij} is called the noise amplitude and $\sigma_{ij} = \sigma_{ji} > 0$ holds true. ω^R is called distance dependent weight function, $\xi_{ij} = \xi_{ji} > 0$ is called randomly fluctuating Gaussian variable having a zero mean and a unit variance, Δt is the time step utilized when solving the DPD

equations. The distance dependent weight function ω^R is calculated via the Eq. (6) below:

$$\omega^R = \begin{cases} 1 - \frac{r_{ij}}{r_C} \; r_{ij} < r_C \\ 0 \; r_{ij} \geq r_C \end{cases} \tag{6}$$

The noise amplitude σ_{ij} in Eq. (5) is related to the friction coefficient γ_{ij} in Eq. (3) via the Eq. (7) below:

$$\sigma_{ij}^2 = 2\gamma_{ij} k_B T \tag{7}$$

Where k_B is the Boltzmann constant (k_B=*1.380649×10⁻²³ J·K⁻¹*) and T is the absolute temperature in units of *K*.

The electrostatic force F_{ij}^E was calculated according to Coulomb's Law as expressed by Eq. (8) below:

$$F_{ij}^E = k_e \frac{q_i q_j}{\varepsilon_r r_{ij}^2} \tag{8}$$

Where k_e is the Coulomb's constant (k_e=*8.99 × 10⁹ N · m² · C⁻²*), q_i and q_j are the electrostatic charges of the bead i and bead j, ε_r is the relative permittivity of the medium.

DPD forces related to bonded interactions are called spring force F_{ij}^S and angle force F_{ijk}^A. The spring force F_{ij}^S simulates the strength of bonds between bead particles and is expressed with the Eq. (9) and Eq. (10) below:

$$F_{ij}^S = -\frac{\delta U^S}{\delta r_{ij}} \tag{9}$$

$$U^S = \sum_j \frac{1}{2} C^b \left(r_{ij} - r_0\right)^2 \tag{10}$$

Where C^b is called the spring constant, r_0 is unstretched bond length between bead particles i and j.

The angle force F_{ijk}^A simulates the stiffness of the angle between two neighboring bonds and calculated using the Eq. (11) and Eq. (12) below:

$$F_{ijk}^A = -\frac{\delta U^A}{\delta r_{ij}} \tag{11}$$

$$U^A = \sum_j \frac{1}{2} C^a \left(cos\theta_{ijk} - cos\theta_0\right)^2 \tag{12}$$

Where C^a is called the angle constant, θ_{ijk} is the actual bond angle, θ_0 is the equilibrium bond angle of *i-j-k* bonds.

2.2 Coarse Graining

Coarse graining is done to transform the actual molecular structure of the component to a mesomolecular structure consisting of bead particles that is suitable for DPD simulation. Coarse graining of the gemini-like surfactant C_{18}-EPPO-C_{18} was done by dissecting the molecule into molecular fragments consisting of 4 or 5 heavy atoms. The dissection was done in a manner to keep the volumes of dissected parts approximately equal or close to each other. Coarse graining of the water molecules was done by combining 3 water molecules into a single bead particle. Coarse graining scheme for C_{18}-EPPO-C_{18} and water molecules is presented in Fig. 1 below.

Volume of a single water molecule is generally taken to be equal to 30 Å^3 in accordance with Groot and Rabone [9]. The total volume of W bead which contains 3 water molecules is generally considered to be 90 Å^3. Bead density of ρ=3 was adopted in-line with a pioneering work on DPD methodology by Groot and Warren [10]. The effective diameter of the beads was taken as equal to the bead interaction cut-off radius r_C and was determined using the Eq. (13) below [9]:

$$r_c = \sqrt[3]{\rho V_W} \tag{13}$$

Where V_W is bead volume of 90 Å^3. Therefore, the effective bead diameter for all beads becomes r_C=6.46 Å.

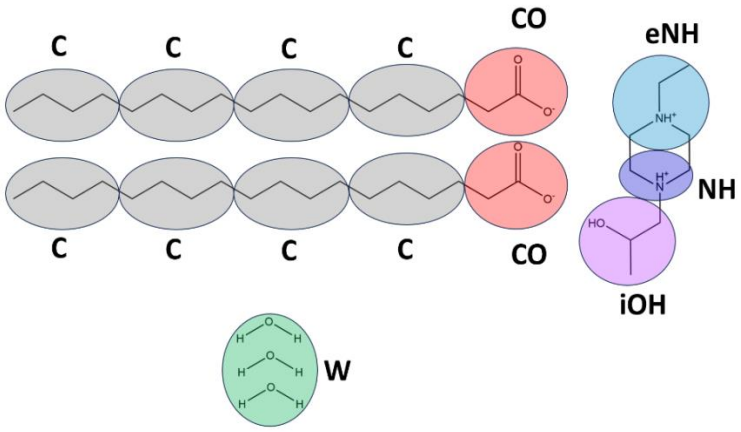

Fig. 1 Coarse graining of C_{18}-EPPO-C_{18} and water molecules

2.3 DPD Parametrization

The conservative force repulsive interaction parameters a_{ij} for the beads shown in Fig. 1 are calculated using the Flory-Huggins solution theory. The Flory-Huggins chi (χ_{ij}) parameter is related to DPD interaction parameter a_{ij} via the Eq. (14) below [9]:

$$a_{ij} = a_{ii} + \frac{\chi_{ij}}{0.231} \tag{14}$$

Where a_{ii} is the DPD interaction parameter between two identical beads, while a_{ij} is the interaction parameter for two differing beads. The Flory-Huggins chi (χ_{ij}) parameters for all bead pairs were calculated in Materials Studio v23 software. a_{ii} is calculated using the Eq. (15) below [9]:

$$a_{ii} = \frac{(16N_m - 1)k_B T}{0.2\rho} \tag{15}$$

Where N_m is the number water of water molecules combined into a single bead and ρ is the bead density. The values of bead interactions parameters a_{ii} and a_{ij} for all bead pairs are listed in Table 1 below.

The friction coefficient γ_{ij} from Eq. (3) above is assigned the value of γ_{ij}=4.5 as recommended by different works on DPD simulations of surfactants [5] [11] [12].

A time step of Δt=0.05 was selected to get good accuracy with optimum computational efficiency.

NH, eNH and CO beads were assigned electrostatic charges of +1, +1 and -1 respectively, while all other beads were electroneutral. The relative permittivity ε_r was set to the value of 78.2, which is the relative permittivity of water at 25°C to simulate the aqueous environment.

The value of spring constant in Eq. (10) was set to $C^b=150$ in-line with recommended value in the literature [12]. The unstretched bond length r_0 for all bead pairs was calculated using the Eq. (16) below [12]:

$$r_0 = r_C[0.1(n_i + n_j) - 0.01] \tag{16}$$

Where n_i and n_j are the number of heavy atoms contained by bonded beads i and j, respectively and r_0 is in units of Å.

The value of angle constant in Eq. (12) was set to $C^a=5$ and equilibrium angle of $\theta_0=180°$ was selected for all bond angles [12].

Table 1. Bead interaction parameters

Bead type	Reference compound	C	CO	iOH	NH	eNH	W
C	C_4H_{10}	78.33					
CO	CH_3COOH	134.22	78.33				
iOH	CH_3CHCH_3OH	89.25	93.35	78.33			
NH	CH_3NHCH_3	82.32	80.68	73.97	78.33		
eNH	$CH_3NCH_3CH_2CH_3$	79.38	77.98	74.75	78.18	78.33	
W	$3 \cdot H_2O$	118.79	80.77	75.50	74.24	72.69	78.33

3. Simulation Results

DPD simulations were run in a simulation box with dimensions of 200 Å × 200 Å × 200 Å at 2 mM, 5 mM, 10 mM and 20 mM surfactant concentrations for 100 000 time steps to reach equilibrated thermodynamic state. The thermostat was set to 298 K at the beginning of each simulation and box dimensions were fixed. All simulations were run in Materials Studio v23.

3.1 Micelle formation

DPD simulations could successfully predict micelle formation at various surfactant concentrations. The snapshots of final system configurations are presented in Fig. 2 below. Water beads have been hidden for clarity. The bead coloring scheme is the same as described in Fig. 1 above.

Fig. 2 indicates that the size and number of the aggregates increases as the concentration becomes greater. In addition, all CO beads, which simulate the polar part of the surface-active molecules, are directed away from the center of the aggregates and are in interaction with the solvent molecules. Certain fraction of the bead particles simulating the counterions with piperazine fragment are also interacting with the aggregates and forming a corona around them. The remaining counterion particles are freely distributed throughout the solution. The overall configuration of mesomolecules within the equilibrated simulation boxes agrees with the actual idea of the micelle formation and counterion binding to the micelles. This indicates that DPD parametrization is done correctly.

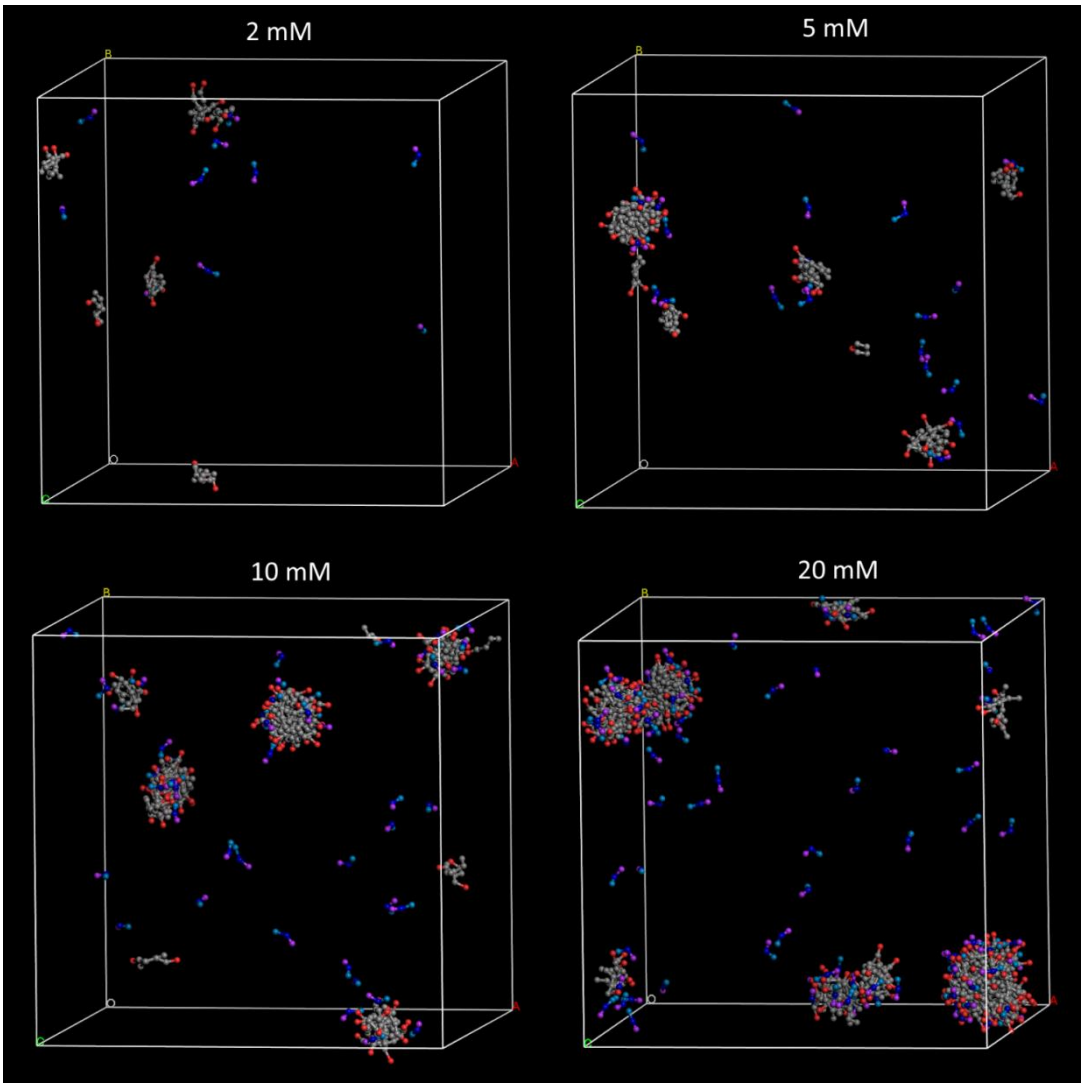

Fig. 2 Snapshots of equilibrated DPD simulation boxes at different concentrations

3.2 Radial Distribution Function (RDF)

Radial distribution function (RDF) describes how local density of the particles varies as a function of radial distance from the reference particle in a multiparticle system. When RDF curves are plotted for a multiparticle system it describes the averaged particle density calculated for each one of the particles over all distances. If a peak appears on an RDF plot at a certain radial distance, this is an indication of an orderly arrangement of the particles at this average distance from each other. RDF plots of C_{18}-EPPO-C_{18} are generated from the analysis of DPD trajectories to identify the structural arrangements of surface-active molecules within the solution space and presented in Fig. 3 below. The data has been normalized to compare the plots for varying concentrations.

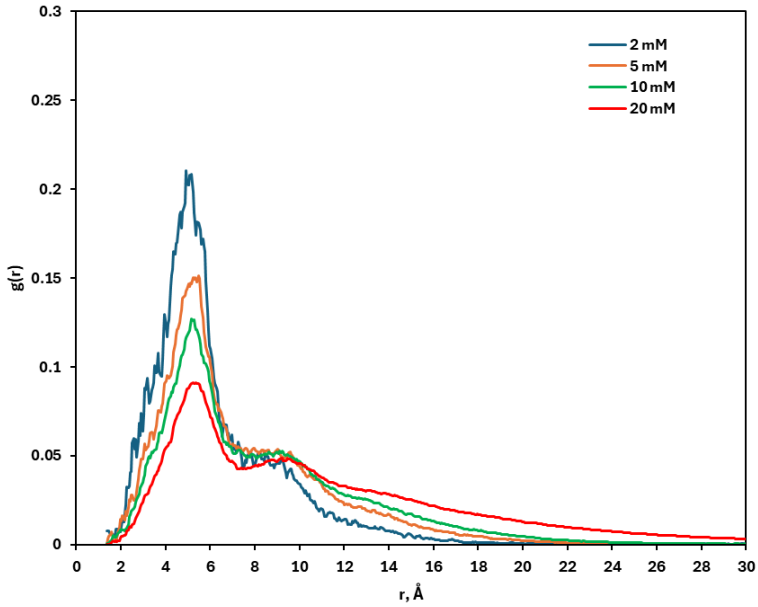

Fig. 3 RDF plots of C_{18}-EPPO-C_{18} at different concentrations

The analysis of Fig. 3 shows that the first RDF peak appears between 5-6 Å at all concentrations. This distance corresponds to the average equilibrium length of the bonds between bead particles. The height of the first peaks becomes smaller as the bulk surfactant concentration increases. A second, much flatter peak appears to the right of the first sharp peak on each one of the RDF curves for different concentrations. The height of the second peak becomes greater as the concentration is increased. While the first RDF peak is related to the intramolecular arrangement of beads, appearance of the second peaks is related to the ordered arrangement beyond the bond length distances. It could be argued that the second peak appears due to formation of the aggregates in the solution. The fact that the second peak becomes greater as the concentration increases supports this statement. The RDF curves decay and approach to zero as the distance increases. It is due to the fact that surface-active molecules are essentially concentrated within aggregates and probability of finding a surfactant molecule within interaggregate space is very low. This fact once more confirms the formation of micellar aggregates in the surfactant solution.

3.3 Prediction of CMC

CMC of a surfactant solution can be evaluated based on DPD trajectory analysis by identifying what fraction of the total dissolved surfactant molecules are freely distributed within the solution and are not part of any aggregates. The concentration of the 'free' surfactant molecules is counted as CMC. If two surfactant molecules are within a certain R_{agg} threshold distance from each other, they are considered to belong to the same aggregate. If the distance between two surfactant molecules is greater than R_{agg}, they are considered to be free from aggregates. R_{agg} is determined from the minimum point between the two peaks on the RDF curve (see Fig. 3). In addition, a cluster of surfactant molecules is considered as micelle if and only if it contains more than n_{mic} number of molecules. If less than n_{mic} number of molecules are in a cluster, all molecules are considered free from micellization. n_{mic} corresponds to the minimum point between two peaks on an aggregate size distribution curve. Aggregate size distribution curves of C_{18}-EPPO-C_{18} at varying concentrations are presented in Fig. 4 below.

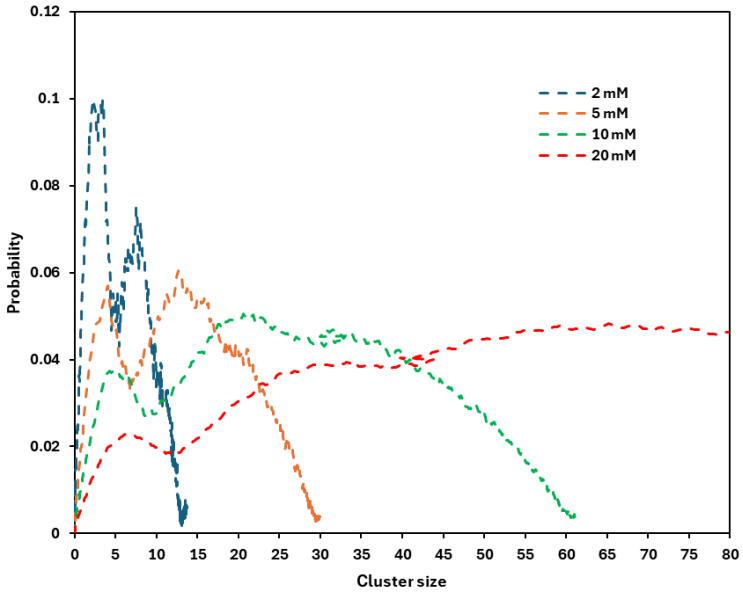

Fig. 4 Aggregate size distribution curves of C_{18}-EPPO-C_{18} at different concentrations

It is obvious from Fig. 4 that n_{mic} shows some variation with concentration. The value of n_{mic} is n_{mic}*=5*, n_{mic}*=7*, n_{mic}*=9 and* n_{mic}*=12* at 2 mM, 5 mM, 10 mM, and 20 mM concentrations, respectively. Theoretically evaluated CMC value was 1.054 mM, 1.157 mM, 1.398 mM and 0.681 mM for 2 mM, 5 mM, 10 mM, and 20 mM total concentrations, respectively. This level of fluctuation of CMC value with concentration can be considered normal. The average value of theoretical CMC was 1.073 mM whereas experimentally determined CMC value of C_{18}-EPPO-C_{18} is 0.390 mM [6]. In fact, several other studies reported a difference between experimental and theoretical CMC values of surfactants. Vishnyakov et al. [3] predicted the CMC values of non-ionic surfactants C_8E_8, DDAO and MEGA-10 as 11.8 mM, 1.3 mM, and 7.5 mM, respectively. The experimental CMC values of these surfactants are 10 mM, 1-2 mM, and 6-7 mM. Anderson et al. [11] predicted the CMC values of ionic n-alkyl sulfate surfactants S6S, S8S, S10S and S12S as 210 mM, 78 mM, 22.5 mM, and 6.7 mM, whereas their experimental CMC values were 420 mM, 130 mM, 33 mM, and 8.2 mM, respectively. Overall, theoretical and experimental CMC values of C_{18}-EPPO-C_{18} are in the same order of magnitude, which can be considered a very good agreement between simulation and experiment.

4. Conclusion

DPD simulation of a gemini-like surfactant C_{18}-EPPO-C_{18} constructed from propoxylated ethyl piperazine and stearic acid has been performed to model its micellization behavior. Repulsive interaction parameters have been evaluated utilizing the Flory-Huggins chi parameters. Simulations performed at different surfactant concentrations successfully predicted aggregate formation and its dependence on concentration. Aggregate formation has been verified from the analysis of RDF plots having a secondary peak at intermolecular range. The RDF curves are decaying and approaching zero at long distances, which points out that local concentration of surface-active molecules is very low outside the aggregate space. The average theoretically evaluated CMC value of C_{18}-EPPO-C_{18} was higher than experimental CMC value. However, the difference between theoretical and experimental CMC values is small and good agreement of simulation results with experimental outcomes is observed.

5. REFERENCES

[1] Ivanova, A. A., Koltsov, I. N., Groman, A. A., & Cheremisin, A. N. (2023). Molecular Dynamics Simulations for Surfactant Research (A Review). *Petroleum Chemistry*, *63*(8), 867–885. https://doi.org/10.1134/S0965544123060142

[2] Santo, K. P., & Neimark, A. V. (2021). Dissipative particle dynamics simulations in colloid and Interface science: a review. *Advances in Colloid and Interface Science*, *298*(October), 102545. https://doi.org/10.1016/j.cis.2021.102545

[3] Vishnyakov, A., Lee, M. T., & Neimark, A. V. (2013). Prediction of the critical micelle concentration of nonionic surfactants by dissipative particle dynamics simulations. *Journal of Physical Chemistry Letters*, *4*(5), 797–802. https://doi.org/10.1021/jz400066k

[4] Gong, J., Song, Y., Sun, Y., Sun, Q., Liu, C., Tan, J., Zhao, L., & Xu, B. (2024). Vesicle-to-micelle transition in a double chain quaternary ammonium surfactant system: Interfacial behavior and molecular insights. *Journal of Molecular Liquids*, *394*(August 2023), 123714. https://doi.org/10.1016/j.molliq.2023.123714

[5] Goodarzi, F., & Zendehboudi, S. (2020). Effects of salt and surfactant on interfacial characteristics of water/oil systems: Molecular dynamic simulations and dissipative particle dynamics. *Industrial and Engineering Chemistry Research*, *58*(20), 8817–8834. https://doi.org/10.1021/acs.iecr.9b00504

[6] Hasanov, E. E., Rahimov, R. A., Abdullayev, Y., & Ahmadova, G. A. (2023). Symmetric and Dissymmetric Pseudo-gemini Amphiphiles Based on Propoxylated Ethyl Piperazine and Fatty Acids. *ChemistrySelect*, *8*(48), e202303942. https://doi.org/10.1002/slct.202303942

[7] Hoogerbrugge, P. J., & Koelman, J. M. V. A. (1992). Simulating microscopic hydrodynamic phenomena with dissipative particle dynamics. *Epl*, *19*(3), 155–160. https://doi.org/10.1209/0295-5075/19/3/001

[8] Espanol, P., & Warren, P. (1995). Statistical mechanics of dissipative particle dynamics. *Epl*, *30*(4), 191–196. https://doi.org/10.1209/0295-5075/30/4/001

[9] Groot, R. D., & Rabone, K. L. (2001). Mesoscopic simulation of cell membrane damage, morphology change and rupture by nonionic surfactants. *Biophysical Journal*, *81*(2), 725–736. https://doi.org/10.1016/S0006-3495(01)75737-2

[10] Groot, R. D., & Warren, P. B. (1997). Dissipative particle dynamics: Bridging the gap between atomistic and mesoscopic simulation. *Journal of Chemical Physics*, *107*(11), 4423–4435. https://doi.org/10.1063/1.474784

[11] Anderson, R. L., Bray, D. J., Del Regno, A., Seaton, M. A., Ferrante, A. S., & Warren, P. B. (2018). Micelle Formation in Alkyl Sulfate Surfactants Using Dissipative Particle Dynamics [Research-article]. *Journal of Chemical Theory and Computation*, *14*(5), 2633–2643. https://doi.org/10.1021/acs.jctc.8b00075

[12] Li, Y., Zhang, H., Bao, M., & Chen, Q. (2012). Aggregation Behavior of Surfactants with Different Molecular Structures in Aqueous Solution: DPD Simulation Study. *Journal of Dispersion Science and Technology*, *33*(10), 1437–1443. https://doi.org/10.1080/01932691.2011.620897

[13] Anderson, R. L., Bray, D. J., Ferrante, A. S., Noro, M. G., Stott, I. P., & Warren, P. B. (2017). Dissipative particle dynamics: Systematic parametrization using water-octanol partition coefficients. *Journal of Chemical Physics*, *147*(9). https://doi.org/10.1063/1.4992111

2024. Volume 8, Number 1 ***Pages 13-22***

UOT: 544.5, 543.2
https://doi.org/10.30546/2521-6317.2024.402

INVESTIGATING THE DECHLORINATION PATHWAY OF HEXACHLOROBENZENE IN ACETONE THROUGH GAMMA IRRADIATION

Samir KARIMOV[1*], Elshad ABDULLAYEV[2], Muslum GURBANOV[3], Lala GASIMZADA[1]

[1]*French-Azerbaijani University under Azerbaijan State Oil and Industry University,*

Baku, Azerbaijan

[2]*Sumgait State University,*

Sumgait, Azerbaijan

[3]*Institute of Radiation Problems,*

Baku, Azerbaijan

[*]Corresponding author.

E-mail: samir.karimov@ufaz.az (S. Karimov), elshad.abdullayev@sdu.edu.az (E. Abdullayev)

ARTICLE INFO

Article history:

Received:2024-07-26

Received in revised form:2024-09-13

Accepted:2024-10-18

Available online

Keywords:
Hexachlorobenzene
Radiation chemistry
Nuclear energy
POPs
Environmental remediation
JEL CODES: Q53, Q55, Q57,Q65

ABSTRACT

Hexachlorobenzene (HCB), a persistent organic pollutant, poses significant environmental and health risks due to its stability and bioaccumulation. This study investigates the degradation of HCB in acetone using gamma irradiation. Gamma radiolysis was performed using a ^{60}Co source, and the resultant radiolytic products were analyzed through Gas Chromatography-Mass Spectrometry (GC-MS). Mass spectral analysis revealed the formation of various by-products, including lower chlorinated benzenes (CBs) – penta- (PCB), tetra-(TeCB), trichlorobenzene (TCB) – and other chlorinated and non-chlorinated compounds, indicating a complex dechlorination pathway. Detailed investigation of the degradation pathway suggested sequential dechlorination and breakdown of the HCB molecule under gamma irradiation. The effects of different radiation doses on the degradation efficiency were also explored. Results demonstrated significant reduction in HCB concentration, highlighting gamma irradiation as a viable method for the remediation of HCB-contaminated environments.

1. Introduction

HCB is a persistent organic pollutant (POP) known for its environmental persistence, bioaccumulative nature, and toxicity to both human health and ecosystems [1]. Historically used as a fungicide and industrial chemical, HCB has been banned or restricted in many countries due to its hazardous properties including Azerbaijan [2]. Despite these measures, significant amounts of HCB remain in the environment, necessitating effective remediation techniques.

Traditional methods for the degradation of HCB, such as thermal, chemical, and biological treatments are applied [3, 4, 5]. These methods often face limitations in efficiency, cost, and potential secondary pollution [6, 7, 8]. Consequently, alternative approaches are being explored to address these challenges including advanced oxidation processes [9, 10, 11, 12, 13, 14]. One promising technique is gamma radiolysis, which involves the use of high-energy gamma photons from a ^{60}Co source to induce chemical reactions that break down complex pollutants into simpler, less harmful compounds [15, 16, 17, 18].

Gamma radiolysis has shown potential in the degradation of various chlorinated compounds due to its ability to generate reactive species such as hydroxyl radicals (•OH) and solvated electrons ($e^-_{sol.}$) [19, 19]. These reactive species can effectively cleave carbon-chlorine bonds, leading to the dechlorination of the target pollutants. Previous studies, including our own on the gamma radiolysis of TCB in methanol, ethanol, hexane, and benzene, have demonstrated the efficacy of gamma radiolysis and revealed that the choice of solvent significantly influences the degradation pathway and products formed [16].

This study focuses on the gamma radiolysis of HCB in acetone, a widely used solvent known for its high solubility and moderate reactivity. Acetone's unique properties may affect the stability and reactivity of the intermediates formed during radiolysis, thereby influencing the overall degradation process. By identifying the primary and secondary products of HCB degradation in acetone, this research aims to elucidate the mechanisms involved and assess the potential of gamma radiolysis as a viable method for the remediation of HCB-contaminated environments.

2. Materials and methods

The similar method applied in our previous investigation has been applied in this study as well [15].

>99% pure HCB was purchased from Merck, while acetone was of gradient grade and obtained from LiChrosolv. All chemicals were used as received without further purification. Standard solutions of HCB were prepared in acetone at a concentration of approximately 0.06 g/L for the gamma irradiation experiments and calibration of GC-MS.

Irradiation was performed using an MRX-γ-25 apparatus equipped with a ^{60}Co source. The solutions were irradiated without degassing to maintain the presence of air. The samples were subjected to various doses to investigate the dose-dependent degradation of HCB.

Post-irradiation, the samples were analyzed using gas chromatography-mass spectrometry (GC-MS) to identify the degradation products of HCB. The GC-MS analysis was conducted using a Shimadzu QP2010 SE instrument equipped with a Rxi-5ms capillary column (30 m ×

0.25 mm, 0.25 μm film thickness). The following conditions were used for the analysis: Helium was used as the carrier gas at a flow rate of 1 mL/min. The injection mode was split with an injection volume of 1 μL. The oven temperature program started at an initial temperature of 30°C (held for 2 minutes), ramped to 320°C (held for 2 minutes) at 10°C/min rate. MS detection was conducted in electron impact ionization (EI) mode at 70 eV, with the mass spectrometer operating in Scan mode to enhance sensitivity and selectivity for the chlorinated products.

3. Results and Discussion

The gamma radiolysis of HCB in acetone results in a diverse array of degradation products. Below, we provide a detailed analysis and discussion of the findings, supported by chromatograms, mass spectra, and a summary table of the identified compounds.

3.1. Chromatographic Analysis

The gas chromatograms of the HCB solution before and after, 25.1 kGy gamma irradiation are shown in Figure 1. GC chromatogram of HCB in acetone: A) before gamma irradiation; B) after 25.1 kGy gamma irradiation. A and B respectively.

The pre-irradiation chromatogram displays a single dominant peak corresponding to HCB at a retention time of 17.47 minutes. Post-irradiation, additional peaks appear at different retention times, indicating the formation of degradation products such as dechlorination products of PCB and TeCBs.

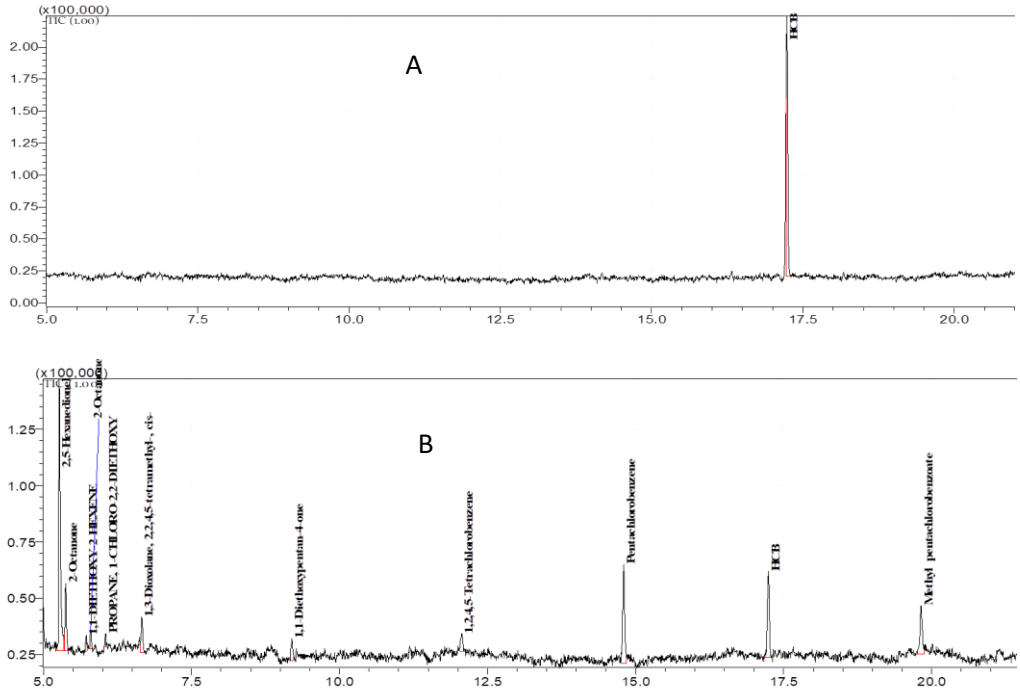

Figure 1. *GC chromatogram of HCB in acetone: A) before gamma irradiation; B) after 25.1 kGy gamma irradiation.*

3.2. Mass Spectrometric Analysis

Mass spectra for the products were obtained to confirm their identities. For instance, the mass spectrum of pentachlorobenzene (PeCB) (Figure 2 (2)) shows a molecular ion at 250 m/z, with significant fragment ions at m/z 215 and 180, while the mass spectrum of

tetrachlorobenzene (TeCB) (Figure 2Figure 2. Mass spectra and appropriate structures of identified products post-irradiation. (10)) shows a molecular ion at 216 m/z, confirming their identity.

All 20 identified products and HCB at different radiation doses have been numbered according to their respective numbers in

Table 1. The corresponding peak areas of these compounds have also been provided at the relevant absorbed doses. Although it is not the primary aim of this report, information on the quantitative changes can also be inferred from the peak areas of the compounds in the chromatograms given in

Table 1.

3.3. Mechanistic Insights of product formations

The gamma radiolysis of HCB in acetone leads to the formation of a wide variety of products through several distinct mechanisms:

1. Dechlorination: Dechlorination of HCB results in compounds such as PCB, 1,2,4,5-TeCB and 1,2,4-TCB. These intermediates suggest a stepwise removal of chlorine atoms facilitated by the high-energy gamma photons. These products indicate interactions between hydrogen radicals – forms from the radiolysis of acetone – and HCB.

2. Oxidation: The radiolytic conditions favor oxidation reactions, producing ketones, including: 2,5-hexanedione; 3,4-dihydroxy-3,4-dimethyl-hexan-2,5-dione; 2-octanone; 1,1-diethoxypentan-4-one; 4-methyl-pent-4-en-2-one and 2-hexanone, 6-(acetoxy). The formation of carboxylic acid - 2-ethyl-butanoic acid further highlights the oxidative pathways. Those products are expected to form due to interaction between oxygen and other compounds available in irradiated systems.

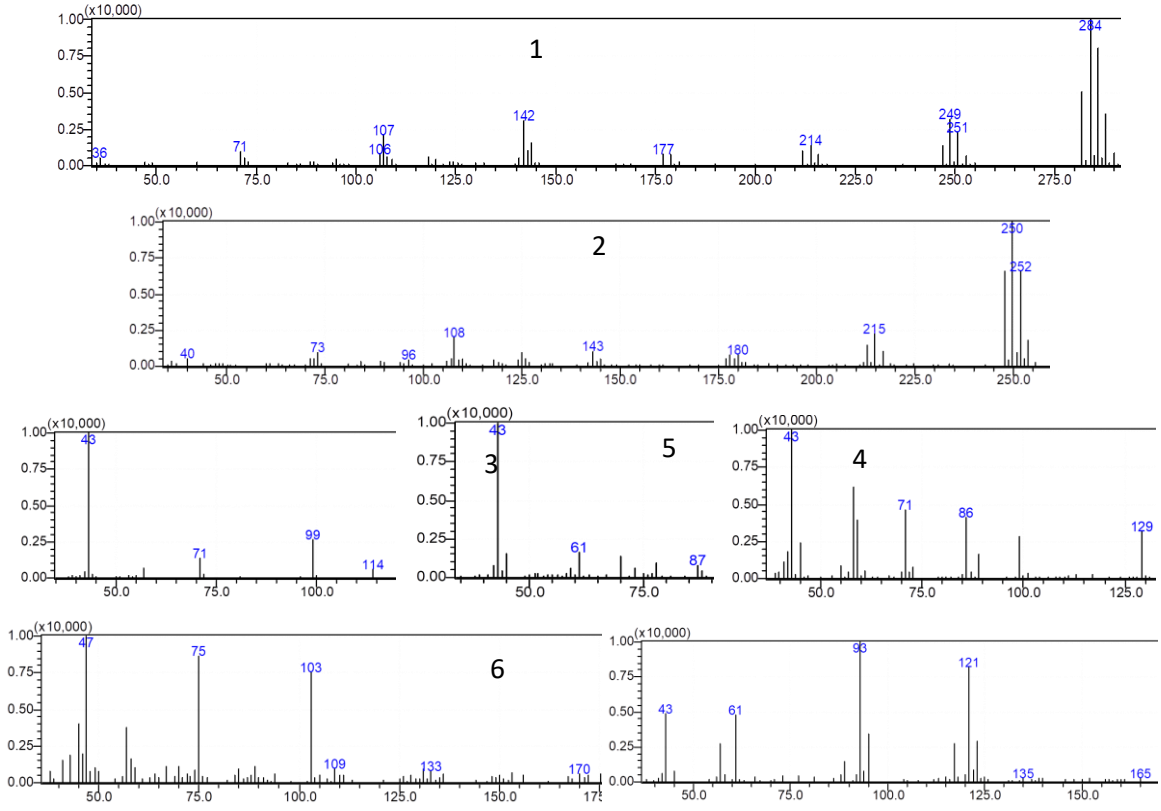

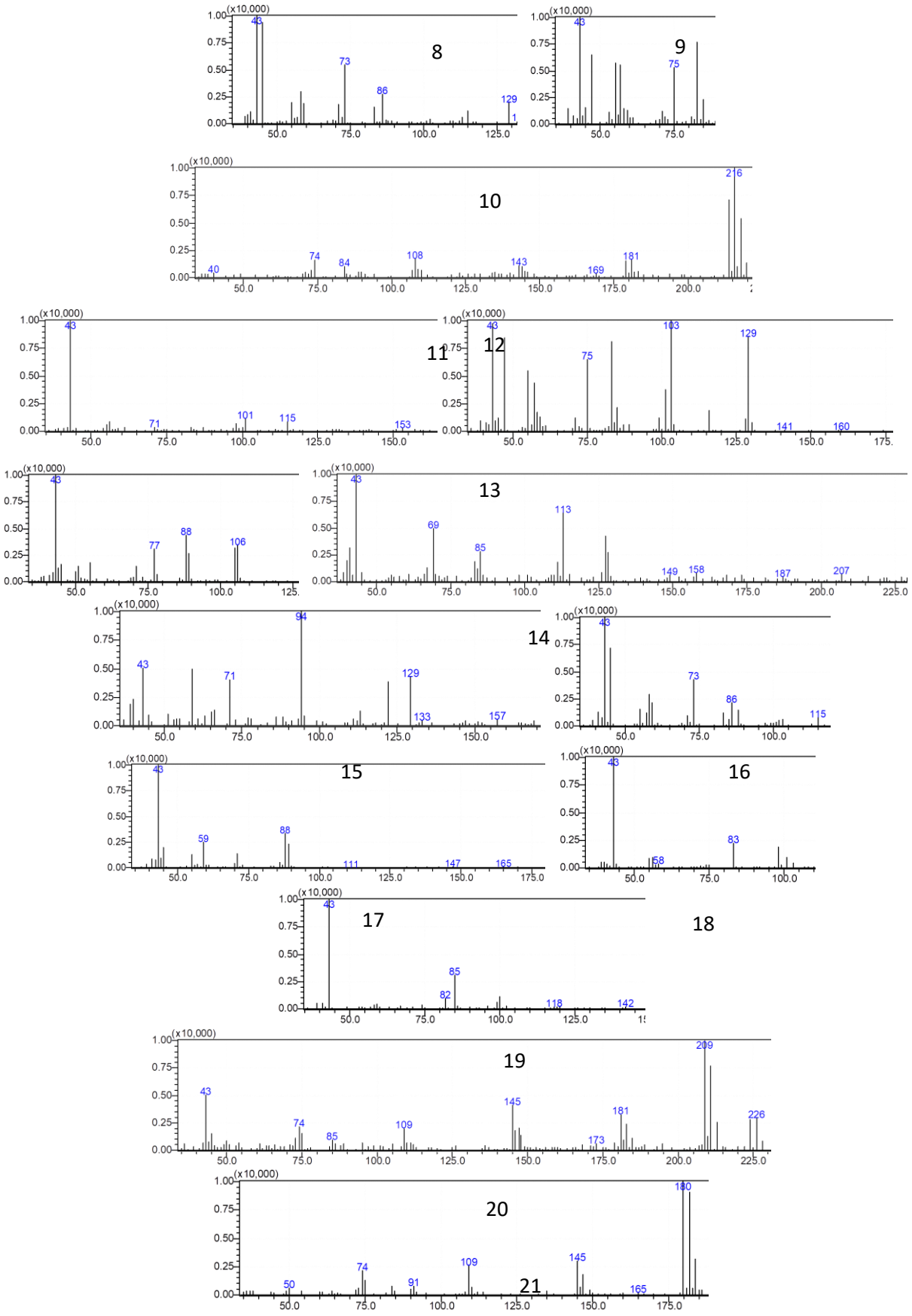

Figure 2. *Mass spectra and appropriate structures of identified products post-irradiation.*

3. Substitution and Esterification: The formation of methyl pentachlorobenzoate; ethyl acetate; pentanoic acid 3-hydroxy-5,5-dimethoxy-3-methyl-,ethyl ester; phenyl butyrate; acetic acid 1-methyl-3-oxo-but-1-enyl ester points to substitution and esterification reactions. These products indicate interactions between the reactive species – primary products of radiolysis of acetone – and acetone itself.

4. Formation of Ethers and Acetals: Compounds 1,1-diethoxy-hexen-2; 1-chloro-2,2-diethoxy-propane demonstrate the incorporation of ethoxy groups, indicating the formation of ether and acetal structures.

5. Reduction: The presence of alcohols – 1-(2,4,5-trichlorophenyl)-ethanol and 1-propoxy-2-propanol suggests reduction reactions are also occurring, reducing the chlorinated intermediates to their corresponding alcohols.

These results illustrate the complex interplay of radiolytic reactions occurring during the gamma irradiation of HCB in acetone. The identification of diverse products underscores the versatility of gamma radiolysis in degrading POPs. This study's findings provide a comprehensive understanding of the degradation pathways and highlight the potential of gamma irradiation for environmental remediation applications.

Table 1. *Identified products from gamma irradiated acetone solutions of HCB*

No.	Name of products	Dose, kGy							
		0	**3.1**	**6.3**	**12.6**	**25.1**	**50.2**	**100.5**	**169.5**
		Area of the peaks							
1	HCB	351385	404961	358657	89111	43369	0	0	0
2	PCB	0	0	27165	82967	99272	76092	22069	0
3	2,5-hexanedione	0	0	0	116593	229362	277026	401050	865129
4	Ethyl acetate	0	0	0	19967	0	0	0	0
5	2-octanone	0	0	0	0	49594	9883	26850	0
6	1,1-diethoxy-2-hexene	0	0	0	0	8342	13266	-	30405
7	Propane,-1-chloro-2,2-diethoxy	0	0	0	0	8082	0	0	0
8	1,3-dioxolane, 2,2,4,5-tetramethyl-, cis-	0	0	0	0	30860	0	0	28090
9	1,1-diethoxypentan-4-one	0	0	0	0	20935	53370	139574	0
10	1,2,4,5-TeCB	0	0	0	0	19720	50262	31735	0
11	Methyl pentachloro benzoate	0	0	0	0	61106	38570	0	0
12	2-hexanone, 6-(acetoxy)	0	0	0	0	0	11872	31985	12639
13	2-ethylbutanoic acid	0	0	0	0	0	0	24869	0
14	Pentanoic acid, 3-hydroxy-5,5-dimethoxy-3-methyl-,ethyl ester	0	0	0	0	0	0	10109	0
15	Phenyl butyrate	0	0	0	0	0	0	20474	0
16	1-propoxy-2-propanol	0	0	0	0	0	0	43389	81081
17	3,4-dihydroxy-3,4-dimethyl-hexan-2,5-dione	0	0	0	0	0	0	0	33877
18	4-methyl-pent-4-en-2-one	0	0	0	0	0	0	0	20624
19	Acetic acid 1-methyl-3-oxo-but-1-enyl ester	0	0	0	0	0	0	0	12639
20	1-(2,4,5-trichlorophenyl) ethanol	0	0	0	0	0	0	0	15015
21	1,2,4-Trichlorobenzene	0	0	0	0	0	0	14015	0

3.4. Analysis of Degradation Patterns Under Gamma Radiation

The observed changes in the peak areas of various compounds subjected to increasing doses of gamma radiation illustrate distinct degradation and formation patterns as shown in Figure 3 as well.

Initially, HCB displays a high peak area at 0 kGy, which gradually decreases with increasing dose, becoming 0 by 25.1 kGy. This trend indicates that HCB undergoes extensive degradation as the radiation dose increases.

PCB is not detected at lower doses but emerges at 6.3 kGy, with its peak area increasing up to 25.1 kGy before diminishing at higher doses. This suggests that PCB is a by-product of HCB degradation and itself undergoes further degradation with higher radiation exposure.

The compound 2,5-hexanedione appears at 12.6 kGy, with its peak area steadily

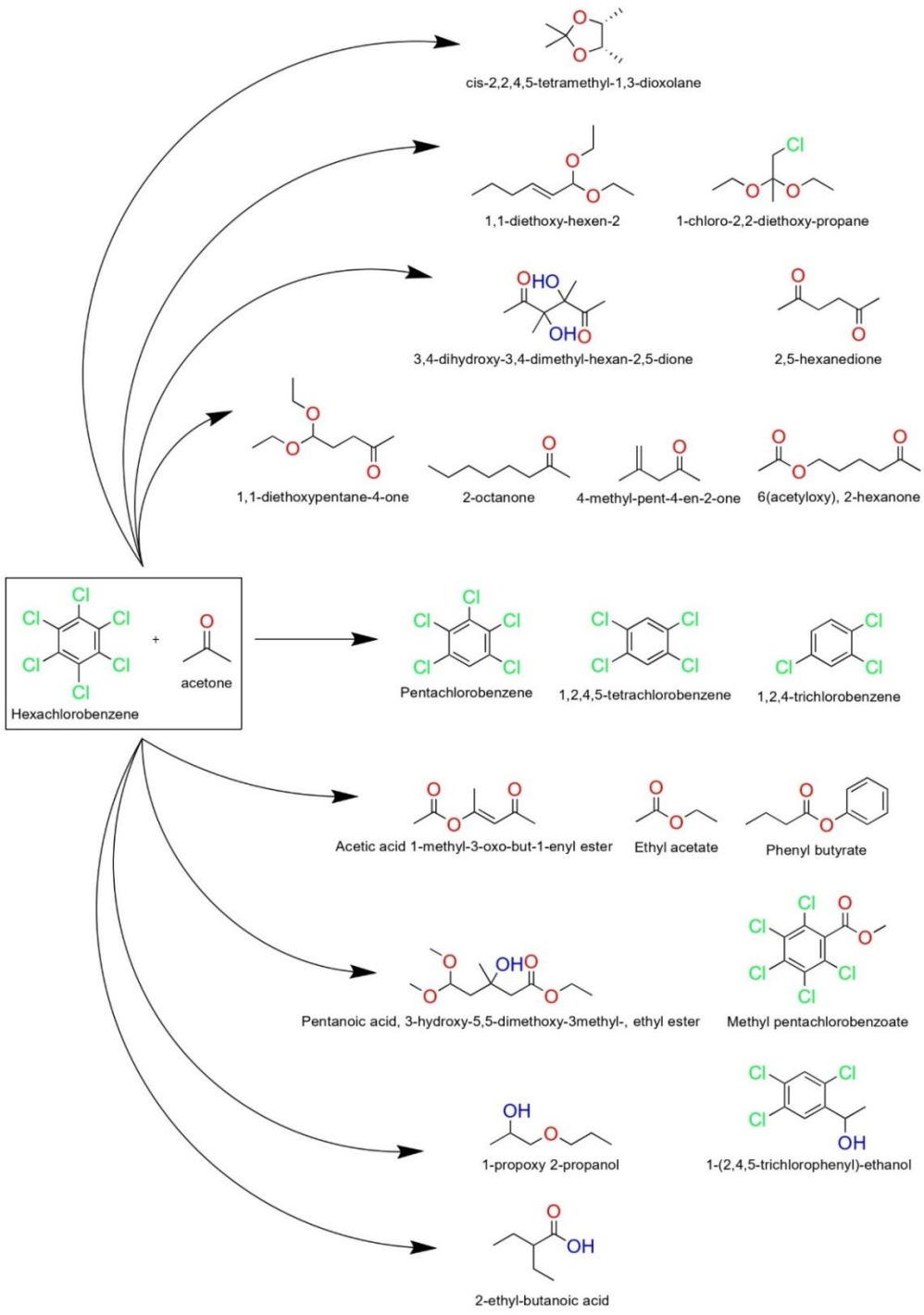

Figure 3. *Overall pathways of HCB +acetone irradiataion under gamma rays*

increasing up to 169.5 kGy, indicating it is a stable by-product formed at higher doses. Ethyl acetate is detected only at 12.6 kGy, suggesting transient formation and instability at higher doses. Similarly, 2-octanone appears at 25.1 kGy, increases at 50.2 kGy, but is not present at higher doses, indicating formation at intermediate doses followed by degradation or volatility.

The presence of 1,1-diethoxy-2-hexene is first detected at 50.2 kGy, with its peak area increasing at 100.5 kGy before slightly diminishing, indicating late formation and some stability under high radiation. Propane-1-chloro-2,2-diethoxy is only present at 50.2 kGy, suggesting specific formation conditions that do not persist at higher doses. Similarly, 1,3-dioxolane, 2,2,4,5- tetramethyl-, cis- appears at 50.2 kGy but not at higher doses, indicating formation under specific conditions and instability at higher radiation levels.

The compound 1,1-diethoxypentan-4-one appears at 50.2 kGy and significantly increases at 100.5 kGy, suggesting formation at higher doses and stability. 1,2,4,5-TeCB is detected from 50.2 kGy, with its peak area increasing and stabilizing at 100.5 kGy, indicating it is a stable degradation by-product.

Methyl pentachloro benzoate appears at 50.2 kGy, with significant peaks at 100.5 kGy, indicating formation and stability at high radiation doses. The compound 2-hexanone, 6-(acetoxy) appears at 100.5 kGy, maintaining a stable peak at 169.5 kGy, suggesting formation and stability at high doses. 2-ethylbutanoic acid and pentanoic acid, 3-hydroxy-5,5-dimethoxy-3-methyl-,ethyl ester are both detected at 100.5 kGy, indicating formation under specific high-dose conditions.

Phenyl butyrate, present at 100.5 kGy, and 1-propoxy-2-propanol, which increases from 100.5 kGy to 169.5 kGy, further indicate formation and stability at high doses. The compound 3,4-dihydroxy-3,4-dimethyl-hexan-2,5-dione is only detected at 169.5 kGy, along with 4-methyl-pent-4-en-2-one and acetic acid 1-methyl-3-oxo-but-1-enyl ester, indicating formation under very high radiation doses. Lastly, 1-(2,4,5-trichlorophenyl)ethanol and 1,2,4-trichlorobenzene (TCB) are present at 169.5 kGy, indicating they are degradation products formed at high doses.

4. Conclusion

The study demonstrates the effective degradation of HCB in the presence of acetone under gamma irradiation. As the radiation dose increases, HCB significantly degrades, showing the efficacy of gamma rays in breaking down this compound. The process leads to the formation of various by-products, which appear at different stages of irradiation. Intermediate products such as PCB and TeCB emerge at lower doses and either stabilize or degrade further at higher doses into compounds like TCB. The formation of specific compounds at high doses indicates complex degradation pathways and secondary product formation. Overall, the results highlight the potential of gamma irradiation for environmental remediation, providing insights into the mechanisms of radiolytic degradation and the stability of the resulting by-products.

REFERENCE LIST

1. Starek-Świechowicz, B., Budziszewska, B., & Starek, A. (2017). Hexachlorobenzene as a persistent organic pollutant: Toxicity and molecular mechanism of action. *Pharmacological Reports*, *69*(6), 1232–1239. https://doi.org/10.1016/j.pharep.2017.06.013
2. Miyoshi, K., Nishio, T., Yasuhara, A., Morita, M., & Shibamoto, T. (2004). Detoxification of hexachlorobenzene by dechlorination with potassium–sodium alloy. *Chemosphere*, *55*(11), 1439–1446. https://doi.org/10.1016/j.chemosphere.2004.01.025
3. Yin, K., Gao, X., Sun, Y., Zheng, L., & Wang, W. (2013). Thermal degradation of hexachlorobenzene in the presence of calcium oxide at 340–400°C. *Chemosphere*, *93*(8), 1600–1606. https://doi.org/10.1016/j.chemosphere.2013.08.014
4. Nie, M., Li, Y., Dong, Y., Song, Z., Zhao, C., & Chen, S. (2022). Mechanochemical degradation of hexachlorobenzene with a combined additive of SiC and Fe. *Process Safety and Environmental Protection*, *177*, 167–173. https://doi.org/10.1016/j.cherd.2021.10.035
5. Hirano, T., Ishida, T., Oh, K., & Sudo, R. (2007). Biodegradation of chlordane and hexachlorobenzenes in river sediment. *Chemosphere*, *67*(3), 428–434. https://doi.org/10.1016/j.chemosphere.2006.09.087
6. Barra, G., Guadagno, L., Raimondo, M., Santonicola, M. G., Toto, E., & Ciprioti, S. V. (2023). A Comprehensive review on the thermal stability assessment of polymers and composites for aeronautics and space applications. *Polymers*, *15*(18), 3786. https://doi.org/10.3390/polym15183786
7. Guo, S., Feng, D., Li, Y., Liu, L., & Tang, J. (2024). Innovations in chemical degradation technologies for the removal of micro/nano-plastics in water: A comprehensive review. *Ecotoxicology and Environmental Safety*, *271*, 115979. https://doi.org/10.1016/j.ecoenv.2024.115979
8. He, Y., Deng, X., Jiang, L., Hao, L., Shi, Y., Lyu, M., Zhang, L., & Wang, S. (2024). Current advances, challenges and strategies for enhancing the biodegradation of plastic waste. *Science of the Total Environment*, *906*, 167850. https://doi.org/10.1016/j.scitotenv.2023.167850
9. Devendrapandi, G., Liu, X., Balu, R., Ayyamperumal, R., Arasu, M. V., Lavanya, M., Reddy, V. R. M., Kim, W. K., & Karthika, P. (2024). Innovative remediation strategies for persistent organic pollutants in soil and water: A comprehensive review. *Environmental Research*, 118404. https://doi.org/10.1016/j.envres.2024.118404
10. Noor, S., Ashar, A., Taj, M. B., & Bhutta, Z. A. (2022). Advanced oxidation processes for remediation of persistent organic pollutants. In *CRC Press eBooks* (pp. 203–212). https://doi.org/10.1201/9781003165958-17
11. Boulkhessaim, S., Gacem, A., Khan, S. H., Amari, A., Yadav, V. K., Harharah, H. N., Elkhaleefa, A. M., Yadav, K. K., Rather, S., Ahn, H., & Jeon, B. (2022). Emerging trends in the remediation of persistent organic pollutants using nanomaterials and related processes: a review. *Nanomaterials*, *12*(13), 2148. https://doi.org/10.3390/nano12132148
12. Nguyen, V., Smith, S. M., Wantala, K., & Kajitvichyanukul, P. (2020). Photocatalytic remediation of persistent organic pollutants (POPs): A review. *Arabian Journal of Chemistry*, *13*(11), 8309–8337. https://doi.org/10.1016/j.arabjc.2020.04.028
13. Venny, N., Gan, S., & Ng, H. K. (2012). Current status and prospects of Fenton oxidation for the decontamination of persistent organic pollutants (POPs) in soils. *Chemical Engineering Journal*, *213*, 295–317. https://doi.org/10.1016/j.cej.2012.10.005
14. Shrestha, R. A., Pham, T. D., & Sillanpää, M. (2009). Effect of ultrasound on removal of persistent organic pollutants (POPs) from different types of soils. *Journal of Hazardous Materials*, *170*(2–3), 871–875. https://doi.org/10.1016/j.jhazmat.2009.05.048
15. Karimov, S., Abdullayev, E., Gurbanov, M., & Gasimzada, L. (2024). The kinetic properties of gamma - radiolysis of HCB in selected organic solvents. *Scientific News*, *24*(2), 24–29. https://doi.org/10.54758/16801245-2024-24-2-24
16. Karimov, S., Abdullayev, E., Millet, M., & Gurbanov, M. (2024). Radiolytic degradation of 1,2,4-trichlorobenzene (TCB) in some organic solvents by gamma rays: The kinetic properties of complete dechlorination of TCB and its pathway. *Heliyon*, *10*(10), e31547. https://doi.org/10.1016/j.heliyon.2024.e31547

17. Albarrán, G., & Mendoza, E. (2020). Radiolysis induced degradation of 1,3-dichlorobenzene and 4-chlorophenol in aqueous solution. *Radiation Physics and Chemistry*, 109318. https://doi.org/10.1016/j.radphyschem.2020.109318
18. З.И. Искендерова, М.А. Курбанов, Радиационно-химическая деградация 1,2,4-трихлорбензола в водной среде, *Химическая безопасность*, 2 (2) (2018), pp. 112-118, 10.25514/CHS.2018.2.14108
19. Venturi, M., Breccia, A., Busi, F., & Mulazzani, Q. (1976). Gamma and pulse radiolysis of methanolic solutions of triphenylphosphine. *International Journal for Radiation Physics and Chemistry*, *8*(6), 673–677. https://doi.org/10.1016/0020-7055(76)90039-5
20. Barker, R. (1963). Gamma-radiolysis of liquid acetone. *Transactions of the Faraday Society*, *59*, 375. https://doi.org/10.1039/tf9635900375

JOURNAL OF BAKU ENGINEERING UNIVERSITY-ADVANCES IN CHEMISTRY AND CHEMICAL ENGINEERING
2024. Volume 8, Number 1 ***Pages 23-28***

UOT: 678.049:53
https://doi.org/10.30546/2521-6317.2024.404

HEAT- AND FIRE-RESISTANT COMPOSITION BASED ON N, N'-(4,4'- DIPHENYLMETHANE) BISIMIDOMALEIN-1,2,3,4-TETRACHLOROCYCLOHEXA-1,3-DIENE-5,6-DICARBOXYLIC ACID AND EPOXY RESIN ED-20

Aygun ALIKHANOVA[1*], Shahana GULIYEVA[2], Bakhtiyar MAMMADOV[1]

[1]Institute of Polymer Materials of Ministry of Science and Education of the Republic of Azerbaijan,

Sumgait, Azerbaijan

[2]Azerbaijan Medical University,

Baku, Azerbaijan

*E-mail**: aygun81@mail.ru

ARTICLE INFO

Article history:

Received:2024-09-20

Received in revised form:2024-10-11

Accepted:2024-10-18

Available online

Key words:

fire resistance;

heat-resistant polyimides;

composite materials;

adhesive composites;

epoxy resin;

modification

JEL CODES: O33

ABSTRACT

A new adhesive composition based on epoxy resin ED-20 and N, N′-(4,4′-diphenylmethane) bismaleimide-1,2,3,4-tetrachlorocyclohexa-1,3-diene-5,6-dicarboxylic acid was obtained. Its properties have been studied and it has been found that it possesses high physical and mechanical characteristics. It operates effectively in a temperature range from -80 to +96°C without forming cracks, making it suitable as a heat-resistant adhesive for bonding photo-, optical, and semiconductor components in devices with photosensitive elements. Additionally, the obtained adhesive composition based on N, N′-(4,4′-diphenylmethane) bismaleimide-1,2,3,4-tetrachlorocyclohexa-1,3-diene-5,6-dicarboxylic acid and epoxy resin ED-20 is used for sealing and pouring in the manufacture of the above-mentioned devices and appliances.

1. Introduction

The need to create heat-resistant and non-combustible polymers is associated with the development of electronics, electrical engineering, aerospace and other industries [1]. The development of modern microelectronics would be unthinkable without the creation of special polymers that possess fire resistance, heat resistance, as well as high elasticity and solubility in organic solvents. However, at present, all commercial polyimides have significant drawbacks:

a) The traditional method of obtaining polyimides is primarily based on a two-stage process, with the second stage of this process typically implemented through thermal cyclization [2, 3];

b) insolubility of polyimides in traditional organic solvents, which complicates their processing into a product

In order to eliminate such individual disadvantages of polyimide polymers, attempts have been made to modify their structures. Special attention was paid to the development of halogen-containing polyimides, whose composition and specific structure of the elementary units create the possibility of partially, and sometimes completely, eliminating the aforementioned drawbacks.

Few works are devoted to the synthesis and development of chlorinated polyimides. However, it is known [4–6] that halogen-containing polyimides with a specified spatial structure are perspective compounds for obtaining monomers containing imide rings, as well as various functional groups. Such monomers are capable of undergoing polycondensation reactions with other bifunctional monomers, leading to the formation of flame-resistant and heat-resistant polymeric materials that can withstand abrupt changes in temperature [7-9].

Based on the above, we have developed a method of obtaining chlorinated cyclic bisimidodienes suitable for their application as fire- and heat-resistant adhesives for bonding of separate elements of photographic, optical and semiconductor devices. The selection and application of such adhesives and sealants for cooled photovoltaic elements in photo materials is a rather complex task [10].

At present in photodetectors for bonding of optical elements silicon-organic polyurethane composites UK-1 and UK-2 are used. The operating temperature range for compound UK-2 is from +80 to -80°C, while for UK-1 it is from +80 to -60°C [11]. However, for bonding a germanium carrier substrate with an optical plate made of Cd×Hg Te (CMT), the adhesive, in addition to being effective at low temperatures, must have high adhesion strength and chemical resistance to a range of aggressive environments (acids, bases, various solvents), as well as mechanical strength against detachment.

The aim of the work was to obtain an adhesive composition that meets the properties mentioned above. The present article is devoted to the synthesis of N, N'-(4,4'-diphenylmethane) bismaleimide-1,2,3,4-tetrachlorocyclohexa-1,3-diene-5,6-dicarboxylic acid prepared according to the scheme:

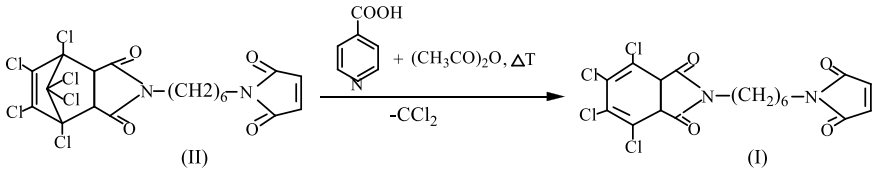

This reaction was carried out by heating bisimide (II) in dimethylformamide (DMF) medium in the presence of the acceptor isonicotinic acid and acetic anhydride. The obtained imidodiene is used as a modifier of ED-20 epoxy resin to produce an adhesive composition.

2. Experimental part

N,N'-(4,4'-diphenylmethane) bisimidamalein-1,2,3,4-tetrachlorocyclohexa-1,3-diene-5,6-dicarboxylic acid (I) was synthesized as follows:

0.01 mol of N,N'-(4,4'-diphenylmethane) bisimidamalein-1,4,5,6,7,7,7-hexachlorobicyclo-[2.2.1.1]-hept-5-ene-2,3-dicarboxylic acid was dissolved in 50 ml of DMF. The mixture was stirred until a homogeneous mass was formed. Then,10 ml of acceptor (a mixture of isonicotinic acid and acetic anhydride - 1:1 molar ratio) was added to the mixture. The reaction proceeded exothermically with temperature increase up to 45-50°C. After the temperature decreased to 20°C, the mixture was heated for an additional 2 hours at 120°C. Then, the mixture was poured into ice-cold water while stirring. The resulting precipitate was filtered through a Schott filter, recrystallized from isopropyl alcohol, and dried at 60°C. The yield of the product was 75%. T_m 135°C, R_f 0.58. In the UV spectrum, a peak at 285 nm was observed, characteristic of a diene system. The obtained bisimide (I) is a white powdery product. M=548. Formula: $C_{25}H_{14}Cl_4N_2O_4$. Calculated %: C 54.74, H 2.55, Cl 25.91, N 5.10. Found %: C 54.17, H 2.41, Cl 25.01, N 4.98.

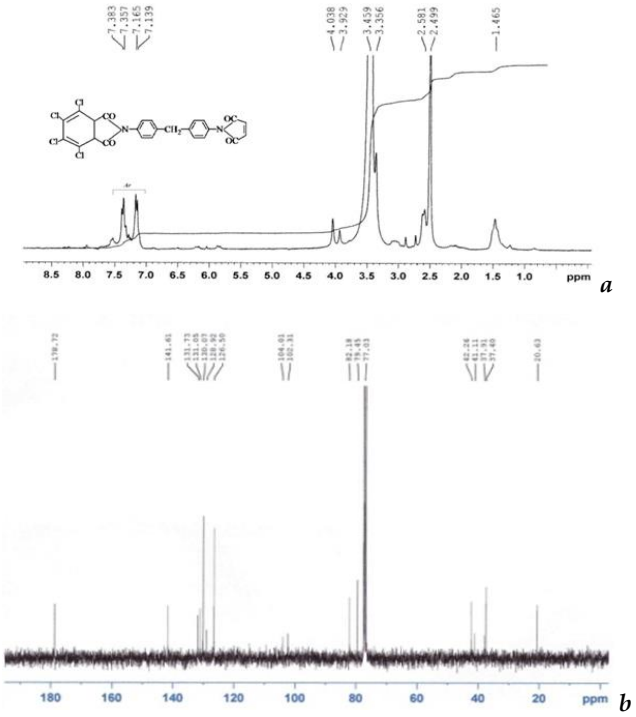

Figure 1. NMR ^1H ***(a)*** and ^{13}C ***(b)*** spectra of N,N'-(4,4'-diphenylmethane) bismaleimide-1,2,3,4-tetrachlorocyclohexa-1,3-diene-5,6-dicarboxylic acid

The structure of N,N'-(4,4'-diphenylmethane) bisimide of 1,2,3,4-tetrachlorocyclohexa-1,3-diene-5,6-dicarboxylic acid (1) has been confirmed by ^{1}H and ^{13}C NMR and IR spectra [12, 13]. The signals of the protons were identified as follows from the 1H NMR (BRUKER-Fourier 300.18 MHz, acetone-d6, δ): 1.46 (triplet, CH), 2.58, 2.49 (CH_2), 3.45, 3.56 (singlet, 4H, CH), 3.92 (singlet, CH_2), 3.92 (singlet, 6H), 4.03 (singlet, 2H, CH_2), 7.38, 7.35, 7.16-7.13 (6H, CH, Ar). The 13C NMR signals are: 20.63 (CH), 37.40 (CH_2), 79.45 (Cl-C-C), 104.01 (Cl-C-Cl), 126.50, 128.92, 131.05, 131.73, 141.61 (C, Ar), 130.07 (C-Cl), 178.72 (C=O).

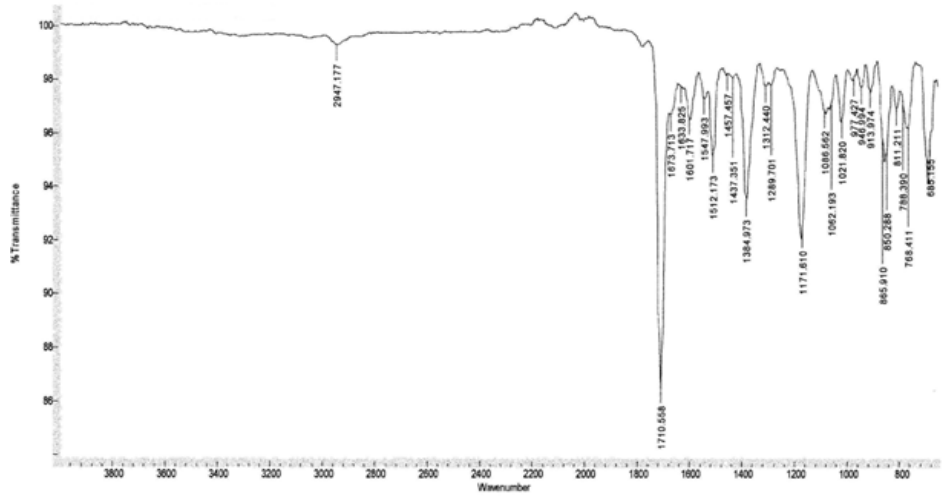

Figure 2. IQ spectrum of N, N'-(4,4'-diphenylmethane) bismaleimide-1,2,3,4-tetrachlorocyclohexa-1,3-diene-5,6-dicarboxylic acid

In the IR spectrum, characteristic absorption bands were observed for the C=C bond at 1601 cm^{-1}, for the imide rings at 1710 cm^{-1}, and for the C-Cl bond at 685 cm^{-1}.

The adhesive epoxy composition was prepared at the following ratios of components; (mass fraction): ED-20-(80 and 90); modifier (I) - (10 and 20) hardener PEPA -8.

For the preparation of the composition, industrial resin ED-20 (GOST 10587-63) was used, which contains 18% epoxy groups.

Modification of ED-20 was carried out as follows: to 80 or 90 mass fraction of ED-20 was added 20-10 mass fraction of modifier (I) and stirred for 30-35 minutes at 90-95° C to obtain a homogeneous mass, then the mixture was cooled to 20° C and 8 mass fraction of polyethylene polyamine hardener (PEPA) was added as a hardener under stirring. The mixture was then vacuumed to remove air bubbles and applied to the photosensitive elements and the CMT (CdxHg Te) substrate or poured into a mold for curing and bonding for 48 hours at room temperature To determine the physical and mechanical parameters, the samples were made in the form of spatulas with the size of 80×7×5 mm and thickness of 2 mm. The performance of the samples was evaluated based on the results of at least three parallel determinations.

3. Results and discussion

The obtained adhesive composition was tested for bonding optical plates of CMT with a germanium carrier substrate.

The composition of the adhesive composition and test results are given in the table 1.

Table 1. Composition and parameters of the adhesive composition

Component names and parameters	ED-20 without modifier	Composites	
		I	Known
Amount of ED-20, parts	100	90	90
Amount of modifier (I), parts	–	10	10
Amount of curing agent PEPA, parts	8	8	8
Vicat softening point, °C	138	195	180
Brinell hardness, MPa	5.48	13.7	14
Resistance to uniform direct pull, MPa			
at 20°C	–	1120	–
at 50°C	–		
Impact strength, MPa	–	24.5	–
Adhesive strength, MPa	82	200	210
Water absorption, (48 h.) %	0.69	Absent	absent
Crack formation after 72 temperature gradient cycles from -80 to +96°C	cracks	Does not form cracks	can't withstand subzero
Degree of curing, %	96	98	temperatures
Curing time, h.	24	24	98
Chemical resistance in 50% H_2SO_4 solution at 20-60°C (after 24 h. exposure)	–	13.5	24 –
Chemical resistance in 50% NaOH solution at 20-60°C (after 24 h. exposure)	–	13.2	–

The study of resistance to temperature change of the adhesive composition showed that the adhesive compound is workable at the temperature of liquid nitrogen and at repeated temperature changes from minus 80 to plus 120 °C during repeated thermocycling.

From the results of the study, it can be seen that the obtained adhesive composition has high tensile strength (9.02-9.72 MPa) and adhesion strength (1.47-1.86 MPa), at temperatures ranging from -80 to +96 °C. The quality of adhesion after 72 hours of thermocycling does not change. High frost resistance of the adhesive composition is due to the presence of double bonds in the polymer chain.

In addition, it is shown that bonded samples of CMT optical plates with germanium substrate are resistant to aggressive environments and moisture for 48 hours.

Thus it has been established that the obtained adhesive composition based on ED-20 and compound (I) is workable in the temperature range from minus 80 to plus 96 °C and can be used for gluing optical parts to photosensitive elements, as well as for sealing and casting semiconductor devices.

REFERENCE LIST

1. Bessonov, M.I., Koton, M.M., Kudryavchev, V.R., Layus, L.A. (1983). *Poliimidi – klass termostoykix polimerov*. M.: Ximiya.
2. Vinoqradova, S.V., Vasnev, V.A. (2000). *Polikondenchionnie prochessi i polimeri.* M.: Nauka.
3. Salakhov, M.S., Umaeva, V.S., Alikhanova, A.İ. (2007). New cryogenic epoxy adhesive composites for photodetectors, *International polymer science and technology*, 34(5),1-3
4. Batirov, I. I., Korshak, V. V., Rusanov, A.L. (1978). Sintez i issledovanie poliimidov na osnove 1,7-difenil-2,6-di-(aminofenil)benzo-[1,2-d; 4,5-d']-diimidazolov, *Visokomolekulyarnoe soidineniya* A., 20(5), 1036.
5. Kolyamshin, O. A., Danilov, V.A., Kolchov, N.I. (2012). Osobennosti sinteza i svoystva nekotorix maleinimidov, *Butlerovskie soobsheniya*, 32(12), 26-30.
6. Salakhov, M.S., Umaeva, V.S., Alikhanova, A.İ. (2008). Oqnestokie epoksidnie kompozichii, *Plasticheskie massi*, 7, 11-13.
7. Mostovoy, A.S., Nurtazina, A.S., Kadykova, Y.A., Bekeshev, A.Z. (2019). Highly Efficient Plasticizers-Antipirenes for Epoxy, *Polymers Inorganic Materials: Applied Research,* 10, 1135–1139.
8. Mostovoy, A.S., Plakunova, E.V., Panova, L.G. (2014). Development of fireproof epoxy composites and their-structure and properties, *Perspektivnie Materiali,* 1, 37–43.
9. Shirshova, E.S., Tatarintseva, E.A., Plakunova, E.V., Panova, L.G. (2006). The effect of modifiers on the properties of epoxy compositions, *Plasticheskie massi*, 12, 34–36.
10. Ekivina, N.I., Lyuxobobenko, Q.A. (1982). Ximicheski stoykiy krioqenniy kley dlya priyemnikov luchistoy enerqii XSK, *Voprosi oboronnoy texniki*, 11(84), 19.
11. Antipova, M.A. (1973). Priminenie poliuretanovix kompaundov UK-1 и UK-2 v texnoloqii izqotovleniya priyemnikov IK-izlucheniya na osnove fosfora, *Voprosi oboronnoy texniki*, 11(25), 37.
12. Trujillo-Ferrara, J., Santillan, R., Beltrán, H.I., Farfán, N., Höpfl, H. (1999). ^{1}H and ^{13}C NMR spectra for a series of arylmaleamic acids, arylmaleimides, arylsuccinamic acids and arylsuccinimides, *Magnetic Resonance in Chemistry*, 37(9), 682-686.
13. Prec, E., Byulman, F., Affolter, K. (2006). *Opredelenie stroeniya orqaniceskix soedineniy*. M: Mir.

JOURNAL OF BAKU ENGINEERING UNIVERSITY-ADVANCES IN CHEMISTRY AND CHEMICAL ENGINEERING
2024. Volume 8, Number 1 ***Pages 29-34***

UOT:504, 54, 556

https://doi.org/10.30546/2521-6317.2024.503

ECO-CHEMICAL STUDY OF FRESHWATER SOURCES CONTAMINATED WITH MINING WASTEWATER

[1]Aiten SAMADOVA, [1]Sevinj HAJIYEVA, [2]Islam MUSTAFAYEV

[1]Baku State Universityi,

[2]Radiation Poblems Institute

aytan.samad@gmail.com

ARTICLE INFO

Article history:

Received:2024-06-13

Received in revised form:2024-07-04

Accepted:2024-10-18

Available online

Key words:

iron, manganese, hardness, ecology, mining industry

ABSTRACT

The study of environmental objects is of special importance in order to eliminate the increasing ecological imbalance in recent times. In this regard, it is important to control the eco-chemical state of freshwater resources for living creatures. For this purpose, water samples have been taken from the territory of Okchuchay to Azerbaijan and conducted their eco-chemical study. As an example, an eco-chemical study was conducted on the samples taken from the beginning, middle and lower streams, taking into account the degree of pollution and the self-regulating property of the river. Their physico-chemical parameters have been determined. At the same time, some cations and anions were investigated. In particular, the amount of iron and manganese ions, which are important in the integrity of the ecosystem, were compared with the permissible concentration limits. The effect of chemical pollutants on the ecosystem, on living organisms, on the unity of the biocenosis has been studied.

Entrance

When conducting an eco-chemical assessment in the environment, the hydrosphere should be considered first. Because pollutants can spread rapidly in the underlying hydrosphere compared to soil. A fresh water body was selected for the purpose of investigating the effect of the hydrosphere on the organisms entering the ecosystem. At this time, we took samples from three points of Okchuchay that passes through Azerbaijan, which was affected by the waste water of the mining industry. They were taken from the upper, middle and lower parts of the river, respectively (Burunlu, Shayiflı, Jahangirbeyli areas).

Experimental Part

First, water samples were taken, and their physical parameters were determined. The hydrogen indicator is determined by pH-meters for pH, oxygen for solved oxygen, conduitometers for electrical engineering, sulphate, ammonium, nitrites and nitrates ions, and metals by optical emissions spectrometer and atomic absorbsion spectrometer. Sample studies have been conducted three times for accuracy (table 1, 2, 3)

Table 1. Analysis of water samples taken from the river at 01.03.2023

№	Name of component	Unit	Amount of component			Maximum Permissible Concentration
			Okchuchay-Zengilan village			
			Jahangirbayli village	Shayifli village	Burunlu village	
1	pH	–	8.0	7.6	7.8	6.5-8.5
2	Dissolved oxygen	mqO_2/l %	6.5 67.0	4.8 58.0	5.6 61.0	≥4.0
3	Electrical transmission	μSm/sm	1386	1264	1268	–
4	Transparency	Sm	14	10	17	>30
5	Hardness	mg-ekv/l	**10.39**	**10.6**	**10.48**	7.0
6	Calcium ion, Ca^{2+}	mg/l	139.8	148.7	147.0	–
7	Magnesium ion, Mg^{2+}	mg/l	41.5	38.7	38.2	–
8	Chloride ion, Cl^-	mg/l	23.7	19.99	20.66	350
9	Hydrocarbonate ions, HCO_3^-	mg/l	256.0	241.0	259.0	-
10	Carbonate ions, CO_3^{2-}	mg/l	0	0	0	-
11	Sulphate ion, SO_4^{2-}	mg/l	321.6	372.9	348.82	500
12	Ammonium ion, NH_4^+	mg/l	**1.02**	**1.49**	**1.58**	0.5
13	Nitrogen ion, NO_2^-	mg/l	0	0.43	0.44	3.3
14	Nitrate ion, NO_3^-	mg/l	5.2	4.4	3.9	45.0
15	Zink, Zn	mkg/l	135.4	137	122	1000
16	Iron, Fe	mkg/l	**709**	**875**	**900**	300
17	Cobalt, Co	mkg/l	2.06	1.9	3.25	100
18	Lead, Pb	mkg/l	1.5	<LOD	3.76	30
19	Nickel, Ni	mkg/l	0.414	0.755	0.745	100
20	Molybdenum, Mo	mkg/l	228	234	241	250
21	Manganese, Mn	mkg/l	**398**	**427**	**439**	100
22	Copper, Cu	mkg/l	64.0	71.3	70.6	1000

As can be seen from Table 1, according to the analyzes carried out on water samples, in the sections passing through the villages of Jahangirbeyli, Shayifli and Burunlu of Okchuchay, the concentration of hardness - 1.5 times, ammonium ion - 2.0 times in the village of Jahangirbeyli, 3.0 times in the village of Shayifli, 3.2 times in the village of Burunlu, iron - 2.4

times in the village of Jahangirbeyli. , 2.9 times in Shayifli village, 3 times in Burunlu village, manganese – 4.0 times in Jahangirbeyli village, 4.3 times in Shayifli village, 4.4 times in Burunlu village.

The parameter of water, such as hardness, is influenced by the presence of magnesium and calcium ions. [10] According to literature, magnesium affects a number of plants. It is also part of the chlorophyline, which is made up of nuclides, phosphates, and pectins. Magnesium is inorganic in plant fibers. In addition to activating plant-based enzyme systems, magnesium affects the cell's metabolism. It participates in the respiratory processes of living things that enter the ecosystem. In biochemistry plants, the battery of military acid accelerates (the magnesium ion reacts with unsuspecting dienol groups of military acid, weakening or stopping oxidation processes; its effects are greatly strengthened in acidic environments). Water plants affect oxidation-reducing reactions [10].

An excess of magnesium is accompanied by an excess of sodium [8]. [9] literature states that magnesium sulfate (MgSO4) is a common contaminant in mine waters and is usually obtained from accelerated oxidation of sulfides and subsequent dissolution of magnesium minerals in exposed ore, waste rock, or tailings.

Manganese blocks phosphorus and calcium ions. Manganese is antagonistic elements with elements like Fe and Zn. That is, the amount of one should be less compared to the amount of the other elements. The excess of these two elements is related to its anthropogenic factors as well [11].

Table 2. Analysis of water samples taken from the river at 09.03.2023

№	Name of component	Unit	Amount of component			Maximum Permissible Concentration
			Okchuchay-Zengilan village			
			Jahangirbayli village	Shayifli village	Burunlu village	
1	pH	–	7.8	7.5	7.5	6.5-8.5
2	Dissolved oxygen	mq O_2/l %	6.4 71.0	4.0 41.0	4.9 54.0	≥4.0
3	Electrical transmission	μSm/sm	1220	1212	1210	–
4	Transparency	Sm	12	11	15	30
5	Hardness	mg-ekv/l	**10.43**	**10.8**	**11.2**	7.0
6	Calcium ion, Ca2+	mg/l	146.3	151.5	157.1	–
7	Magnesium ion, Mg^{2+}	mg/l	38.0	39.4	40.9	–
8	Chloride ion, Cl^-	mg/l	21.0	19.4	20.7	350
9	Hydrocarbonate ions, HCO_3^-	mg/l	254.0	250.0	263.0	-
10	Carbonate ions, CO_3^{2-}	mg/l	0	0	0	-
11	Sulphate ion, SO_4^{2-}	mg/l	350.3	381.2	411.0	500
12	Ammonium ion, NH_4^+	mg/l	**0.93**	**1.60**	**1.62**	0.5
13	Nitrogen ion, NO_2^-	mg/l	0.1	0.34	0.29	3.3
14	Nitrate ion, NO_3^-	mg/l	6.1	4.9	4.2	45.0
15	Zink, Zn	mkg/l	87.3	194	270	1000
16	Iron, Fe	mkg/l	**459**	**1040**	**1220**	300
17	Cobalt, Co	mkg/l	3.41	3.82	6.2	100
18	Lead, Pb	mkg/l	1.1	2.28	3.1	30
19	Nickel, Ni	mkg/l	<LOD	<LOD	2.27	100
20	Moibden, Mo	mkg/l	164	170	180	250
21	Manganese, Mn	mkg/l	**110**	**386**	**665**	100
22	Copper, Cu	mkg/l	46.5	57.1	93.5	1000

As it can be seen from Table 2, according to the analyzes carried out on water samples, hardness - 1.6 times in Burunlu village, 1.5 times in Shayifli and Jahangirbeyli villages, ammonium ion - 1.9 times in Jahangirbeyli village, 3.2 times in Shayifli village and Burunlu villages, iron - 1.5 times in Jahangirbeyli village, 3.5 times in Shayifli village, 4.1 times in Burunlu village, manganese – 1.1 times in Jahangirbeyli village, 3.9 times in Shayifli village, 6.7 times in Burunlu village.

The same parameters were re-analyzed at the end of March. The results were shown in table 3.

Table 3. Analysis of water samples taken from the river at 28.03.2023

№	Name of component	Unit	Amount of component			Maximum Permissible Concentration
			Okchuchay-Zengilan village			
			Jahangirbayli village	Shayifli village	Burunlu village	
1	pH	–	7.8	7.7	7.8	6.5-8.5
2	Dissolved oxygen	mqO_2/l %	6.9 75.0	5.5 59.0	5.5 60.0	≥4.0
3	Electrical transmission	µSm/sm	1228	1202	1207	–
4	Transparency	Sm	23	20	22	>30
5	Hardness	mg-ekv/l	**10.1**	**9.94**	**9.97**	7.0
6	Calcium ion, Ca^{2+}	mg/l	141.7	139.4	139.9	-
7	Magnesium ion, Mg^{2+}	mg/l	36.8	36.3	36.4	-
8	Chloride ion, Cl^-	mg/l	19.0	18.9	18.9	350
9	Hydrocarbonate ions, HCO_3^-	mg/l	299.0	267.0	261.0	-
10	Carbonate ions, CO_3^{2-}	mg/l	6.4	0	0	-
11	Sulphate ion, SO_4^{2-}	mg/l	249.0	247.0	250.4	500
12	Ammonium ion, NH_4^+	mg/l	**0.7**	**1.6**	**2.0**	0.5
13	Nitrogen ion, NO_2^-	mg/l	0.32	0.45	0.53	3.3
14	Nitrate ion, NO_3^-	mg/l	7.1	4.9	3.72	45.0
15	Zink, Zn	mkg/l	61.6	181	166	1000
16	Iron, Fe	mkg/l	**420**	**1830**	**2200**	300
17	Cobalt, Co	mkg/l	2.53	7.29	6.79	100
18	Lead, Pb	mkg/l	2.1	7.4	9.7	30
19	Nickel, Ni	mkg/l	1.47	0.147	5.22	100
20	Moibden, Mo	mkg/l	180.0	233	248	250
21	Manganese, Mn	mkg/l	**111.0**	**625**	**669**	100
22	Copper, Cu	mkg/l	36.5	143.0	147.0	1000

As it can be seen from Table 3, according to the analyzes carried out on water samples, iodine - 1.4 times in Jahangirbeyli, Shayifli and Burunlu villages, ammonium ion - 1.4 times in Jahangirbeyli village, 3.2 times in Shayifli village, 4 times in Burunlu village, iron - 1.4 times in Jahangirbeyli village, Shayifli village 6.1 times, 7.3 times in Burunlu village, manganese - 1.1 times in Jahangirbeyli village, 6.3 times in Shayifli village, 6.7 times in Burunlu village.

It should be noted that the Permissible Hardness Limits for Surface Waters are from the document "Rules for the Protection of Surface Waters from Wastewater Pollution" approved by the State Ecology and Nature Use Control Committee of the Republic of Azerbaijan by Order No. 01 of January 4, 1994. taken.

Magnesium has a chronic toxic effect on five species of ecosystems [9]. The excess amount of magnesium affects in a mutagenic way. This is due to its cumulating properties. It is associated with a sudden deterioration in the liver, kidneys and gastrointestinal tract. In

children's organism, magnesium causes excessive neurotoxicity and intellectual ability in adults.

Manganese is considered a major pollutant. Its presence in the environment creates serious environmental problems. Its excess in the hydro environment is related only to the anthropogenic factors. Manganese can bioaccumulate in the environment, so it can have ecotoxic effects. If it exposed to a high dose for a long time, the creatures of the ecosystem can be destroyed [11].

The biogeochemical and ecological status of iron in freshwater ecosystems has been extensively investigated, as various anthropogenic influences have strongly modified lentic and lotic ecosystems over recent decades. In freshwater ecosystems, iron is considered an essential element as it affects numerous ecosystem functions and organisms both directly and indirectly.

Conclusion

According to the information above, it can be concluded that pollutant ions such as sodium, ammonium, iron, manganese, which are very important in the eco-chemical assessment of the environment, were many times higher than the norm in March. These are parameters that pose a serious threat to the existence of living things in those water ecosystems.

REFERENCES

1. Abbasov V.M., Aliyeva R.A., Salimova N.A. and others. *Introduction to environmental chemistry*. Baku: Maarif, 2002
2. Hajiyeva S.R., Mustafayev İ.İ., Abdullayeva R.Z. *Study of ecotoxıcants ın the dıscharge of mınıng wastewater ın Okchuchay,* Azerbaijan Journal of Chemical News. Vol 6, №1, p.4-8, 2024
3. Samadova A.A. *Eco-chemıcal research of pollutants ın envıronmental objects*, Proceedings Of Azerbaijan High Technical Educational Institutions. Vol 2 İSSUE 148, p.502-508, 2024
4. Samadova A. Ümummilli Lider Heydər Əliyevin anadan olmasının 100-cü ildönümünə həsr olunmuş doktorant, magsitr və gənc tədqiqatçıların "Kimya və Kimya texnologiyası" II Respublika Elmi Konfransı, "*Study of methods of decontamination of waste water of mining industry", 04-05 may, 2023, pp.228-229*
5. Воронова Г.А., Юрмазова Т.А. *Химические элементы в биосфере.* Томск: Изд-во Томского политехнического университета, 2010.
6. Мирошниченко Ю.Ю., Юрмазова Т.А. *Химические загрязнения в биосфере и их определение*. Томск: Изд-во Национального исследовательского Томского политехнического университета, 2010.
7. Исидоров В.А. *Экологическая химия* Химиздат. С.П., 2001
8. Angela Potasznik, Sławomir Szymczyk, Potasznik A., Szymczyk S. 2015. *Magnesium and calcium concentrations in the surface water and bottom deposits of a river-lake system*. Journal of Elementology, 20(3): 677-692. DOI: 10.5601/jelem.2015.20.1.788
9. Rıck A. Van Dam, Alıcıa C. Hogan, Cherıe D. Mcc Ullough, Melanıe A. Houston, Chrıs L.Humphrey, and Andrew J. Harford. *Aquatıc Toxıcıty Of Magnesıum Sulfate, And The Influence Of Calcıum,In Very Low Ionıc Concentratıon Water* Environmental Toxicology and Chemistry, Vol. 29, No. 2, pp. 410–421, 2010
10. Власюк П.А. *Биологические элементы в жизнедеятельности растений.* Издательство «Наукова Думка», Киев, 1969
11. Vera A. Matveeva, Alexey V. Alekseenko, Daniel Karthe and Alexander V. Puzanov. *Manganese Pollution in Mining-Influenced Rivers and Lakes*: *Current State and Forecast under Climate Change in the Russian Arctic*/Water, 14, 1091, 2022

This work was supported by the Azerbaijan Science Foundation-

Grant №AEF-MQM-QA-1-2021-4(41)-8/07/4-M-07

JOURNAL OF BAKU ENGINEERING UNIVERSITY-ADVANCES IN CHEMISTRY AND CHEMICAL ENGINEERING
2024. Volume 8, Number 1 ***Pages 35-43***

UOT:661
https://doi.org/10.30546/2521-6317.2024.105

THE PHYSICAL-COLLOIDAL PROPERTIES OF COMPLEXES FORMED COMPLEXES FORMED BY OCTADECANOIC ACID WITH MONOETHANOLAMINE, DIETHANOLAMINE AND TRIETHANOLAMINE

SHAHVERDIYEVA Asya [*]; Nargiz SALAMOVA

Academician Y.H. Mammadaliyev Institute of Petrochemical Processes of the

Ministry of Science and Education of the Republic of Azerbaijan,

Baku, Azerbaijan

[*]Corresponding author.

E-mail: sahverdiyeva.asya@mail.ru (Shahverdiyeva Asya).

ARTICLE INFO

Article history:
Received:2024-10-8
Received in revised form:2024-10-05
Accepted:2024-10-08
Available online

Keywords:
octadecanoic acid, surface activity, petro-collecting

ABSTRACT

The article presents the results of the study of the surface activity substances, physical-colloidal parameters, and elemental composition calculated using the tensiometer of the complexes formed by the monobasic saturated carboxylic acid octadecanoic acid with monoethanolamine, diethanolamine, triethanolamine with different concentrations. As a result of surface tension measurements, parameters such as critical micelle formation density, surface pressure, minimum surface area per molecule, and micelle formation and adsorption Gibbs free energy were calculated based on electrical conductivity values. These measurements provided important information about the properties of the synthesized materials. Finally, experiments were conducted on three different water samples with different mineral content to investigate the effectiveness of the synthesized surfactants in removing oil spills from the water basin, oil collection and oil dispersing properties.

1. Introduction

Like other water bodies around the world, the Caspian Sea also faces unique challenges, such as the pollution of its water reservoir and the resulting deterioration of its ecological condition.

Currently, the main causes of pollution in the Caspian Sea are accidents that occur during oil extraction from oil fields and the transportation of oil.

The characteristic features of pollution by oil and its products include contamination of environmental components, their dispersion across large water areas, accumulation in sediments at the seabed, and other forms of pollution. Oil spills degrade water quality and negatively impact oxygen levels, disrupting the balanced interaction between the upper water layers and the atmosphere, which leads to a disturbance in the overall ecological regime.

Oil-based films that reflect sunlight prevent the absorption of energy by the water, which is essential for the life activities of marine organisms. The Caspian Sea is home to many species of fish, including 95% of the world's sturgeon population, making the removal of such oil spills particularly crucial for their survival.

After the accident on the crude oil platform in the Gulf of Mexico, urgent safety measures were implemented in the oil fields of the Caspian Sea, one of the largest centers of hydrocarbon resources. Among these measures, addressing the consequences of such incidents holds great importance. During mechanical cleaning of spilled oil, some of it remains on the water surface in the form of slicks. These slicks can only be removed through certain physico-chemical methods, using dispersants and collectors.

Surfactants (SAMs) used to remove thin oil films from the water surface are categorized into oil dispersants and oil collectors [1-10].

2. Materials And Experimental Methods

Octadecanoic acid, with the chemical formula $C_{17}H_{35}COOH$, is a saturated monobasic carboxylic acid that appears as white, crystalline, odorless solid. It is insoluble in water but soluble in ether. Its relative molecular mass is 284.5 g/mol, with a melting point of 69.6°C and a boiling point of 361°C.

Monoethanolamine (MEA) is a strong base with a molar mass of 61.1 g/mol. It is a colorless, transparent substance that can mix with water in any proportion.

Diethanolamine (DEA) is a strong base with a molar mass of 105.2 g/mol. It is a colorless, transparent substance that can mix with water in any proportion.

Triethanolamine (TEA) is a weak base with a molar mass of 149.19 g/mol. It is a colorless, transparent substance with an ammonia-like odor.

Infrared spectra were identified in the wavenumber range of 400-4000 cm^{-1} using a BIO-RAD FTS 3000 MX spectrometer (Germany).

The surface tension values were defined at the air-water interface via a du Nouy tensiometer with a ring method (KSV Sigma 702, Finland). [11].

The petro-collecting and dispersing properties of the synthesized surfactants were performed according to the methodology given in [12].

The petro-collecting properties were characterized by the collecting coefficient (K) (the ratio of the initial surface area of the petroleum film to the surface area of the thickened petroleum spot formed under the influence of the reagent) and the duration effect (τ) of the collected petroleum.

3. Results and Discussion

The reaction between octadecanoic acid and monoethanolamine (MEA) was conducted under laboratory conditions at a 1:1 molar ratio, with intensive stirring at a temperature of 70-75°C over the course of one day.

The reaction scheme is as follows:

$C_{17}H_{35}COOH + NH_2C_2H_4OH \rightarrow [\ C_{17}H_{35}COO^-\ N^+\ H_3\ C_2H_4OH]$

The relative molecular mass of the obtained complex is 345.6 g/mol. Based on the calculation method, the mass fractions of the elements in the quaternary ammonium salt formed from octadecanoic acid and MEA are as follows:

- Carbon (C): 69.5%
- Hydrogen (H): 12.7%
- Oxygen (O): 13.8%
- Nitrogen (N): 4%

These percentages reflect the distribution of each element's mass in the complex.

The reaction between octadecanoic acid and diethanolamine (DEA) was conducted under laboratory conditions at a 1:1 molar ratio, with intensive stirring at a temperature of 70-75°C over the course of one day.

The reaction scheme is as follows:

$C_{17}H_{35}COOH + NH(C_2H_4OH)_2 \rightarrow [\ C_{17}H_{35}COO^-\ N^+\ H_2(C_2H_4OH)_2]$

The relative molecular mass of the obtained complex formed from the reaction between octadecanoic acid and diethanolamine (DEA) is 433.4 g/mol.

Based on the calculation method, the mass fractions of the elements in the quaternary ammonium salt formed from octadecanoic acid and diethanolamine (DEA) are as follows:

- Carbon (C): 67.8%
- Hydrogen (H): 12.1%
- Oxygen (O): 16.5%
- Nitrogen (N): 3.6%

These percentages indicate the distribution of each element's mass in the complex.

The reaction between octadecanoic acid and triethanolamine (TEA) was conducted under laboratory conditions at a 1:1 molar ratio, with intensive stirring at a temperature of 70-75°C over the course of one day.

The reaction scheme can be represented as follows:

$C_{17}H_{35}COOH + N(C_2H_4OH)_3 \rightarrow [\ C_{17}H_{35}COO^-\ N^+\ H(C_2H_4OH)_3]$

The relative molecular mass of the obtained complex formed from the reaction between octadecanoic acid and triethanolamine (TEA) is 433.7 g/mol. Based on the calculation method, the mass fractions of the elements in the quaternary ammonium salt are as follows:

- Carbon (C): 66.4%

- Hydrogen (H): 11.8%

- Oxygen (O): 18.5%

- Nitrogen (N): 3.3%

these percentages indicate the distribution of each element's mass in the complex.

The octadecanoic acid with MEA was identified by IR-spectroscopy (Fig. 1). Spectral results are listed below: Stretching vibrations of N–H and O-H bonds at 3293 cm^{-1}, 2915 və 2848 cm^{-1} stretching vibration of C-H bond in CH_3 and CH_2 groups, stretching vibration of C=O bond at 1639 cm^{-1}, stretching vibrations of N-H bond at 1554 cm^{-1}, 1464, 719 cm^{-1} stretching vibration of C-H bond in CH_3 və CH_2 groups.

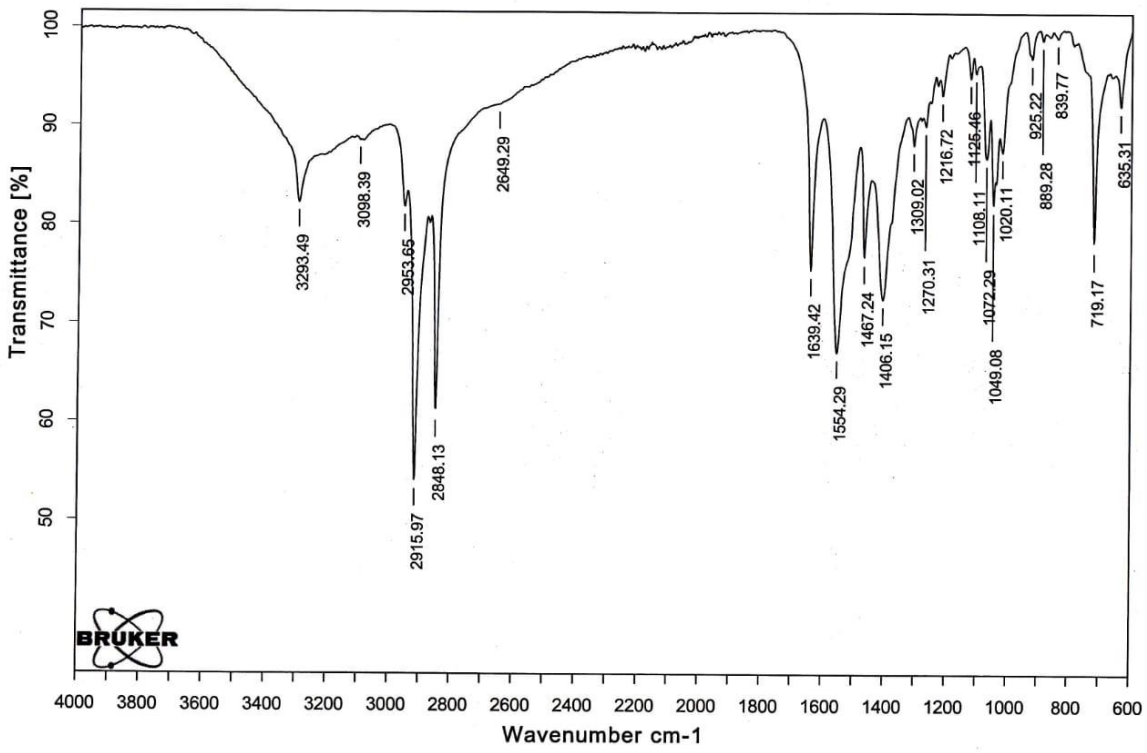

Fig. 1. FTIR spectra of octadecanoic acid with MEA

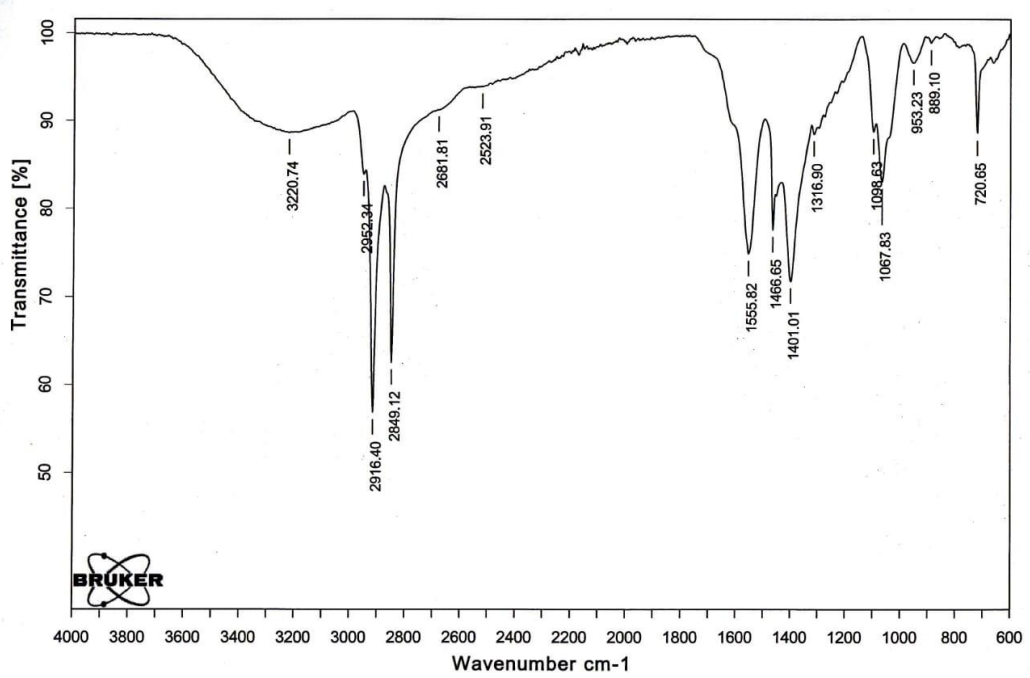

Fig. 2. FTIR spectra of octadecanoic acid with DEA

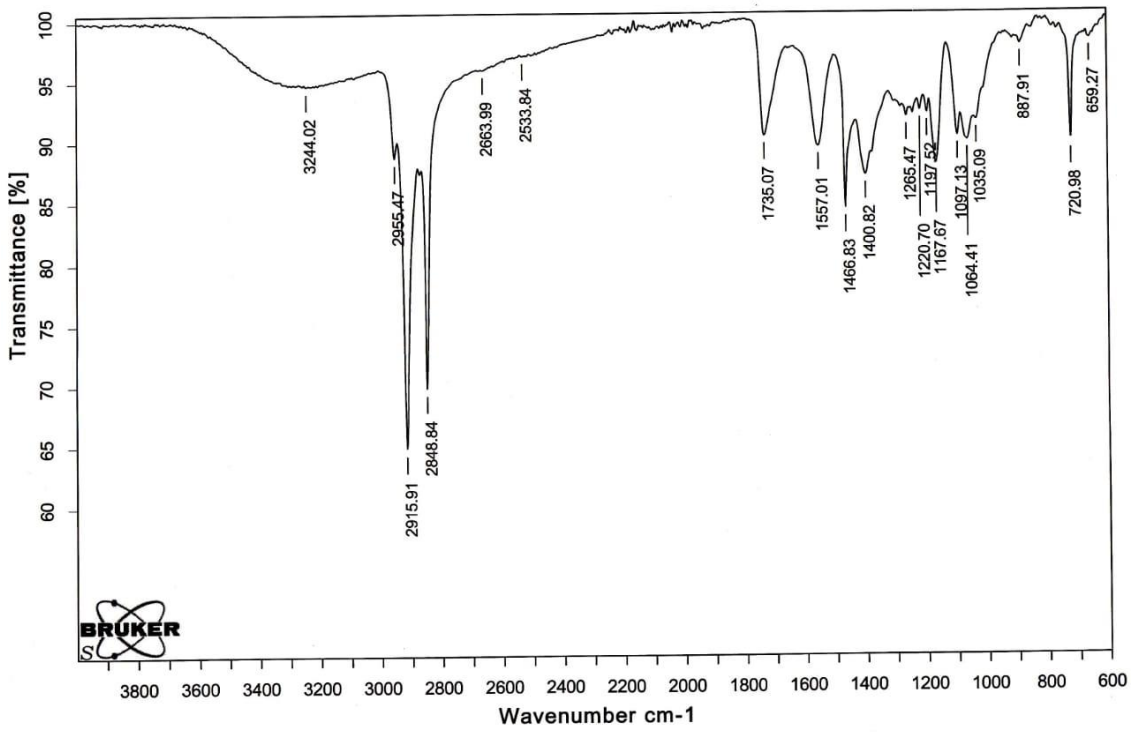

Fig. 3. FTIR spectra of octadecanoic acid with TEA

Identification of the structure of complexes formed by octanoic acid with MEA, DEA and TEA by IR spectroscopic method also proves that the reactions proceed according to the above scheme (Figure 1, 2,3).

Based on the measured surface tension values obtained using the tensiometric method, surface tension isotherms were established (Figure 4).

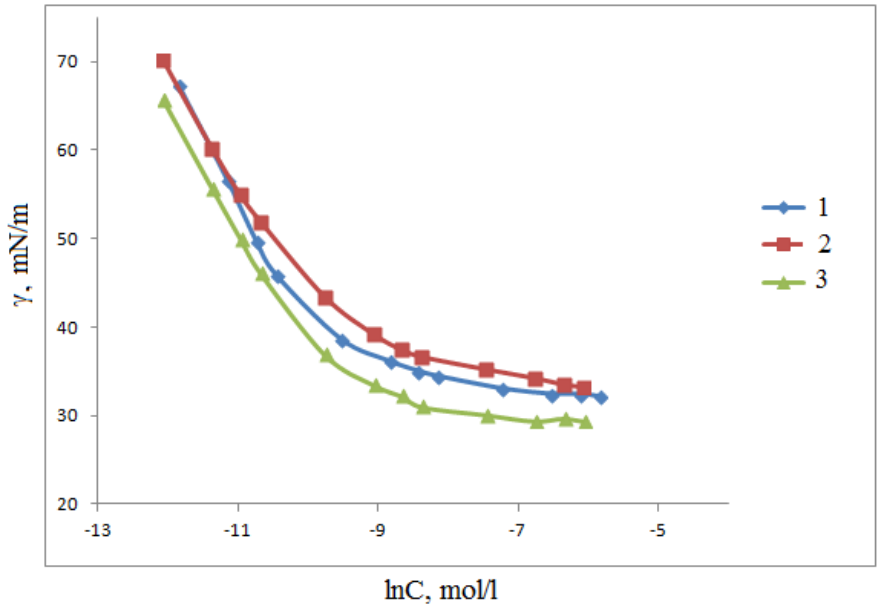

Figure 4. The surface tension isotherms of the salts formed by octadecanoic acid with MEA (1), DEA (2), and TEA (3).

Based on this figure, the value of *γ–lnC* was determined graphically [13]. In the absence of reagents, the surface tension at the air-water interface is equal to 72.0 mN·m^{-1}. The stabilization of the surface tension values for the salts formed by octadecanoic acid with MEA, DEA, and TEA occurs at approximately 32.5, 33.5, and 29.4 mN·m^{-1}, respectively.

According to the figure, the value of d/dlnC was determined graphically. By putting this value into the Gibbs equation, the adsorption value – G is calculated:

$$\Gamma_{max} = -\frac{1}{nRT}\left(\frac{\partial\gamma}{\partial \ln C}\right)_T$$

where d/dlnC – surface activity (tangent of the slope of the dependence on lnC at constant temperature T); R – universal gas constant (8.314 J·/mol K).

The minimum cross-sectional area of the polar group of the synthesized surfactants was calculated using the formula:

$$A_{\min} = \frac{1}{\Gamma_{max} N_A},$$

where N_A is Avogadro's number (6.023·1023).

The value of efficiency (pC20), characterizing the concentration at which surface tension decreases by 20 mN/m, was calculated using the equation:

$$pC_{20} = -\lg C_{(-\Delta\gamma=20)}.$$

Surface pressure or efficiency (π_{CMC}) of aqueous solutions of synthesized substances at the water-air interface is determined by the formula:

$$\pi_{CMC} = \gamma_0 - \gamma_{CMC}$$

where γ_0 is the surface tension in the absence of a surfactant, γ_{CMC} is the surface tension of the solution with CMC.

It is known from the literature that for nonionic surfactants, the thermodynamic parameters of micellization, namely the change in the Gibbs free energy, are calculated using the equation

$$\Delta G_{mis} = (2-\alpha)RT \ln CMC$$

where lnKKM is the surfactant concentration at the CMC point.

The value of ΔG_{ad} was calculated using the equation [13]

$$\Delta G_{ad} = (2-\alpha)RT \ln CMC - \pi_{CMC} A_{CMC.}$$

The colloid-chemical parameters of the synthesized surfactants (SAMs) were calculated based on the equations provided in [13], and the results are presented in Table 1.

Table 1– Colloid-chemical parameters of the new surfactants formed by octadecanoic acid with MEA, DEA, and TEA.

Surfactants	*CMC×10^{-3}, mol·dm^{-3}*	*G_{max}×10^{-10}, mol·sm^{-2}*	*A_{min}×10^{-2}, nm^2*	*γ_{CMC}, mN·m^{-1}*	*π_{CMC}, mN·m^{-1}*	*pC_{20}*	*ΔG_{mis}, kJ/mol^{-1}*	*ΔG_{ad}, kJ/mol^{-1}*
1	1.45	1.78	93.6	32.5	39.5	4.73	-25.89	-48.14
2	1.73	2.46	67.6	33.5	38.5	4.65	-25.44	-41.13
3	1.15	2.19	75.80	29.4	42.6	4.82	-26.23	-45.68

Note:

- CMC – Critical micelle concentration (CMC)

- γ_{CMC} – Surface tension of the solution at CMC

- G_{max} – Maximum adsorption

- A_{min}– Minimal surface area of the polar group

- π_{CMC} – Surface pressure or effectiveness

- pC_{20} – Efficiency value

- ΔG_{mis}– Enthalpy change during micelle formation

- ΔG_{ad} – Enthalpy change during the adsorption process.

Table 2 Research results of oil collection and oil dispersing ability of complexes formed by octanoic acid with MEA, DEA and TEA (Balakhana oil; thickness 0.17 mm)

Surfactants	The case of giving the reagent to the surface of the oil	Distilled water		Drinkable water		Sea water	
		τ, saat	K(K_D,%)	τ, saat	K(K_D,%)	τ, saat	K(K_D,%)
Octadecanoic acid +MEA	Undiluted product	0-24 48-72 72-96	Disp 66.2% Disp 78.6% Disp 86.6%	0-24 48-72 72-96	Disp 79.9% 12.2 Disp 86.6%	0-24 48-72 72-96	Disp 66.2% Disp 78.6% Disp 86.6%
	5% aqueous dispersion	0-24 48-72 72-96	Disp 66.2% Disp 78.6% Disp 86.6%	0-24 48-72 72-96	Disp 79.9% 12.2 Disp 86.6%	0-24 48-72 72-96	Disp 69.2% Disp 87.6% Disp 81.1%
Octadecanoic acid +DEA	Undiluted product	0 1.0-4.0 21.0-76.0	Disp 70.9% Disp 78.6% Disp 82.6%	0 1.0-4.0 21.0-76.0	Disp 70.9% Disp 78.6% Disp 82.6%	0 1.0-4.0 21.0-76.0	
	5% aqueous dispersion	0 1.0-4.0 21.0-76.0	Disp 60.9% Disp 68.6% Disp 72.6%	0 1.0-4.0 21.0-76.0	Disp 60.9% Disp 88.7% Disp 82.9%	0 1.0-4.0 21.0-76.0	Disp 73.5% Disp 78.6% Disp 72.6%
Octadecanoic acid +TEA	Undiluted product	1.0-5.0 21.0-76.0	Disp 78% Disp 86.8%	1.0-5.0 21.0-76.0	Disp 63.7% Disp 75%	1.0-5.0 21.0-76.0	Disp 72.6% Disp 65.9%
	5% aqueous dispersion	1.0-5.0 21.0-76.0	Disp 75% Disp 79.2%	1.0-5.0 21.0-76.0	Disp 72% Disp 82.4%	1.0-5.0 21.0-76.0	Disp 78.6% Disp 86.8%

As can be seen from Table 2, the complex of ocadecanic acid and MEA, DEA, TEA exhibits the ability to disperpsed oil in seawater for both application forms of the reagents.

4. Conclusion

Based on the results of the research, it was found that the complex formed by octadecanoic acid with MEA increased the surface tension from 72.0 mN/m to 32.5 mN/m at that boundary, and the complex formed by octadecanoic acid with DEA increased the surface tension from 72.0 mN/m to 33.5 mN/m, at that the complex formed by octadecanoic acid with TEA shows high surface activity by reducing the surface tension from 72.0 mN/m to 29.4 mN/m at that limit.

REFERENCES

1. *Liang Y., Li H., Li M., Mao X., Li Y., Wang Zh., Xue L., Chen X., Hao X.* Synthesis and physicochemical properties of ester-bonded gemini pyrrolidinium surfactants and comparison with single-tailed amphiphiles // Journal of Molecular Liquids, 2019, v. 280, p. 319-326.
2. *Ao. M., Xu G.Y., Zhu Y., Bai Y.* Synthesis and *properties* of ionic liquid-type Gemini imidazolium surfactants // Journal of colloid and interface science, 2008, v. 326, p. 490-495.
3. *Tehrani-Bagha A.R., Holmberg K., van Ginkel C.G., Kean M.* Catonic gemini surfactants with cleavable spacer: chemical hydrolysis, biodegradation and toxicity // Journal of colloid and interface science, 2015, v. 449, p. 72-79.
4. *Vorobyev Yu.L., Akimov V.A., Sokolov Yu.İ.* Preduprejdeniye i likvidasiya avariynıx razlivov nefti i nefteproduktov. M.: İn-oktavo, 2005. 368 s.
5. *Mariano A.J., Kourafalou V.H., Srinivasan A., Kang H., Halliwell G.R., Ryan E.H., Roffer M.* On the modeling of the 2010 Gulf of Mexico Oil Spill // Dinamics of Atmospheres and Oceans, 2011, v. 52, p. 322-340.
6. *Hamdan L.J., Fulmer P.A.* Effects of COREXIT® EC9500A on bacteria from a beach oiled by the Deepwater Horizon spill // Aquatic microbial ecology, 2011, v. 63, p. 101-109.
7. *Wang Z., Stouts.* Oil spill environmental forensics: fingerprinting and source identification. – London: Elsevier, 2010, 565 p.
8. Asadov, Z. H., Rahimov, R. A., Salamova, N. V., Zarbaliyeva, I. A., Ahmedova, G. A. (2014). Green synthesis of surfactants for removing crude oil films off water surface. *İnternational Oil Spill Conference Proceedings*, 1, 299689.
9. Salamova N. V. (2023). Polucheniye, fiziko-ximicheskiye xarakteristiki, neftesobirayushiye i neftedispergiruyushiye svoystva novix poverxnostno-aktivnix veshestv na osnove trigliseridov soyevogo masla, etilendiamina i alkildigalogenidov. *Bashkirskiy ximicheskiy jurnal,* 30(3), 85-90.
10. Asadov, Z. H., Rahimov, R. A., Salamova, N. V. (2012). Synthesis of animal fats ehylolamide, ethylolamide phosphates and their petroleum-collecting and dispersing properties. *Journal of the American Oil Chemists Society*, 89(3), 505-511.
11. Triphonova M.Yu., Bondarenko S.V., Tarasevich Yu.İ. İssledovaniye binarnıx smesey poverxnostno-aktivnix veshestv razlichnoy prirodı // Ukrainskiy ximicheskiy jurnal, 2009, t. 75, №1, s. 28-32.
12. *Gumbatov G.G., Dashdiyev R.A.* Primeneniye PAV dlya likvidasii avariynıx razlivov nefti na vodnoy poverxnosti. - Baku: Elm, 1998, 210 s.
13. *Rozen M.J.* Surfactants and interfacial phenomena. - 3rd edn, New York: John Wiley and Sons Inc., 2004, 444 p.

2024. Volume 8, Number 1 ***Pages 44-51***

UOT:628.1
https://doi.org/10.30546/2521-6317.2024.602

ANTIMICROBIAL PROPERTIES AND BACTERIAL CONTAMINATION IN WESTERN CASPIAN SEA COASTAL WATERS: A STUDY OF COLIFORM, E. COLI, AND ENTEROCOCCUS

V.M.ABBASOV, E.A. AYDINSOY✉, D.B. AGHAMALIEVA, Z.Z. AGHAMALIEV

Institute of Petrochemical Processes, named after Yu.G. Mamedaliyev,

Ministry of Science and Education of Azerbaijan.

Baku, Azerbaijan

e-mail: emil.aydinsoy@gmail.com

ARTICLE INFO

Article history:

Received: 2024-09-20

Received in revised form: 2024-09-23

Accepted:2024-10-18

Available online

Keywords:

Caspian Sea;

Antimicrobial Properties;

Coliform Bacteria;

Escherichia coli (E. coli);

Enterococcus

JEL CODES: Q25, Q5, Q57

ABSTRACT

This study evaluates the antimicrobial properties and bacterial contamination of coastal waters in the western Caspian Sea, focusing on Coliform, Escherichia coli (E. coli), and Enterococcus bacteria. Water samples were collected from four coastal locations—Neftchala, Sumgayit, Bilgah, and Pirallahi—and analysed to determine bacterial concentrations against the minimum acceptable rates for safe water quality. The analysis showed variability in bacterial contamination levels across the sites, with Neftchala displaying undetectable levels of Coliform and E. coli. At the same time, Sumgayit, Bilgah, and Pirallahi exhibited varying concentrations, some exceeding the minimum acceptable rate thresholds. These findings provide insights into the potential antimicrobial properties of certain coastal waters and emphasise the need to investigate environmental and anthropogenic factors influencing microbial presence. Further research is necessary to explore the natural processes contributing to bacterial inhibition in these waters and to develop effective water management strategies for the Caspian Sea region.

1. Introduction

The Caspian Sea, the world's largest enclosed inland body of water, is a vital ecological and economic resource for the surrounding countries. Understanding the antimicrobial properties and bacterial contamination levels of its coastal waters is crucial for water quality management and public health. Bacteria such as Coliform, Escherichia coli (E. coli), and Enterococcus serve as critical indicators of microbial contamination in aquatic environments. Their presence often results from anthropogenic activities such as untreated sewage discharge, agricultural runoff, and industrial pollution, leading to significant ecological and health concerns [1,2]. Monitoring these bacteria in coastal waters provides insights into the environmental health and potential risks associated with waterborne pathogens [3,4].

Microbial contamination in coastal waters can be heavily influenced by local environmental conditions and human activities. For example, studies conducted on the southern Caspian Sea coast have documented varying levels of E. coli contamination in water samples from areas influenced by agricultural and urban runoff, highlighting the importance of location-specific monitoring [2]. In the western Caspian Sea, locations such as Neftchala, Sumgayit, Bilgah, and Pirallahi present a diverse range of contamination levels, which reflect different environmental and anthropogenic influences [4]. This variability underlines the need for continuous monitoring and assessment of bacterial contamination and its implications for public health and marine ecosystems [1,5]

Antimicrobial resistance (AMR) among waterborne pathogens is a growing concern, particularly with the increasing detection of resistant strains in marine environments. Enterococcus species, for instance, have shown resistance to multiple antibiotics, complicating infection control measures and necessitating the study of resistance patterns in coastal waters [1]. Research has demonstrated that waters with frequent human interaction, such as recreational beaches, often harbour resistant bacterial strains, indicating the potential role of such environments in the dissemination of AMR [6,7]. Studies on the molecular detection of antibiotic resistance and virulence gene determinants in Enterococcus species from coastal waters further emphasise the need to address AMR as a critical factor in water quality [4,8-10].

Recent investigations have explored the potential of natural and synthesised antimicrobial agents to reduce microbial contamination in marine settings. For example, deep-sea water has been shown to possess natural antimicrobial properties that can inhibit the growth of E. coli and Staphylococcus aureus, suggesting a promising alternative to chemical-based disinfection methods [6]. Similarly, the exploration of synthesised compounds, such as dipentylammonium (Z)-3-carboxylate complex, has revealed effective bactericidal properties against a range of pathogens, highlighting the potential of these agents for environmental and public health applications [3,7]. The application of such natural and synthetic agents offers a sustainable approach to water management, reducing the reliance on traditional chemical treatments and potentially mitigating the spread of resistant strains [3,8].

Further research on antimicrobial agents derived from marine environments, including deep-sea water, has demonstrated their ability to inhibit a broad spectrum of bacteria, providing a potential solution for microbial control in coastal waters [4-6]. Additionally, understanding the mechanisms underlying the natural antimicrobial properties of seawater can inform the development of new biotechnological applications for environmental safety [7].

This study aims to assess the bacterial contamination and potential antimicrobial properties of coastal waters in the western Caspian Sea, focusing on Coliform, E. coli, and Enterococcus bacteria. By comparing bacterial concentrations across different locations and assessing their alignment with the minimum acceptable rates for water quality, this research provides a comprehensive understanding of microbial dynamics in the region. The findings will contribute to developing more effective water management strategies and exploring the natural antimicrobial processes that may help maintain water quality in the Caspian Sea [4,6,7]

2. Methodology:

This study was conducted to evaluate the antimicrobial properties and bacterial contamination levels of coastal waters in the western Caspian Sea, explicitly focusing on the presence of Coliform, Escherichia coli (E. coli), and Enterococcus bacteria. Water samples were collected from four coastal locations—Neftchala, Sumgayit, Bilgah, and Pirallahi—representing different environmental conditions and levels of anthropogenic influence.

2.1 Sample Collection:

Water samples were collected from the four locations during a period of stable weather conditions to avoid variations due to rainfall or storm events. At each site, samples were taken from a depth of approximately 1 meter to ensure consistency. Sterilised glass bottles were used for sample collection, and each bottle was labelled with the location, date, and time of collection. The samples were immediately stored in an icebox to maintain a low temperature and were transported to the laboratory for analysis within one week. This timeframe ensured that microbial integrity was preserved while allowing for logistical considerations. Figure 1 illustrates the sites from which water samples were collected.

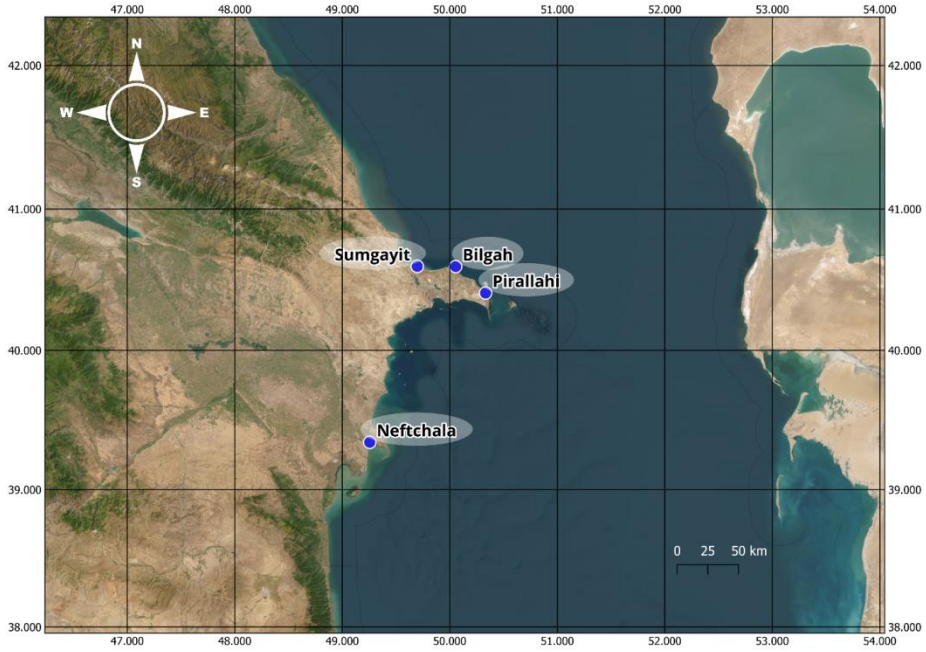

Fig 1. *Locations of conducted experiments on the map*

2.2 Bacterial Analysis:

The concentrations of Coliform, E. coli, and Enterococcus bacteria in the water samples were determined using a Biotrak-4250 analyser conducted under the supervision of the Ministry of

Ecology and Natural Resources of the Republic of Azerbaijan. The analysis was carried out at a temperature of 37°C for 24 hours under fully sterile conditions in a controlled environment. For each analysis, 1 ml of the faecal water sample was mixed with 9 ml of nutrient media, specifically BiMedia 155A, BiMedia 160C, and BiMedia 330A, to provide the optimal conditions for bacterial growth and detection. BiMedia 155A was used for Coliform, BiMedia 160C for E. Coli and BiMedia 330A for Enterococcus.

The Biotrak-4250 analyser was used to detect and quantify bacterial concentrations automatically. This equipment enables precise analysis of bacterial growth in the nutrient media, providing accurate results for Coliform, E. coli, and Enterococcus levels in the samples. After 24 hours of incubation at 37°C, the bacterial concentrations were recorded. Results were expressed in bacterial units per litre (unit/l) for each type of bacteria, based on the growth observed in the BiMedia-specific nutrient conditions.

This automated analysis method allows for a standardised and compassionate approach to monitoring bacterial contamination levels in coastal waters, ensuring that the measurements are reliable and reproducible across different samples and locations [4].

2.3 Determination of Minimum Acceptable Rate:

To assess whether the bacterial contamination levels were within safe limits, the concentrations of Coliform, E. coli, and Enterococcus were compared against the Minimum Acceptable Rates for water quality. These Minimum Acceptable Rates values serve as benchmarks for determining whether the observed bacterial levels pose a potential health risk. The values used in this study 2000 n/L for Coliform, 1000 n/L for E. coli, and 1000 n/L for Enterococcus—are based on the standards reported [4], which are specifically determined for the studied region and water type in the Caspian Sea context (see Table 1).

Additionally, the results were cross-referenced with the **WHO guidelines for safe recreational water environments**, which provide criteria for bacterial concentrations in recreational waters (see Table 2). For other uses, such as drinking water, the WHO sets much stricter standards (see Table 3). This dual reference allows for a more comprehensive understanding of how the contamination levels compare both regionally and internationally. [10-12]

***Table 2. Minimum Acceptable Rates based on** (Guliyeva et al., 2024)*

Bacteria Type	Minimum Acceptable Rates **Values**
Coliform	2000 n/L
E. coli	1000 n/L
Enterococci	1000 n/L

Table 3. WHO Guidelines for Recreational Water Quality

Bacteria Type	**Excellent Quality**	**Good Quality**	**Poor Quality**
Coliform	Not specified	Not specified	Not specified
E. coli	≤ 250 CFU/100 mL	251–500 CFU/100 mL	501–1,000 CFU/100 mL
Enterococci	≤ 40 CFU/100 mL	41–200 CFU/100 mL	201–500 CFU/100 mL

Table 4. WHO Guidelines for Drinking Water Quality

Bacteria Type	**Acceptable Limit**
Coliform	0 CFU/100 mL
E. coli	0 CFU/100 mL
Enterococci	0 CFU/100 mL

2.4 Statistical Analysis:

The bacterial counts obtained from the different locations were statistically analysed to determine significant differences in contamination levels across the study sites. Due to the limited sample size and the non-normal distribution of the data, the **Kruskal-Wallis test**, a non-parametric alternative to one-way ANOVA, was used to test for differences in bacterial concentrations (Coliform, E. coli, and Enterococcus) between the four locations—Bilgah, Pirallahi, Sumgayit, and Neftchala. The Kruskal-Wallis test ranks the data and compares the median ranks across groups. A p-value of less than 0.05 was considered statistically significant, indicating differences in bacterial contamination levels among the sites. If substantial differences were detected, further pairwise comparisons were conducted using post-hoc tests to identify specific groups that differed from each other.

2.5 Assessment of Antimicrobial Properties:

The study assessed the potential antimicrobial properties of the coastal waters by analysing the bacterial contamination levels at each location—Bilgah, Pirallahi, Sumgayit, and Neftchala. The assessment was based on the comparison of bacterial counts (Coliform, E. coli, and Enterococcus) across these locations to identify any site-specific variations that may indicate natural antimicrobial effects. Lower bacterial counts in specific locations could suggest the presence of natural conditions or environmental factors that inhibit microbial growth. The findings were interpreted in the context of the Minimum Acceptable Rates from (Guliyeva et al., 2024) and cross-referenced with **WHO guidelines for recreational water quality** to provide a comprehensive understanding of the water quality and potential antimicrobial properties in the western Caspian Sea region. [10-12]

3. Results and Discussion

To evaluate the microbial safety and potential antimicrobial properties of coastal waters in the western Caspian Sea, this study analysed bacterial contamination levels across four different locations: Bilgah, Pirallahi, Sumgayit, and Neftchala. The presence of Coliform, E. coli, and Enterococcus bacteria was quantified and assessed relative to the region-specific Minimum Acceptable Rates provided by (Guliyeva et al., 2024) and the internationally recognised **WHO guidelines** for recreational water quality.

3.1 Bacterial Contamination Levels Across Locations:

The bacterial analysis across the four locations—Bilgah, Pirallahi, Sumgayit, and Neftchala—revealed varying levels of Coliform, E. coli, and Enterococcus bacteria. The concentrations of these bacteria were measured at specific time points to evaluate their presence in the water samples relative to the Minimum Acceptable Rates and WHO guidelines. As shown in Table 4, Bilgah exhibited Coliform levels of 58,000 unit/l, which is below the Minimum Acceptable Rate of 2000 unit/l, but E. coli levels were 55,000 unit/l, far exceeding the acceptable limit of 1000 unit/l. Pirallahi showed even higher bacterial concentrations, with Coliform levels reaching 114,000 unit/l and E. coli levels at 110,000 unit/l. Sumgayit also showed notable bacterial presence, with Coliform levels at 52,000 unit/l and E. coli at 48,000 unit/l. In contrast, Neftchala recorded bacterial levels below the detection limits for both Coliform and Enterococcus and 14,700 unit/l for E. coli, indicating a relatively better water quality that might naturally inhibit microbial growth.

Table 5. *Bacterial Contamination Levels at Different Time Points Across Locations*

Location	Bacteria Type	Environment (BiMedia Type)	Concentration (unit/l)	Minimum Acceptable Rate (unit/l)
Bilgah	**Coliform**	**BiMedia 155A**	**58,000**	**2000**
Bilgah	**E. coli**	**BiMedia 160C**	**55,000**	**1000**
Bilgah	**Enterococcus**	**BiMedia 330A**	**0**	**1000**
Pirallahi	**Coliform**	**BiMedia 155A**	**114,000**	**2000**
Pirallahi	**E. coli**	**BiMedia 160C**	**110,000**	**1000**
Pirallahi	**Enterococcus**	**BiMedia 330A**	**0**	**1000**
Sumgayit	**Coliform**	**BiMedia 155A**	**52,000**	**2000**
Sumgayit	**E. coli**	**BiMedia 160C**	**48,000**	**1000**
Sumgayit	**Enterococcus**	**BiMedia 330A**	**0**	**1000**
Neftchala	**Coliform**	**BiMedia 155A**	**0**	**2000**
Neftchala	**E. coli**	**BiMedia 160C**	**14,700**	**1000**
Neftchala	**Enterococcus**	**BiMedia 330A**	**0**	**1000**

3.2 Comparison with Minimum Acceptable Rates and WHO Guidelines:

The findings across the locations were compared to the Minimum Acceptable Rates, which were 2000 unit/l for Coliform, 1000 unit/l for E. coli, and 1000 unit/l for Enterococcus. Except for Neftchala, all other locations exceeded these thresholds, especially for E. coli and Coliform, indicating poor water quality that could pose health risks if used for recreational activities.

Additionally, these results were compared with the WHO guidelines for recreational water quality, which specify that for E. coli, concentrations should be ≤ 250 CFU/100 mL for excellent quality and up to 1,000 CFU/100 mL for poor quality. For Enterococci, ≤ 40 CFU/100 mL is considered exceptional, and up to 500 CFU/100 mL is poor quality. The contamination levels observed in Bilgah, Pirallahi, and Sumgayit far exceed these WHO limits, underscoring the need for immediate interventions and continuous monitoring to prevent potential health risks.

3.3 Statistical Analysis of Bacterial Contamination Levels:

The **Kruskal-Wallis H test** was used to evaluate differences in bacterial contamination levels (Coliform, E. coli, and Enterococcus) across the four locations: Bilgah, Pirallahi, Sumgayit, and Neftchala. This non-parametric test, appropriate for non-normally distributed data, assesses whether the median ranks of multiple groups differ significantly. The test statistic HIs calculated using:

$$H = \frac{12}{N(N+1)} \sum \left(\frac{{R_i}^2}{n_i} \right) - 3(N+1) \qquad (1)$$

where NIs the total number of observations, $R_i$is the sum of ranks for the i -th group and n_i is the number of observations in that group.

The test showed significant differences in **Coliform** and **E. coli** levels among the locations ($p < 0.05$), with post-hoc tests indicating higher contamination at Bilgah, Pirallahi, and Sumgayit compared to Neftchala. No significant differences were found for **Enterococcus** ($p > 0.05$), reflecting consistently low levels across all sites. These findings suggest localised factors driving bacterial contamination, requiring targeted interventions.

3.4 Implications for Water Quality and Management:

The results highlight significant microbial contamination in several coastal areas, with Bilgah, Pirallahi, and Sumgayit showing levels far beyond both regional and international safety guidelines. This suggests potential sources of pollution, such as untreated sewage discharge,

agricultural runoff, or other anthropogenic influences that must be addressed to ensure safer water for recreational and public use. In contrast, Neftchala's relatively lower contamination levels indicate a more favourable water quality profile, which could be further investigated to understand the factors contributing to these conditions.

3.5 Recommendations and Future Research:

The findings call for targeted water quality management strategies to mitigate contamination sources and improve the overall safety of coastal waters in the Caspian Sea. Future research should involve more frequent and comprehensive sampling across different seasons and environmental conditions, coupled with chemical analyses to identify specific pollutants or natural antimicrobial compounds influencing bacterial growth.

4. Conclusion

This study provides a comprehensive assessment of bacterial contamination levels across four coastal locations in the western Caspian Sea—Bilgah, Pirallahi, Sumgayit, and Neftchala—by quantifying the presence of Coliform, E. coli, and Enterococcus bacteria and comparing them against established minimum acceptable rates and WHO guidelines for recreational water quality. The findings reveal significant microbial contamination in Bilgah, Pirallahi, and Sumgayit, where bacterial levels, particularly for Coliform and E. coli, substantially exceed both regional and international safety thresholds. These results suggest that these areas are heavily impacted by anthropogenic pollution, such as untreated sewage discharge, agricultural runoff, and possibly industrial activities, necessitating immediate intervention and targeted water management strategies to mitigate potential health risks.

In contrast, the comparatively lower bacterial counts observed in Neftchala indicate more favourable water quality conditions, which may be attributed to natural factors or reduced human impact. This highlights the potential for certain coastal areas to exhibit natural antimicrobial properties that warrant further investigation. The use of both regional and international guidelines provided a robust framework for evaluating contamination levels, emphasising the need for harmonised standards in assessing water quality for public health safety.

The study underscores the urgent need for enhanced monitoring and regulatory measures in the Caspian Sea region. Implementing regular, high-frequency water quality monitoring, coupled with advanced microbial source tracking techniques, could provide deeper insights into pollution dynamics and inform more effective mitigation strategies. Additionally, future research should focus on understanding the ecological and public health implications of such contamination, exploring the presence of antimicrobial resistance in marine pathogens, and investigating natural antimicrobial compounds that could offer sustainable solutions for water quality management.

Overall, this study contributes to the growing body of knowledge on coastal water quality in the Caspian Sea and provides critical insights for policymakers, researchers, and environmental managers. By addressing both immediate contamination issues and exploring sustainable long-term solutions, the region can move towards safer, cleaner, and healthier marine environments.

REFERENCES

1. Issazadeh, K., Razban, S., & Pahlaviani, M. (2014). Isolation and identification of Enterococcus species and determination of their susceptibility patterns against antibiotics and heavy metals in coastal waters of Iran. International Journal of Advanced Biological and Biomedical Research. 2(6), 2026-2030
2. Seifi, S., & Shirzad, M. R. (2017). Antimicrobial susceptibility of Escherichia coli isolated from free-range poultry or wild birds at the southern Caspian Sea coast of Iran. Journal of the Hellenic Veterinary Medical Society, 64(4), 249-254. https://doi.org/10.12681/jhvms.15504
3. Abbasov, V. M., Aghamaliyeva, D. B., Abbasov, M. M., Talibov, A. H., Amirli, F. A., Afandiyeva, L. M., & Aghamaliyev, Z. Z. (2024). Exploration of the antibacterial effect of dipentylammonium (Z)-3-carboxylate complex. Processes of Petrochemistry and Oil-Refining (PPOR), Special Issue 1, 199-205.

   https://doi.org/10.62972/1726-4685.si2024.1.199
4. Guliyeva, S. I., Alikhanova, A. I., Rasulov, N. S., Garayev, E. A., & Mammadov, B. A. (2024). Synthesis of copolymerisation of meta-carboxphenylmaleinimide with styrene and study of antimicrobial properties. Processes of Petrochemistry and Oil-Refining (PPOR), 25(1), 153-162. https://doi.org/10.62972/1726-4685.2024.1.153
5. Korajkic, A., McMinn, B. R., Staley, Z. R., Ahmed, W., & Harwood, V. J. (2020). Antibiotic-resistant Enterococcus species in marine habitats: A review. Current Opinion in Environmental Science & Health, 16, 92–100. https://doi.org/10.1016/j.coesh.2020.07.003
6. Chandran, G. R., Dailin, D. J., Manas, N. H. A., El-Ensashy, H. A., Man, M., Edis, Z., Fatriasari, W., & Azelee, N. I. W. (2023). Antimicrobial properties of deep-sea water towards Escherichia coli and Staphylococcus aureus. Journal of Bioprocessing and Biomass Technology (BBT), 2(1), 13–17.

   https://doi.org/10.11113/bioprocessing.v2n1.22
7. Vingino, A., Roberts, M. C., Wainstein, M., West, J., Norman, S. A., Lambourn, D., Lahti, J., Ruiz, R., D'Angeli, M., Weissman, S. J., & Rabinowitz, P. (2021). Surveillance for antibiotic-resistant E. coli in the Salish Sea ecosystem. Antibiotics, 10(10), 1201. https://doi.org/10.3390/antibiotics10101201
8. Adeniji, O. O., Sibanda, T., & Okoh, A. (2020). Molecular detection of antibiotic resistance and virulence gene determinants of Enterococcus species isolated from coastal water in the Eastern Cape Province, South Africa. International Journal of Environmental Studies, 78(2), 208–227. https://doi.org/10.1080/00207233.2020.1785759
9. Dyakova, S., Volodina, V., Galyautdinova, E., Menkova, A., & Soprunova, O. (2020). The current state of heterotrophic bacterioplankton and bacteriobenthos in the northern and middle parts of the Caspian Sea. KnE Life Sciences. 5(1), 262–273. https://doi.org/10.18502/kls.v5i1.6066
10. Verhougstraete, M. P., Pogreba-Brown, K., Reynolds, K. A., Condé Lamparelli, C., Zanoli Sato, M. I., Wade, T. J., & Eisenberg, J. N. S. (2020). A critical analysis of recreational water guidelines developed from temperate climate data and applied to the tropics. *Water Research, 170*, 115294. https://doi.org/10.1016/j.watres.2019.115294
11. Petri, O., Ulqinaku, D., Kika, B., & Abazaj, E. (2022). Trends of recreational water quality in Albania's coastal during 2016–2020. *Journal of Environmental Science and Health, Part A: Toxic/Hazardous Substances and Environmental Engineering, 57*(4), 327-334. https://doi.org/10.1080/10934529.2022.2075653
12. assanein, F., Masoud, I. M., Fekry, M. M., et al. (2023). Environmental health aspects and microbial infections of the recreational water. *BMC Public Health, 23*, 302. https://doi.org/10.1186/s12889-023-15183-z

JOURNAL OF BAKU ENGINEERING UNIVERSITY-ADVANCES IN CHEMISTRY AND CHEMICAL ENGINEERING
2024. Volume 8, Number 1 ***Pages 52-58***

UOT:661
https://doi.org/10.30546/2521-6317.2024.108

SYNTHESIS OF SURFACTANTS BASED ON SOYBEAN OIL TRIGLYCERIDES, N-(2-HYDROXYETHYL) ETHYLENEDIAMINE, AND PROPYLENE OXIDE, AND THE STUDY OF THEIR PETRO-COLLECTING AND PETRO-DISPERSING PROPERTIES

Nargiz SALAMOVA*, Gulnara AHMADOVA,
Gular BAYRAMOVA, Seyid Zeynab HASHIMZADA

Academician Y.H. Mammadaliyev Institute of Petrochemical Processes of the

Ministry of Science and Education of the Republic of Azerbaijan,

Baku, Azerbaijan

*Corresponding author.

E-mail: e_nargiz@mail.ru (Nargiz Salamova).

ARTICLE INFO

Article history:

Received:2024-09-23

Received in revised form:2024-10-18

Accepted:2024-10-18

Available online

Keywords:

soybean oil triglycerides;

surface activity;

specific electrical conductivity;

petro-collecting;

petro-dispersing.

ABSTRACT

An aminoamide containing a hydroxyl group was synthesized from the reaction of a soybean oil acid mixture with hydroxyethylethylenediamine. The obtained aminoamide was then oxypropylated with propylene oxide. The composition and structure of the synthesized aminoamide and its oxypropyl derivatives were determined by FTIR spectroscopy. The synthesized products were characterized by their important physico-chemical properties, and conductometric measurements of their aqueous solutions at different concentrations were carried out. The colloid-chemical parameters of the synthesized surfactants were studied, and their adsorption properties were determined experimentally. Simultaneously, the critical micelle concentration, surface pressure, maximum adsorption, minimum surface area of the molecule, adsorption efficiency, and free Gibbs energy of micellization and adsorption were calculated. The petro-collecting and petro-dispersing properties of the obtained products were studied in a thin oil layer on the surface of different types of water.

1. Introduction

It is well-known that one of the main sources of water pollution is oil and petroleum products [1-7]. Oil pollution in marine waters occurs primarily during oil extraction and transportation by tankers. Accidental spills, operational discharges, and leaks during these activities significantly contribute to the presence of oil in the marine environment. The impact of oil pollution on marine life is profound, affecting both the health of aquatic organisms and the overall balance of the ecosystem.

Methods for cleaning water contaminated with oil are carried out in several stages to effectively reduce pollution levels. The first stage usually involves removing the thick layer of oil from the water surface using mechanical methods. These methods include the use of sorbents, skimmers, and booms, which physically separate the oil from the water. For example, sorbents [8,9] absorb or adsorb oil, making it easier to collect and dispose of. Skimmers are used to collect oil from the water surface [10,11], while booms prevent the spread of oil, keeping it from reaching the shoreline and sensitive habitats.

Despite the effectiveness of mechanical methods in removing the bulk of the oil, a thin layer of oil often remains on the water surface. This residual layer is difficult to eliminate, requiring more advanced methods. At this stage, colloidal-chemical methods are used to disperse or break down the thin oil film. These methods include the use of surfactants and dispersants, which reduce the surface tension between the oil and water [12-16].

Ongoing research and development in this field aim to improve the efficiency of these reagents, ultimately leading to cleaner and healthier oceans.

2. Materials and Experimental Methods

Soybean oil was used as a commercial product by the Labinsk branch of LLC "MEZ Yug Rusi" according to GOST R 53510-2009 (Russia). N-(2-hydroxyethyl) ethylenediamine (HEtEDA) – purity 99%, Sigma-Aldrich.Propylene oxide (PO) - purity 99%, Alfa Aesar, Great Britain. The chemical structures of the prepared compounds were confirmed by FT-IR analysis.

Infrared spectra were identified in the wavenumber range of 400-4000 cm^{-1} using a BIO-RAD FTS 3000 MX spectrometer (Germany).

The surface tension values were defined at the air-water interface via a du Nouy tensiometer (KSV Sigma 702, Finland) with a ring method. [17].

The petro-collecting and dispersing properties of the synthesized surfactants were performed according to the methodology given in [18].

The petro-collecting properties were characterized by the collecting coefficient (K) (the ratio of the initial surface area of the petroleum film to the surface area of the thickened petroleum spot formed under the influence of the reagent) and the duration effect (τ) of the collected petroleum.

3. Results and Discussion

An aminoamide containing a hydroxyethyl group was synthesized from the reaction of soybean oil triglycerides with HEtEDA. The reaction was carried out at a temperature of 120-130°C in a 1:3 mol ratio of reagents. The reaction time was 24 hours. The total course of the reactions is given in Scheme 1:

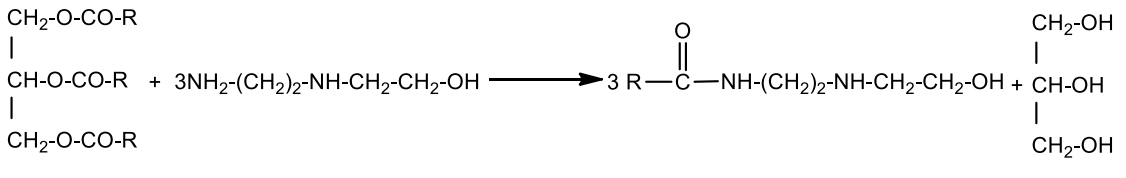

(1)

The aminoamide of the obtained soybean oil acid mixture (SOAM) with hexaethylethylenediamine was identified by IR-spectroscopy (Fig. 1). Spectral results are listed below: Stretching vibrations of N–H and O-H bonds at 3295 və 3271 cm^{-1}, stretching vibrations of CH=CH at 3009 cm^{-1}, 2852 və 2921 cm^{-1} stretching vibration of C-H bond in CH_3 and CH_2 groups, stretching vibration of C=O bond at 1640 cm^{-1}, stretching vibrations of N-H bond at 1558 cm^{-1}, 1464, 1397, 1376 və 720 cm^{-1} stretching vibration of C-H bond in CH_3 və CH_2 groups.

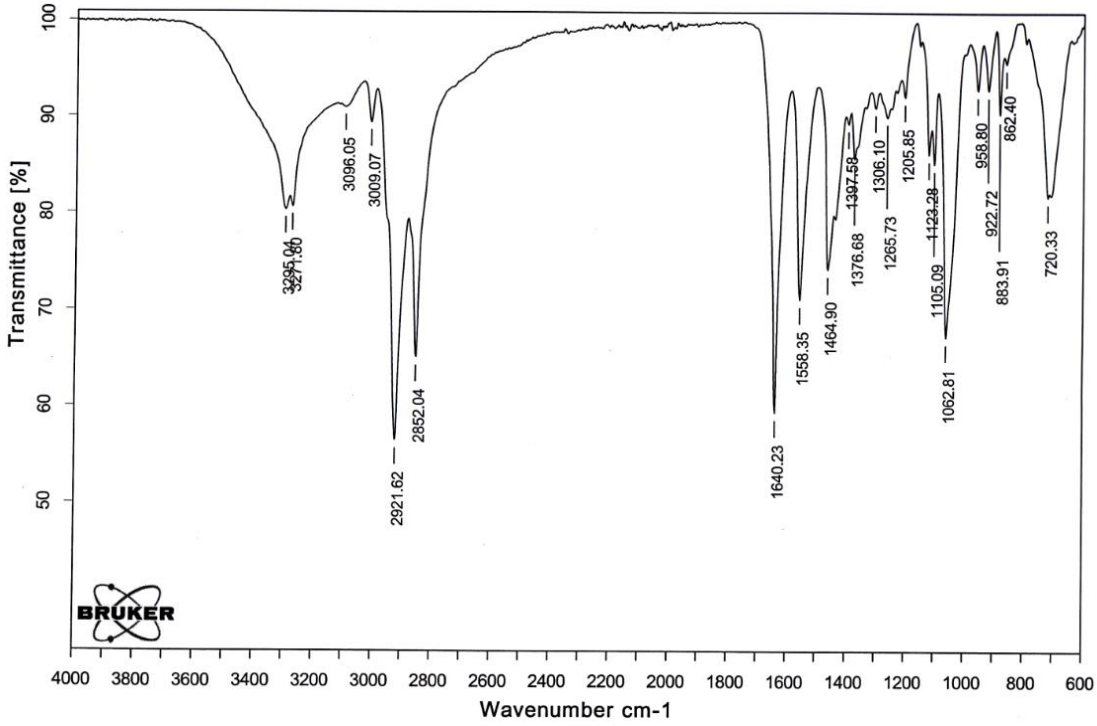

Fig. 1. FTIR spectra of hydroxyethyl aminoamide of SOAM

Synthesis of obtained SOAM aminoamide HEtEDA with PO was carried out and the oxypropyl derivative was synthesized. The reaction was carried out at room temperature in an equimolar ratio of reagents. The reaction lasted 15-16 hours. The general scheme (2) of the reaction is given below:

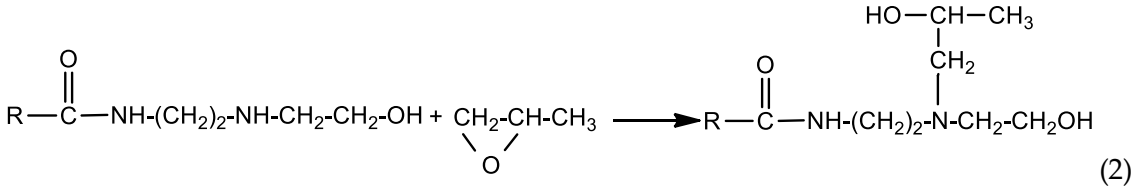

(2)

The structure of the synthesized oxypropyl derivative of the hydroxyethylethylenediamine aminoamide of SOAM was confirmed by IR-spectroscopy (Fig. 2). Absorption bands belonging to the following groups are observed in the spectrum: stretching vibration of the bond at 3321

cm^{-1}, stretching vibration of CH=CH bond at 3008 cm^{-1}, stretching vibration of C-H bond in CH_3 and CH_2 groups at 2853 and 2923 cm^{-1}, the stretching vibration of the C=O bond of the amide group at 1645 cm^{-1}, the stretching vibration of the N-H bond at 1547 cm^{-1}, the stretching vibration of the C-H bond in the CH_3 and CH_2 groups at 1456 and 1372 cm^{-1}, the stretching vibration of the C–O at 1048 cm^{-1}, vibrations belonging to the alkyl chain at 721 cm^{-1}.

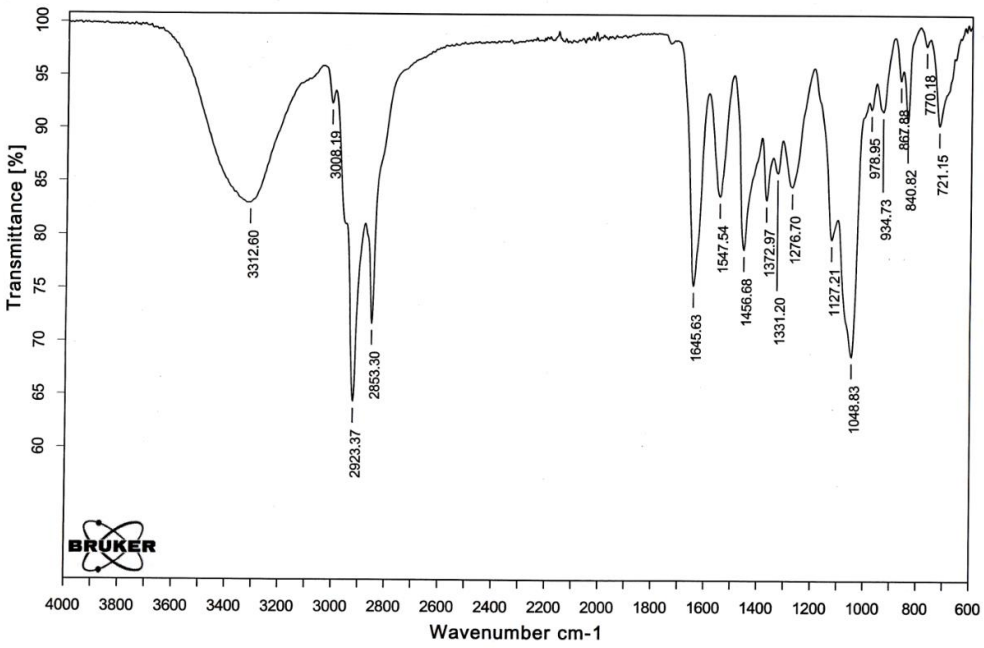

Fig. 2. FTIR spectra of the oxypropyl derivative of the aminoamide of SOAM

Based on the surface tension values of the synthesized SOAM aminoamide and its oxypropyl derivative measured using a tensiometer, surface tension isotherms were constructed in the γ–lnC coordinate (Fig. 3).

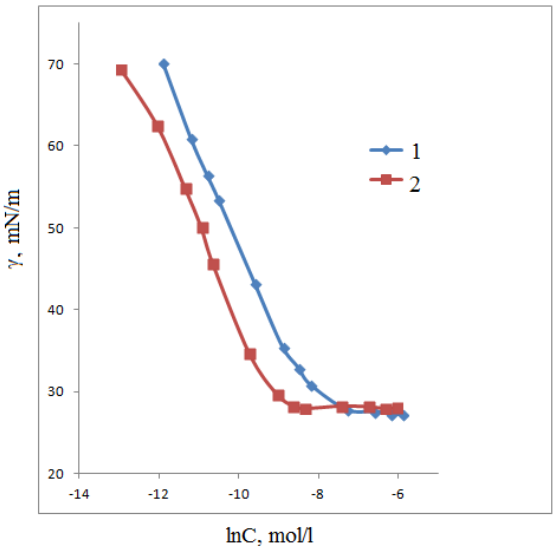

Fig. 3. The surface tension isotherms of the hydroxyethyl aminoamide of SOAM (1) and its oxypropyl derivative (2).

The colloid-chemical parameters of synthesised non-ionic surfactants in Table 1 were calculated according to the equations in reference [19].

Table 1. The colloid-chemical parameters of the hydroxyethyl aminoamide of SOAM (1) and its oxypropyl derivative (2).

Surfactants	CMC×10^{-4}, mol·dm^{-3}	Γ_{max}×10^{-10}, mol·cm^{-2}	A_{min}×10^{-2}, nm^2	γ_{CMC}, mN·m^{-1}	π_{CMC}, mN·m^{-1}	pC_{20}	ΔG_{mic}, kJ/mol^{-1}	ΔG_{ad}, kJ/mol^{-1}
1	6.82	2.50	66.50	27.8	44.2	4.52	-28.9	-45.9
2	1.77	1.19	139.16	28.3	43.7	4.82	-31.6	-68.2

CMC – critical micelle concentration, γ_{CMC} – the surface pressure at the water; Γ_{max}- maximum surface excess, A_{min} – minimum surface area per molecule, π_{KMQ} – surface pressure or effectiveness, pC_{20} – efficiency of absorption, ΔG_{mic} – Gibbs free energy of micellization, ΔG_{ad} – standard Gibbs energy of adsorption

Comparing the colloid-chemical parameters of hydroxyethyl aminoamide of SOAM and its oxypropyl derivative, it is known that the oxypropylation process has a higher effect on CMC and pC_{20}. Thus, the value of CMC for the oxypropyl derivative decreases significantly, while the value of pC_{20} increases.

The research results of petro-collecting and petro-dispersing properties of undiluted and 5% aqueous dispersion surfactants are given in Table 2.

As can be seen from Table 2, hydroxyethyl aminoamide of SOAM shows a petro-collecting effect in fresh and sea water in both diluted and undiluted forms (K_{max} = 13.6 and 16.0). The Oxypropyl derivative of the hydroxyethyl aminoamide of SOAM shows a petro-collecting effect in the first hours in all three applied forms of water and then shows petro-dispersing properties. The maximum petro-dispersing effect shown in distilled, fresh and sea water was 84.7%, 89.0% and 91.1%.

Table 2. Petro-collecting and petro-dispersing properties of the hydroxyethyl aminoamide of SOAM and its oxypropyl derivative (Balakhani oil; thickness ≈ 0.17 mm).

Distilled water		Fresh water		Sea water	
τ, hours	K (K_D, %)	τ, hours	K (K_D, %)	τ, hours	K (K_D, %)
Hydroxyethyl aminoamide of SOAM (Undiluted product)					
0 2.0-27.0 45.0-71.0 109.0	7.4 19.4 86.8% spilling	0 1.0-27.0 45-71 109.0	8.6 12.4 6.7 spilling	0 2.0-13.4 27.0-97.0 109.0	7.7 16.0 8.6 spilling
Hydroxyethyl aminoamide of SOAM (5% wt. aqueous solution)					
0 1.0-5.0 21.0-71.0 109.0	6.7 12.4 91.1% spilling	0 27-69 109.0	8.6 13.6 spilling	0 1.0-5.0 21.0-69.0 109.0	6.7 11.4 8.9 spilling
Oxypropyl derivative of the hydroxyethyl aminoamide of SOAM (Undiluted product)					
0-5.0 23.0-97.5	7.6 78.6%	0-5.0 23.0-97.5	7.6 78.6%	0-2.0 5.0 23.0-89.0 97.5	7.6 91.1% 86.8% spilling
Oxypropyl derivative of the hydroxyethyl aminoamide of SOAM (5% wt. aqueous solution)					
0-2.0 5.0 23.0-97.5	5.1 78.6% 84.7%	0-5.0 23.0-89.0 97.5	5.0 89.0% spilling	0-5.0 23.0-89.0 97.5	86.8% 91.1% spilling

This reagent shows a petro-dispersing effect in the form of a diluted form in seawater. The duration of action of the reagent is ~4 days.

4. Conclusion

Hydroxyethyl aminoamide of a mixture of soybean oil acids, as well as its oxypropyl derivative synthesized using propylene oxide, have been synthesized. Their structures were identified using IR spectroscopy. The research established that the synthesized substances exhibit high surface activity. It should also be noted that the reagents show a high tendency for surface adsorption. It was found that the surface activity properties can vary depending on the structure of the synthesized substances. Furthermore, comparative studies showed that the oxypropyl derivative of hydroxyethyl aminoamide of the mixture of soybean oil acids demonstrates superior properties in dispersing thin oil films on the surface of seawater compared to the original hydroxyethyl aminoamide of the mixture of soybean oil acids.

REFERENCE LIST

1. Mariano, A. J., Kourafalou, V. H., Srinivasan, A., Kang, H., Halliwell, G. R., Ryan, E. H., Roffer, M. (2011). On the modeling of the 2010 Gulf of Mexico Oil Spill. *Dynamics of Atmospheres and Oceans*. 52(1-2), 322-340.
2. Wang, Z., Stouts, S. (2010). *Oil spill environmental forensics: fingerprinting and source identification*. London: Elsevier. 46(15), 254.
3. Hamdan, L .J., Fulmer, P. A. (2011). Effects of COREXIT® EC9500A on bacteria from a beach oiled by the Deepwater Horizon spill. *Aquatic microbial ecology*. 63, 101.
4. Воробьев, Ю. *Л*., Акимов, В. А., Соколов, Ю.И. (2005). *Предупреждение и ликвидация аварийных разливов нефти и нефтепродуктов*. Ин-Актаво. 368.
5. Asadov, Z. H., Rahimov, R. A., Salamova, N. V., Zarbaliyeva, I. A., Ahmedova, G. A. (2014). Green synthesis of surfactants for removing crude oil films off water surface. *İnternational Oil Spill Conference Proceedings*, 1, 299689.
6. Саламова, Н. В. (2023). Получение, физико-химические характеристики, нефтесобирающие и нефтедиспергирующие свойства новых поверхностно-активных веществ на основе триглицеридов соевого масла, этилендиамина и алкилдигалогенидов. *Башкирский химический журнал*, 30(3), 85-90.
7. Asadov, Z. H., Rahimov, R. A., Salamova, N. V. (2012). Synthesis of animal fats ehylolamide, ethylolamide phosphates and their petroleum-collecting and dispersing properties. *Journal of the American Oil Chemists Society*, 89(3), 505-511.
8. Kahramanli, Yu. N. (2010). Sorbents on the basis of foam polyolefins for the sorption of oil and oil products from the water surface during emergency spills. *Oil and gas business. Scientific and technical journal*, Vol. 8, N 1. P. 80.
9. de Folly d'Auris, A., Rubertelli, F., Taini, A., Vocciante M. (2023). A novel polyurethane-based sorbent material for oil spills management. *Environmental Chemical Engineering*, Volume 11, Issue 6, December 2023, 111386
10. Manivel, R., Sivakumar, R. (2020). Boat type oil recovery skimmer. *Materials Today: Proceedings.* V. 21. P. 470-473.
11. Supriyono, S., Nurrohman, D. T. (2020). Floating oil skimmer design using rotary disc method. *Journal of Phys.: Conf. Ser*. V. 1450. 012046.
12. Abo-Riya, M., Tantawy, A. H., El-Dougdoug, W. (2016). Synthesis and evaluation of novel cationic gemini surfactants based on Guava crude fat as petroleum-collecting and dispersing agents. *Journal of Molecular Liquids,* 221, 642–650.
13. de Almeida Andrade, M. R., Silva, S. B., Costa, T. K. O., de Barros Neto, E. L., Lavoie, J. M. (2021). An experimental investigation on the effect of surfactant for the transesterification of soybean oil over eggshell-derived CaO catalysts. *Energy Conversion and Management*, X. (11), 100094.
14. Tabaniag, J. S. U., Abad, M. Q. D., Morcelos, C. J. R., Geraldino, G. V. B., Alvarado, J. L. M., Lopez, E. C. R. (2023). Stabilization of oil/water emulsions using soybean lecithin as a biobased surfactant for enhanced oil recovery. *Journal of Engineering and Applied Science*, 70, 154.
15. Massarweh, O., Abushaikha, A. S. (2020). The use of surfactants in enhanced oil recovery: A review of recent advances. *Energy report*, 6, 3150-3178.
16. Badmus, S. O., Amusa, H. K., Oyehan, T. A., Saleh, T. A.. (2021). Environmental risks and toxicity of surfactants: overview of analysis, assessment, and remediation techniques. *Environmental Science and Pollution Research* 28, 62085-62104.2104, (202
17. Трифонова, М. Ю., Бондаренко, С. В., Тарасевич, Ю. И. (2009). Исследование бинарных смесей поверхностно-активных веществ различной природы. *Украинский химический журнал*. 75 (1), 28-32.
18. Гумбатов, Г. Г., Дашдиев, Р. А. (1998). *Применение ПАВ для ликвидации аварийных разливов нефти на водной поверхности*. Элм. 210.
19. Rozen M.J. (2004). *Surfactants and interfacial phenomena*. John. Wiley and Sons Inc. 444.

2024. Volume 8, Number 1 ***Pages 59-66***

UOT: 547.241.547.497.1
https://doi.org/10.30546/2521-6317.2024.201

STUDY OF THE INFLUENCE OF THE NATURE OF HALOGEN AND TEMPERATURE ON THE DIRECTION OF THE ALKYLATION REACTION OF β-DICARBONYL COMPOUNDS BY MONO- AND POLYHALOGENALKANES

İSMAILOV V.M., MAMEDOV I.A., QASIMOV R.A., İBRAQIMOVA Q.Q, YUSUBOV N.N.

Baku State University, AZ-1148, Baku, Z. Khalilov str. 33

e-mail: yniftali@gmail.com

ARTICLE INFO

Article history:

Received:2024-09-20

Received in revised form:2024-09-26

Accepted:2024-10-24

Available online

Key words:

alkylation, acetylacetone, dichloroethane, trichloropropane, furan

ABSTRACT

The data on the influence of the halogen nature and temperature on the direction of the alkylation reaction of β-dicarbonyl compounds with halogenated alkanes are presented. It is shown that the main products of the reaction of acetylacetone with 1,2-dichloroethane at 80^0C are the product of O,O-intermolecular alkylation, and a small amount of the product of C,O-dialkylation, a furan derivative, is formed. The alkylation of dimedone with dichloroethane proceeds according to a similar scheme, yielding an O,O-dialkylation product. Alkylation of dimedone with 1,2,3-trichloropropane yields only the product of O-alkylation, enol ether. It has been established that dimedone with 1,3-dichloroethane, under identical conditions, gives a bicyclic compound. Acylation of dimedone with chloroacetic acid chloride in the presence of pyridine forms O-acylation products. The reaction of alkylation of ethyl cyanoacetate with dichloroethane leads to the formation of three compounds – intramolecular C, C-alkylation with the formation of heme-ethoxycarbonylnitrile cyclopropane, a product of intermolecular dialkylation of bis(1,4-ethoxycarbonyl-cyano)cyclohexane and a polymer compound.

INTRODUCTION

Systematic studies of alkylation of β-dicarbonyl compounds with halogenated alkanes have shown that depending on the nature of the substrate and alkylating reagent, C- and O-alkylation products were obtained. The effect of solvent and temperature on the direction of the alkylation reaction was shown [1-4].

It was found [5-7] that during alkylation of β-dicarbonyl compounds (acetylacetone, acetoacetic ester, indanedione, etc.) with dibromoethane in DMSO in the presence of potash, C,C-cyclopropylalkylation products were obtained. The study of the indicated condensations

with 1,2-dichloroethane under identical conditions gave distinctive results, which served as the basis for a complete study of the indicated reactions depending on the nature of the halogen, solvent and temperature.

Experimental

^{1}H and ^{13}C NMR spectra were recorded on a Bruker AV 300 [300 (^{1}H) and [300 (1H) and 75 (13C) MHz, respectively] spektrometer, internal standard – TMS. Melting point was determined on an SMP 30 Stuart. Elemental analysis was performed on a Carlo Erba 1106 instrument. The purity of the obtained compounds was monitored by TLC on Silufol UV-254 plates, eluent – acetone-hexane (1:1).

General procedure for alkylation of compounds with an active methylene group. 0.12 mol of the reagent was added dropwise to a mixture of 0.12 mol of the compound with an active methylene group and 0.25 mol of K_2CO_3 in 50 ml of DMSO with stirring. The mixture was stirred for 12 h at 80^0C. Cooled, treated with water and extracted with ethyl ether. The extract was dried with $MgSO_4$, the solvent was distilled off, and the residue was distilled under vacuum.

4-[2-(4-oxopent-2-en-2-yl)oxy)ethoxy]pent-3-en-2-one (1). Yield 28 g (70%), b.p. 145^0C (2 mm Hg). Found,%: C 63.23; H 8.17 $C_{12}H_{18}O_4$ Calculated,: C 63.71; H 7.96. ^{1}H NMR spectrum ($CDCl_3$), δ ppm: 2.15 s (6H, $2CH_3$), 2.3 s (6H, $2OCH_3$), 4.15 s (4H, 2CHO), 5.45 s (2H, 2CH=). ^{13}C NMR spectrum ($CDCl_3$), δ ppm: 19.31, 62.5, 100, 171, 198.

1-(2-methyl-4,5-dihydrofuran-3-yl)ethan-1-one (2). Yield 3.2 g (8%), b.p. 68-70^0C (2 mm Hg). Found,%: C 65.98; H 8.32 $C_7H_{10}O_2$ Calculated,%: C 66.66; H 7.93. ^{1}H NMR spectrum ($CDCl_3$), δ ppm: 1.75 s (3H, CH_3-C=C), 1.95 s (3H, CH_3-C=O), 2.72 t (2H, CH_2-C=), 4.20 s (2H, CH_2O). ^{13}C NMR spectrum ($CDCl_3$), δ ppm: 13, 21,2, 23, 29, 30, 31, 41, 61, 62, 69.5, 108, 112, 168, 204.

3,3-(ethane-1,2-diyl)bis(oxy)bis(5,5-dimethylcyclohex-2-ene-1-one) (3). Yield 15 g (65%), m.p. 143-145 ^{0}C. Found,%: C 70.12; H 18.97 $C_{18}H_{26}O_4$ Calculated,%: C 70.58; H 18.49. ^{1}H NMR spectrum (DMSO-d_6), δ ppm: 1.02 s (12H, $4CH_3$), 2.15 s (4H, $2CH_2$), 2.25 s (4H, $2CH_2$), 4.15 s (4H, $2CH_2$), 5.4 s (2H, 2CH=). ^{13}C NMR spectrum (DMSO-d_6), δ ppm: 19, 22, 41, 51, 63, 101, 176, 198.

3,3,12,12-tetramethyldispiro[5,2,59,26]hexadecane-1,5,10,14-tetraone (4). Yield 7 g (23%), m.p. 300 ^{0}C. Found,%: C 72.76; H 8.68 $C_{20}H_{28}O_4$ Calculated,%: C 72.28; H 8.43. ^{1}H NMR spectrum (DMSO-d_6), δ ppm: 1.02 s (12H, $4CH_3$), 1.8 m (8H, $4CH_2$), 2.30 s (8H, $4CH_2$). ^{13}C NMR spectrum (DMSO-d_6), δ ppm: 22.1 (CH_2-CH_2), 27.3 (CH_3), 32.4 ($(CH)_3C$), 50.4 (C-CO), 68.7 ($C(CH)_2$), 220 (CO).

3-[(2-chloroallyl)oxy]-5,5-dimethylcyclohex-2-en-1-on (5). 10 q (0.07 mol)of the reagent was added dropwise to a mixture of 0.12 mol of the compound with an active methylene group and 0.25 mol of K_2CO_3 in 50 ml of DMSO with stirring. The mixture was stirred for 12 h at 80^0C. Cooled, treated with water and extracted with ethyl ether. The extract was dried with $MgSO_4$, the solvent was distilled off, and the residue was distilled under vac

Found,%: C 51.27; H 5.69; Cl 13.87. $C_{11}H_{15}O_2Cl$ Calculated,%: C 51.86; H 5.9; Cl 13.94. ^{1}H NMR spectrum (DMSO-d_6), δ ppm: 0.98 s (6H, $2CH_3$), 2.1 s (2H, CH_2), 2.25 s (2H, CH_2), 4.35 s (2H, OCH_2), 5.24 s (1H, CH=), 5.45 d (2H, $=CH_2$, $^{2}J_{HH}$ 4 Гц).^{13}C NMR spectrum (DMSO-d_6), δC ppm.: 28, 33, 41.5, 50.5, 70, 101, 113, 133, 175, 198.

7,7-dimethyl-4,6,7,8-tetrahydro-2H-chromene-3,5-dione (6). 10 g (0.09 mol) dichloroacetone were added dropwise to a mixture of 10 g (0.07 mol) and 10 g K_2CO_3 in 30 ml DMSO at room temperature. Partial heating of the mixture (25 ^{0}C) was observed, cooled to room temperature and stirred for 6 h. The color of the mixture changed to orange. The mixture was treated with water, extracted with ether, the extract was dried with $MgSO_4$, and the solvent was distilled off. Yield of precipitated crystals **6** was 9.8 r (54%), m.p. 137-139 ^{0}C. Found,%: C 67.56 H 7.67. $C_{11}H_{14}O_3$ Calculated,%: C 68.0; H 7.21. ^{1}H NMR spectrum (DMSO-d_6), δ ppm.: 1.05 s (6H, $2CH_3$), 1.82 s (2H, CH_2CH=), 1.99 s (CH_2C=O), 3.12 s (2H, =C-CH_2), 5.12 s (2H, O-CH_2). ^{13}C spectrum (DMSO-d_6), δC ppm: 27.2, 27.8, 33.3, 37.9, 78.9, 105.8, 172.6, 205.8.

5,5-Dimetil-3-oxocyclohex-1-en-1-yl-2chloroacetate (7). To a mixture of 3.1 g (0.02 mol) dimedone, 1.8 g (0.02 mol) pyridine in 20 ml of ether, 3 g (0.025 mol) of chloroacetic acid chloride was added drop by drop. The mixture was stirred for 4 hours at room temperature. The ether layer was separated, crystals fell out, recrystallized in benzene. White crystals fell out **7**. Yield 4.2 g (67%), t.pl. 138-140 ^{0}C. Found, %: C 56.3; H 4.86; Cl 20.98 $C_{10}H_{12}O_3Cl$ Calculated,%: C C 55.6; H 5.5; Cl 21.5. ^{1}H NMR spectrum (DMSO-d_6), δ ppm.: 0.96 s (6H, $2CH_3$), 2.07 s (2H, CH_2C=), 2.35 c (2H, CH_2C=O), 4.39 s (2H, CH_2Cl), 5.40 d (1H, CH=). ^{13}C spectrum (DMSO-d_6), δC ppm: 27.2, 32.6, 41.5, 44.6, 47.8, 118.8, 171.7, 189.2.

Method of alkylation of ethyl cyanoacetate with dichloroethane. Drops of 10 g (0.065 mol) of dichloroetan were added to a mixture of 10 g (0.07 mol) of ethyl cyanoacetate and 10 g of K_2CO_3 in 40 ml of DMSO. The mixture was stirred at room temperature for 6 hours. After that, the mixture was treated with water, extracted with ether, $MgSO_4$ dried, and the solvent was distilled.

Ethyl 1-cyanocyclopropane-1-carboxylate (8). Yield 14.8 g (62%), b.p. 145^{0}C (2 mm Hg). Found,%: C 63.23; H 6.17; N 11.16. $C_7H_9O_2N$ Calculated,: C 60.43; H 6.47; N 10.07. ^{1}H NMR spectrum ($CDCl_3$), δ ppm: 1.32 t (3H, CH_3), 1.82-187 m (4H, $2CH_2$), 4.6 k (2H, CH_2)/ ^{13}C NMR spectrum ($CDCl_3$), δ ppm: 9.1, 13.6, 15.2, 61.1, 114.9, 172.4.

Diethyl(1s,4s)-1-carboyl-4-cyanocyclohexane-1,4-dicarboxylate (9).

Crystals fell out of the remaining liquid after 4 days. Yield 5 g (25%), m.p. 173-175^{0}C. Found,%: C 56.12; H 8.97; N 10.15. $C_{14}H_{20}O_5N_2$ Calculated,%: C 56.75; H 6.75; N 9.46. ^{1}H NMR spectrum (DMSO-d_6), δ ppm: 1.1 t (6H, $2CH_3$), 2.15 m (4H, $2CH_2$), 2.25 m (4H, $2CH_2$), 4.25 k (4H, $2CH_2$), 7.4 s (2H, NH_2). ^{13}C NMR spectrum (DMSO-d_6), δ ppm: 16, 22.7, 26.4, 34, 51.8, 63, 124, 172, 178.8, 188.

Triethyl 3-cyano-3.4-diiminopentane-1.3.5-tricaroxylate (10). A mixture consisting of 10 g of ethyl cyanoacet and 3 g of triethyl phosphite was heated for 5 hours in a flask with a reverse cooler at 120 ^{0} C.. Cooled, white crystals fell out, and recrystallized with benzene. The yield of product **10** was 7.8 g (67 %), m.p. 156 ^{0}C. Found,%: C 54.12; H 6.97; N 10.15. $C_{15}H_{21}O_6N_3$ Calculated,%: C 53.09; H 6.20; N 12.40. ^{1}H NMR spectrum (DMSO-d_6), δ ppm: 1.1 t (9H, $3CH_3$), 4.23 m (6H, 3 O-CH_2), 2.25 m (4H, $2CH_2$), 9.4 s (2H, 2NH). ^{13}C NMR spectrum (DMSO-d_6), δ ppm: 16, 44.3 61.8, 114, 164.6, 168.1, 172.

Result and Discussion

As noted above [5], acetylacetone is alkylated with 1,2-dibromoethane in DMSO in the presence of potash to form gem-diacetylcyclopropane (C,C-dialkylation). This reaction under the specified conditions with 1,2-dichloroethane at a temperature of 80 0C yields as the main product – O,O-intermolecular dialkylation (1), where two moles of acetylacetone and one mole of dichloroethane participate in the reaction and a small amount of the C,O-dialkylation product is formed – a furan derivative (2).

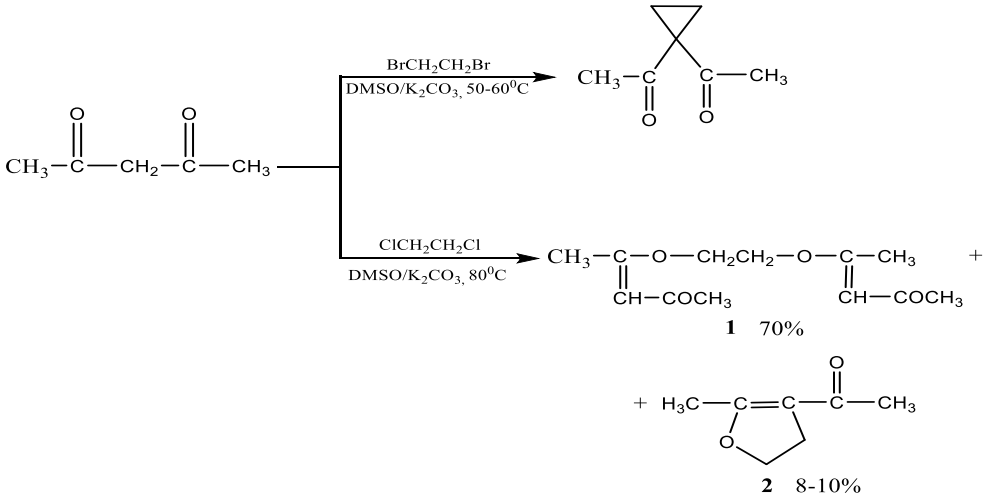

Similar to acetylacetone, indanedione is also alkylated with 1,2-dibromoethane to form a cyclopropane derivative [9], while this reaction with 1,2-dichloroethane has been shown to proceed in a 2:2 ratio to give a product with a dispiro structure.

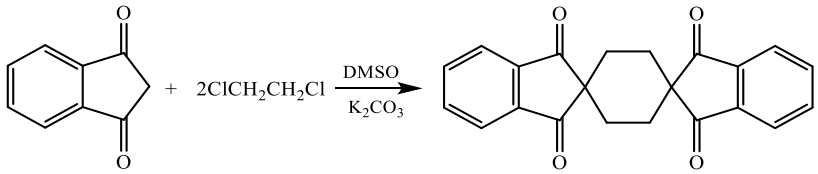

In [10] it was shown that alkylation of cyclohexadione-1,3 with diethyl acetal of bromoacetic aldehyde, contrary to expectations, occurs at position 4, while the active methylene group remains unaffected, whereas alkylation of the said diketone with enol ethers occurs at the active methylene group [11].

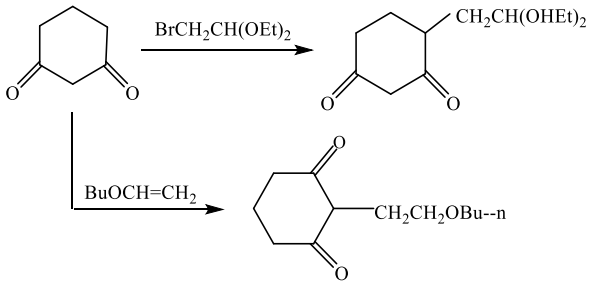

In subsequent studies on the alkylation of dimethylcyclohexadione (dimedone) with acetaldehyde bromoacetal, it was shown that, depending on the nature of the solvent, the reaction proceeds to form O-alkylation products (in DMSO), while in dimethylformamide (DMF) the reaction proceeds via the active methylene group to form a C-alkylation product [12].

However, the condensation of dimedone with 1,2-dichloroethane in DMSO at a temperature of 80^{0}C proceeds via the oxygen atom to form the O,O-intermolecular dialkylation product 3.

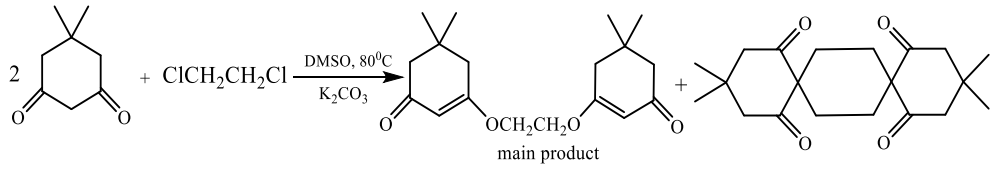

3 **4**

The condensation product of dimedone with 1,2,3-trichloropropane in the presence of potash in DMSO also forms an O-alkylation product. Dehydrochlorination occurs simultaneously, resulting in the formation of the enol ether of dimedone **5**.

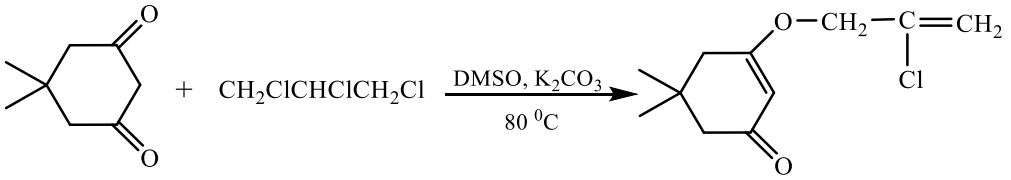

5

Unlike dichloroethane, only one chlorine atom participates in this condensation, which is apparently due to the fact that in the first stage, 1,2,3-trichloropropane, under the action of potash, undergoes dehydrohalogenation with the formation of 2,3-dichloropropene, in which allyl chlorine, being active, enters into condensation with the formation of enol ether **7**.

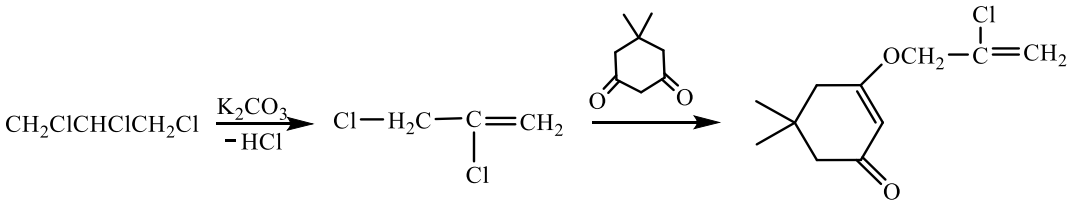

5

This judgment has been confirmed experimentally. Chlorine in the resulting enol ether is passive and does not enter into a substitution reaction under normal conditions.

It should be noted that along with the enol ether 3, an insignificant amount of a crystalline mass is formed, which does not dissolve in common organic solvents, melts at a temperature above 300 0C and, according to the 1H NMR spectrum, is a product of C,C-intermolecular alkylation having a bispiro structure 4, as in the case of indanedione.

In the literature [13], it is noted that the condensation of dimedone with 1,3-dichloroacetone in the presence of potassium hydroxide in methanol gives a product of C,C-intermolecular alkylation, which is subsequently converted into 1,1-bis(2,6-dioxy-4,4-dimethylcyclohexyl)-2-propanone.

We noted that this reaction in DMSO in the presence of potash as a result of intramolecular C,O-cycloalkylation gives a bicyclic compound 6.

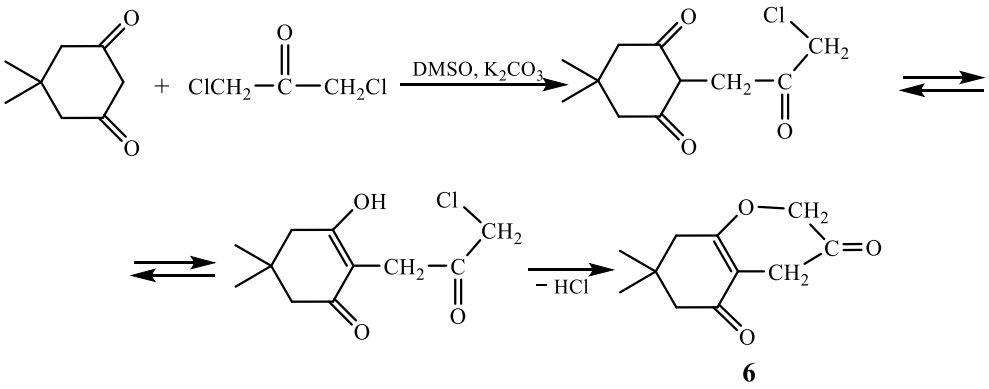

6

Acylation of dimedone with chloroacetic acid chloride in the presence of pyridine leads to the O-acylation product **6**.

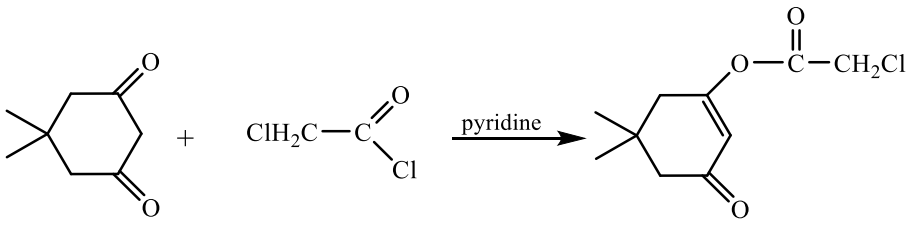

7

Alkylation of ethyl cyanonitrile with 1,2-dichloroethane leads to the formation of three compounds: a product of intramolecular C,C-dialkylation with the formation of gem-ethoxycarbonylnitrile cyclopropane, a product of intermolecular dialkylation with the formation of bis(1,4-ethoxycarbonylcyano)cyclohexane, which under the reaction conditions is partially hydrolyzed by the cyano group with the formation of an amide derivative, and a polymeric product that is formed as a result of the polycondensation of acetonitrile with dichloroethane.

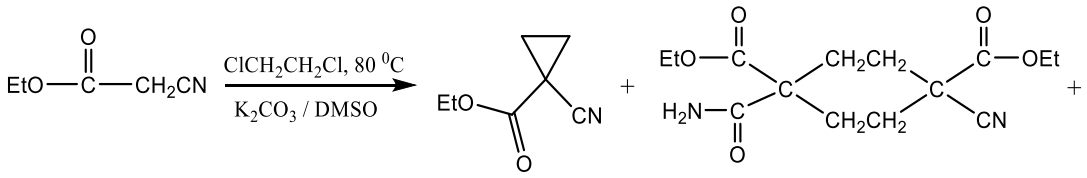

8 **9**

+ polymer

The structure of the first two products is confirmed by the NMR ^{1}H and ^{13}C spectra.

The formation of these three products should be considered as a process of further transformation of the product that is formed in the first stage of the alkylation reaction (A)

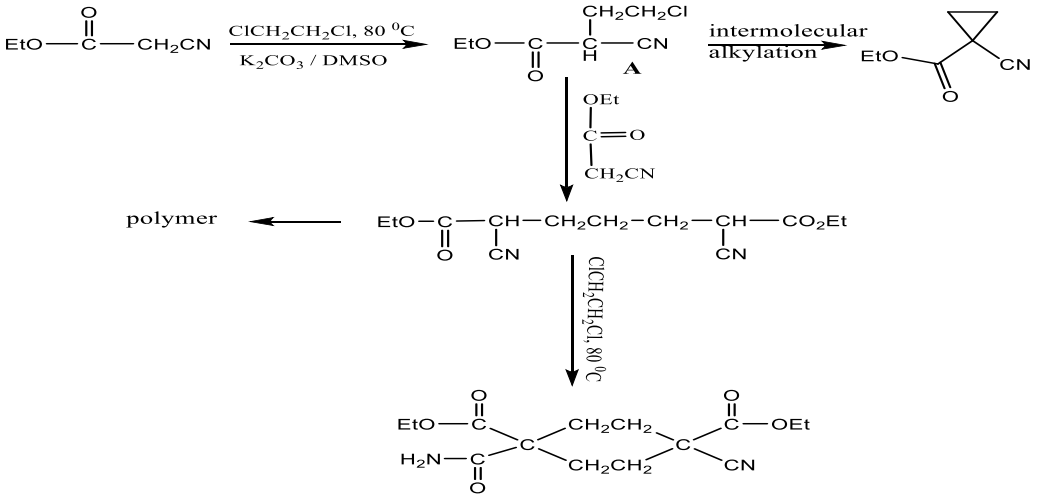

An amorphous glassy phase, which is practically insoluble in water and in organic solvents, according to IR spectra, is a polymer, the structure of which should be studied separately.

It should be noted that ethyl cyanoacetate, in addition to alkylation, also enters into a self-condensation reaction. In [14], it was shown how ethyl cyanoacetate in the presence of an iridium hydride catalyst self-condenses with the participation of two moles of the substrate, resulting in the formation of an enamine.

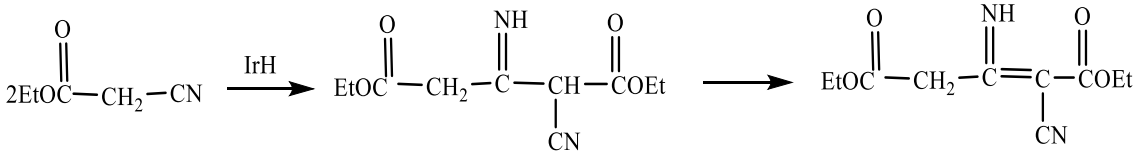

We have shown that in the presence of triethyl phosphite, ethyl cyanoacetate undergoes self-condensation with the participation of three moles of the original. As a result, a product of a different structure is formed, namely, a diimino derivative.

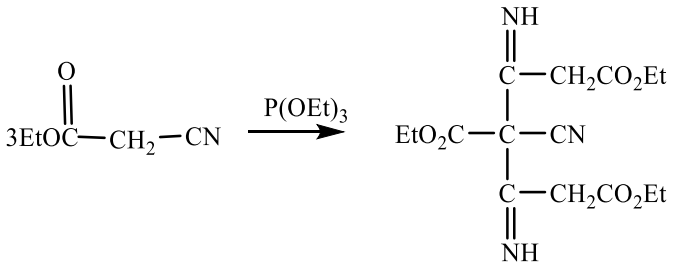

10

LITERATURE

1. Stone M.J., Maplesfone R.A., Rahman S.K. et al. (1991). Syenthisis of 3,5-dihydroxyphenylglycine derivatives and the C-termil dipeptide of vancomycin. Tetrahedron Letters, 32(23), p.2663
2. De, Subhadir; Kinthada, Lakshmana K.; Bisai, Alakesh. (2012). Base-promoted Michael reaction concomitant with alkilateon of cyclic 1,3-diones, an efficient approach to 2-substituted vinylogons esters. Synlett, 23(19), p.2785
3. Rahn N., Bendrath I., Hein M., et al. (2011). Synthesis and characterization of bis-cyclopropanated 1,3,5-tricarbonyl compounds. A combined synthetic, spectroscopic and theoreticalstudy. Organic & Biomolekular Chemistry, 9, p.5172
4. Шокова Э.А., Ким Джун Кын, Ковалев В.В. (2015). 1,3-Дикетоны. Синтез и свойства и свойства . ЖОрХ, 51(6), с.773
5. Зефиров Н.С., Кузнецова Т.С., Кожушков С.И. (1983). Циклоалкилирование α-, ω-дибромидами соединений, содержащих активированную метиленовую группы, как метод синтеза 1,1-дизамещенных C_nH_{2n} циклоалканов. ЖОрХ, 19(3), с. 541
6. Зефиров Н.С., Кузнецова Т.С., Кожушков С.И. и др. (1983). Алкилирование циклических 1,3-дикетонов α,ω-дибромидами ЖОрХ, 19(8), с. 1599
7. Ахмедов Ш.Т., Садыхов Н.Д., Исмаилов В.М., Зефиров Н.С. (1986). Алкилирование β-дикарбонильных соединений с 1,2,3-тригалогенпропаном как метод синтеза замещенных фуранов ХГС, №12, с.1602
8. Ismayilov V.M., Yusubov N.N., Sadikhova N.D. et al. (2016). Alkylation of Methylene – Active Comhounds with Haloacetals and Hydrolysis of the Alkylation Products.Russian Journal of Organic Chemistry, 52(10), p.1390
9. Гюльмалиев Т.М., Исмаилов В.М., Юсубов Н.Н., Москва В.В. (2009). Алкилирование индадиона 1,2-дихлорэтаном и 1,3-дибромпропаном. ЖОрХ, 45(12), с.1836
10. Benard Juma, Muhammed Adeel, Alexander Villinger, Peter Langer. (2008). Efficient synthesis of 2,6-dioxo-1,2,3,4,5,6-hexahydroindoles based on the synthesis and reactions of (2,4-dioxocyclohex-1-yel)acetic acid derivaties. Tetrahedron letters, 49(14), p. 2272
11. Nicola M.Berry, Mark C.P. Darey, Laurence M.Harwood. (1986). Photochemical 2-alkylation of cyclohexone-1.3-diones with enol ethers. Tetrahedron Letters, 27(20), p. 2319
12. Ismayilov V.M., Sadigova N.D., Yusubov N.N. and et al. (2013). Astraightforward synthesis of 2(3) 6,6-trimethyl-6.7-dihydrobenzofuran-4(5)-ones. Mendellev communications, 23(5), p. 292
13. Mattson H., Brigitta S. and Carl Axel Wachtmeister. (1970). Sinthesis of Functionally Substituted Furon and Resorcinal Derivatties from Dimetyl-3-oxopentanedionat. Acta Chemica Scandinavica, 24, p.3326
14. Hikaru Takaya, Takeshi Naota and Shunichi Murahashi. (1998). Indium Hydride Complex Catalyzed Addition of Nitriles to Carbon-Nitrogen Triple Bonds of Nitriles. J. Amerikan Chemistry Sociery, 120(17). p. 4244

2024. Volume 8, Number 1 ***Pages 67-76***

UOT: 547.141:547.539
https://doi.org/10.30546/2521-6317.2024.301

METHANOLYSIS OF DICHLORODIAZADIENES SYNTHESIZED BASED ON 4-METHYLBENZALDEHYDE

[1]Namiq Q. SHIKHALIYEV, [2]Ayten M. QAJAR, [2]Nigar E. AHMEDOVA, [2]Khatira A. GARAZADE, [2]Abel M. MAHARRAMOV, [2]İradə M. ŞIKHALIYEVA, [3]Ayten A. NIYAZOVA

[1]Department of Chemical Engineering,
Baku Engineering University, Hasan Aliyev str, AZ0101,
Baku, Azerbaijan,
[2]Organic Chemistry Department,
Baku State University, Z. Khalilov str. 23, AZ 1148,
Baku, Azerbaijan,
[3]Department of Engineering and Applied Sciences,
Azerbaijan State University of Economics, M. Mukhtarov 194, 1001
Baku, Azerbaijan,
*Corresponding author.
E-mail: namiqst@gmail.com (Namiq Q. Shikhaliyev).

ARTICLE INFO

Article history:

Received:2024-09-27

Received in revised form:2024-09-27

Accepted:2024-10-24

Available online

Keywords:

dichlorodiazadienes, methanolysis reaction, arylhydrazones of α-keto acid esters

ABSTRACT

We carried out methanolysis of dichlorodiazadienes synthesized on the basis of 4-methylbenzaldehyde and as a result of the reaction it was determined that both isomers E/Z of methyl(Z)-2-(2-phenylhydrazineylidene)-2-(p-tolyl) acetate derivatives were obtained. The structures of the obtained compounds were confirmed by NMR and X-ray method. Compared to the E isomer, in the Z isomer, the hydrogen atom of the imine group formed an intramolecular hydrogen bond with the carbonyl group of the ester, which was reflected in the molecular structure. Taking this into account, we proposed two possible mechanisms of the reaction. Based on nucleophilic addition and nucleophilic substitution reactions, we have shown that E/Z isomers have S-cisoid, S-transoid configurations, which is clearly visible in molecular structures. Thus, we proposed a new convenient method for the synthesis of aryl hydrazones of α-keto acid esters from the solvolysis reaction of dichlorodiazadienes in alcohol. Based on the fact that the arylhydrazones of α-keto acid esters obtained as a result of the reaction have many antimicrobial, bactericidal and fungicidal properties, it is worth noting that they are important compounds from the point of view of organic synthesis and pharmacological chemistry.

1. Introduction

We know from the literature that various synthesis methods of α-keto acid esters have been carried out, and transition metal complexes were used as catalysts in these reactions [1-6], which shows how complex and economically expensive the synthesis method is. In general, one of the main problems that arise in conducting this type of syntheses is the occurrence of decarboxylation as a result of the reaction, that is, in other words, decarboxylation occurs after hydrolysis of the ester [7].

An example of the reactions carried out with the direct introduction of α-keto acid ester to the substrate [8] is the reaction in the presence of a platinum catalyst, in which the introduction of the α-keto acid ester group into the molecule occurs as a result of the direct acylation reaction with ethylchloroxoacetate by the method of C-H bond activation [9-13]. Since metalorganic reagents, such as the Grignard reagent, are used in other synthesis methods, as a result of the high reactivity of the latter, conducting the reaction at a very low temperature shows that this method is one of its shortcomings.

During the acylation according to the Friedel-Crafts reaction [14-16], the use of an excess amount of Lewis acid causes many problems in the purification of the reaction mixture, and the selectivity is also not fully observed. In general, α-keto acid esters are included in the composition of many biological and medical organic molecules, and are also used as starting reagents in the synthesis of many important organic compounds (α-hydroxy acids, α-amino acids). In addition, α-keto acid esters are used as important compounds in other areas of organic synthesis, for example, in the synthesis of heterocycles.

Namely, for the reasons mentioned above, the introduction of α-keto acid ester functional group into compounds is of great importance from the point of view of organic synthesis. Taking these into account, the solvolysis reaction of dichlorodiazadienes [17-25] synthesized by us in previous studies was carried out and arylhydrazones of α-keto acid esters [26] were obtained. As a result of these reactions, both isomers of esters were obtained, but the mechanism was not investigated.

Taking into account that arylhydrazones have antimicrobial, bactericidal and fungicidal properties [27] and at the same time have a pharmochor methyl group [28], our research was continued in the direction of methanolysis of dichlorodiazadienes based on 4-methylbenzaldehyde.

2. Results and Discussion

The methanolysis reactions of dienes synthesized on the basis of 4-CH_3-benzaldehyde were studied in order to investigate the mechanism by which both isomers can be obtained simultaneously during the methanolysis reactions of dichlorodiazadienes (Scheme 1).

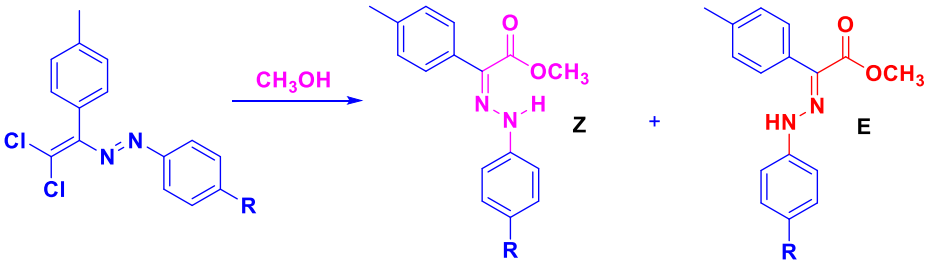

Scheme 1. Methanolysis reaction of dichlorodiazadienes.

The synthesized E/Z isomers were separated from the reaction mixture and the structures of the compounds were confirmed by NMR and X-ray methods. Below are NMR spectra of the E and Z isomers of compound 8 as an example.

It is clear from the 1H NMR spectrum that the signals of the Z isomer of compound 8 shift to a weaker area due to the H bond formed by the hydrogen atom of the imine group with the carbonyl group of the ester in the NMR spectrum. However, in the E isomer of that compound, a stronger field was observed than the Z isomer.

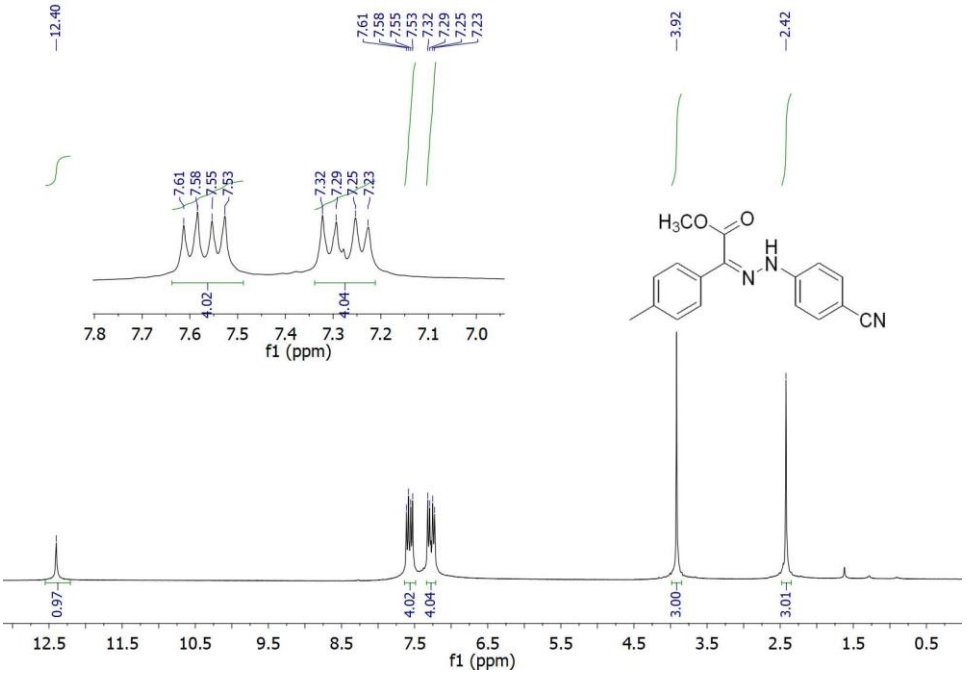

Figure 1. ^{1}H NMR spectrum of compound 8a

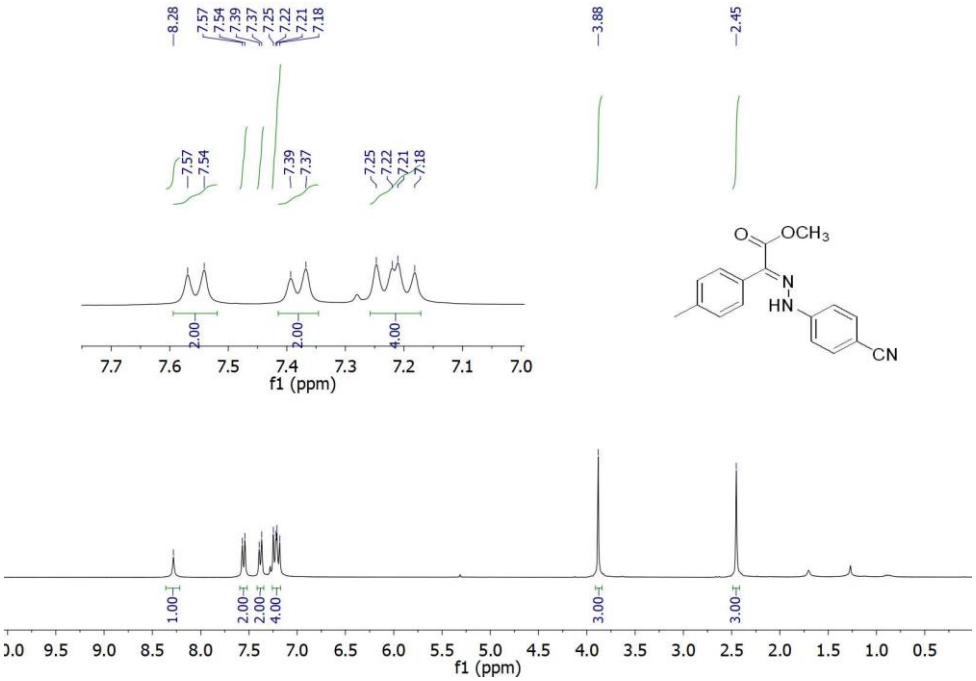

Figure 2. ^{13}C NMR spectrum of compound 8b

The molecular structure of some methyl (Z)-2-(2-phenylhydrazineylidene)-2-(p-tolyl)acetate derivatives was determined again by X-ray method, and the presence of hydrogen bonds is clearly seen from the molecular structure (Figure 3).

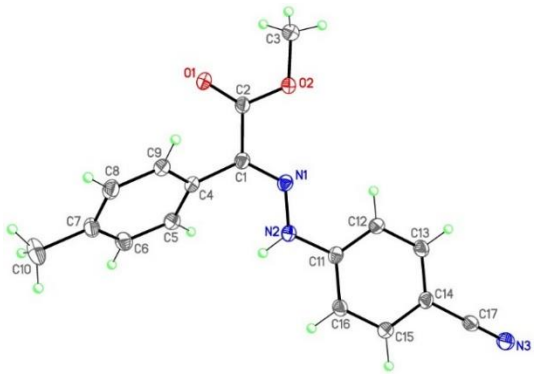

8a

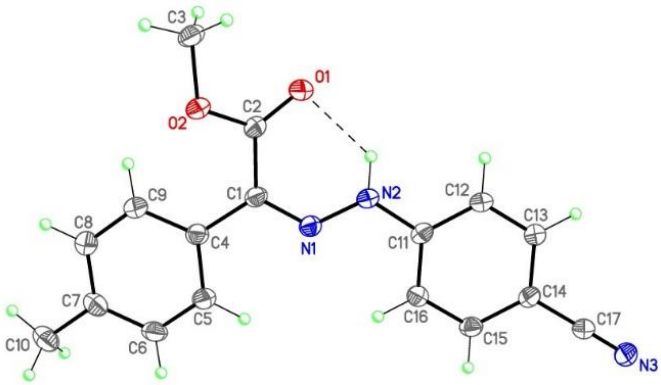

8b

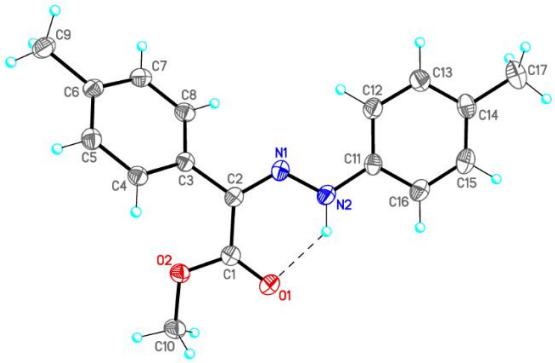

2a

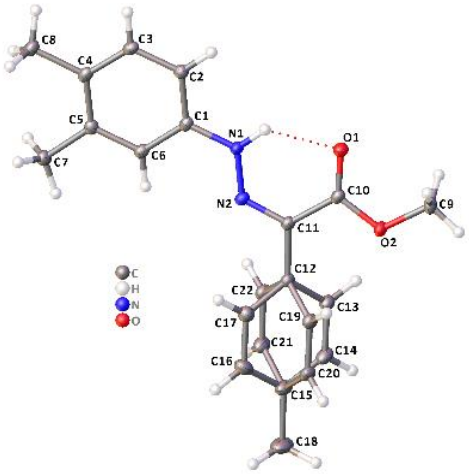

9a

Considering that both isomers are obtained simultaneously during the reaction, two possible reaction mechanisms have been proposed.

1**) Nucleophilic addition reaction to heterodiene**.

As we know, the nucleophilic addition reaction to heterodienes first follows the 1,4-addition reaction. In our reaction, intermediate compound A is probably formed during the 1,4-addition of alcohol. It should be noted that the presence of 2 chlorine atoms in sp^3 hybridized carbon in A and its hydrolysis reaction will lead to obtaining C of carbonyl group B. Thus, one of the methods of obtaining aldehydes is based on the hydrolysis reaction of heminal dichlorinated carbon. Then it is assumed that the hydrolysis of A leads to intermediate B first. Then, depending on which of the heminal hydroxyl groups, which OH group participates in the separation of water, E/Z isomers will be obtained at the same time (Scheme 2).

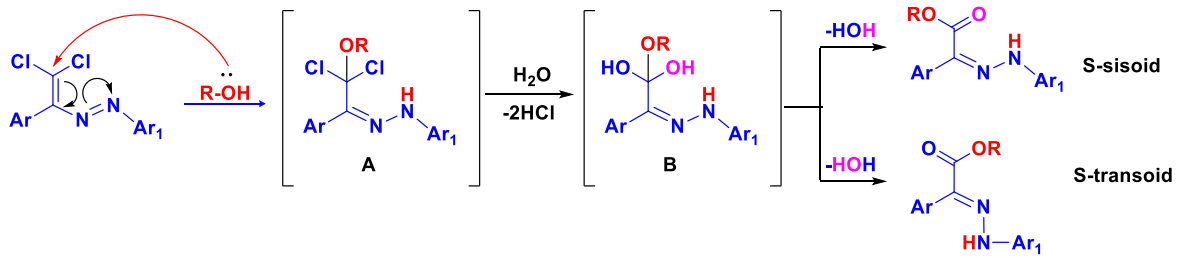

Scheme 2. The first probable mechanism of the reaction.

When we considered the molecular structures of the synthesized esters, we came across an interesting fact. Thus, it was determined that the 1,3-diene system (O=C-C=N-) in the Z-isomers has an S-cisoid configuration, while in the E-isomers have an S-transoid configuration (Figure 3)

1) The second direction is the nucleophilic substitution reaction of the chlorine atom and its hydrolysis:

In the proposed mechanisms for these reactions, taking into account the successive nucleophilic substitution of chlorine atoms, intermediate compound A will be obtained from the substitution of chlorine atom first in this reaction. Then, the hydrolysis of the second chlorine atom leads to the transition to the enol form B, and then to the more stable keto form.

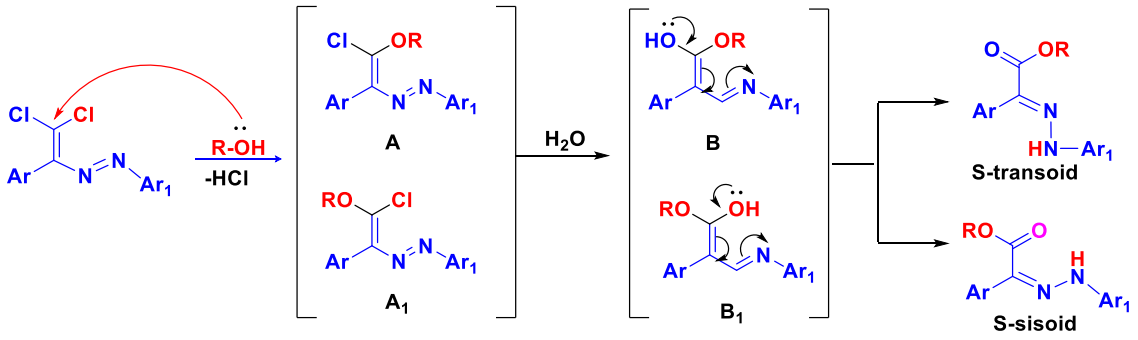

Scheme 3. The second possible mechanism of the reaction.

Thus, both proposed mechanisms involved the production of E/Z-isomers.

Conclusion

Thus, on the basis of a very simple synthesis reaction, the synthesis of methyl (Z)-2-(2-phenylhydrazineylidene)-2-(p-tolyl)acetate derivatives, which is considered an important compound from the point of view of organic synthesis and pharmacological chemistry, was achieved. The synthesis of aryl hydrazones of α-keto acid esters from the solvolysis reaction of dichlorodiazadienes can be considered a new convenient method, and this reaction has created opportunities for the synthesis of compounds with many antimicrobial, bactericidal and fungicidal properties.

Experimental Part

NMR ^{1}H and ^{13}C spectra were also recorded in $CDCl_3$ and DMSO on Bruker Avance 300 (operating frequency 300 MHz spectrometer. SiMe4 was used as an internal standard. UB-254 was performed on NTX Silufol plate, and acidified KMnO4 solution was used for clear visibility of the formed spots and UV lamp rays were used. Column chromatography was performed on silica gel from Merck (63-200).

10 mg of 1,1-dichlorodiazadiene is taken and stirred in 30 ml of ethanol solution for 2 hours using a magnetic stirrer at the boiling temperature of alcohol. After the specified time, the solution is ejected by the rotor. The reaction products are separated by column chromatography. The eluents used for this are dimethyl chloride and n-hexane (1:1), dimethyl chloride and ethanol. The main reaction product fractions separated by thin-layer chromatography are collected and re-evaporated in the rotor and the yield is calculated.

1. **methyl (Z)-2-(2-phenylhydrazineylidene)-2-(p-tolyl)acetate (1a)** yellow solid , (39%), mp 72 ^{0}C, ^{1}H NMR (300 MHz, Chloroform-*d*) δ 2.41 (s, 3H), 3.72 (s, 3H), 7.25 (t, *J* = 2.0 Hz, 1H), 7.42 (d, *J* = 7.5, 2H), 7.57 – 7.47 (m, 2H), 7.64 (d, *J* = 7.5 Hz, 2H), 8.19 (d, *J* = 7.5 Hz, 1H), 12.33 (s, 1 H), ^{13}C NMR (75 MHz, $CDCl_3$) δ 21.6, 54.4, 110.52, 112.5, 127.7, 130.1, 130.4, 131.8, 136.1, 143.4, 146.8, 151.9, 162.9,

   methyl (E)-2-(2-phenylhydrazineylidene)-2-(p-tolyl)acetate (1b) yellow solid , (28%), mp 114 ^{0}C, ^{1}H NMR (300 MHz, Chloroform-*d*) δ 2.38 (s, 3H), 2.68 (s, 3H), 7.15 (t, *J* = 2.0 Hz, 1H), 7.38 (d, *J* = 7.5, 2H), 7.52 – 7.45 (m, 2H), 7.60 (d, *J* = 7.5 Hz, 2H), 8.21 (d, *J* = 7.5 Hz, 1H), 8.53 (s, 1H), ^{13}C NMR (75 MHz, $CDCl_3$) δ 20.9, 50.8, 110.52, 115.7, 127.3, 128.4, 130.8, 135.7, 142.2, 145.7, 150.7, 163.7.

2. **methyl (Z)-2-(p-tolyl)-2-(2-(p-tolyl)hydrazineylidene)acetate (2a)** yellow solid (41%), mp 80 ºC. ^{1}H NMR (300 MHz, Chloroform-d) δ 2.38 (s 3H), 2.36 (s, 3H), 3.89 (s, 3H), 7.27 – 7.05 (m, 6H), 7.56 (d, *J* = 8.1 Hz, 2H), 12.40 (s, 1H). ^{13}C NMR (75 MHz, $CDCl_3$) δ 20.7, 21.2, 51.7, 113.8, 125.0, 126.6, 127.5, 129.6, 130.6, 131.8, 136.1, 140.5,164.3.

   methyl (E)-2-(p-tolyl)-2-(2-(p-tolyl)hydrazineylidene)acetate (2b yellow solid, (22%), mp 102 ^{0}C, ^{1}H NMR (300 MHz, Chloroform-d) δ 2.31 (s, 3H), 2.45 (s, 3H), 3.82 (s, 3H), 7.13 – 7.04 (m, 4H), 7.30 (d, *J* = 9.2 Hz, 2H), 7.57 (d, *J* = 8.4 Hz, 2H), 8.20 (s, 1H). ^{13}C NMR (75 MHz, $CDCl_3$) δ 20.3, 31.7, 52.8, 115.1, 123.5, 126.4, 127.4, 130.4, 133.5, 133.9, 139.5, 150.9,163.9.

3. **methyl (Z)-2-(p-tolyl)-2-(2-(m-tolyl)hydrazineylidene)acetate (3a)** yellow solid, (39%), mp 64 ^{0}C, ^{1}H NMR (300 MHz, Chloroform-d) δ 2.33 (s, 3H), 2.75 (s, 3H), 3.96 (s, 3H), 7.31 – 7.16 (m, 6H), 7.63 (d, *J* = 8.1 Hz, 2H), 11.87 (s, 1H), ^{13}C NMR (75 MHz, $CDCl_3$) δ 24.7, 34.7, 50.8, 111.7, 121.3, 127.6, 128.8, 130.7, 136.7, 137.8, 141.5, 151.5, 164.7.

4. **methyl (E)-2-(p-tolyl)-2-(2-(m-tolyl)hydrazineylidene)acetate (3b)** yellow solid (20%), mp 123^{0}C, ^{1}H NMR (300 MHz, Chloroform-d) δ 2.30 (s, 3H), 3.68 (s, 3H), 3.83 (s, 3H), 7.30 – 7.18 (m, 6H), 7.61 (d, *J* = 8.1 Hz, 2H), 9.21 (s, 1H). ^{13}C NMR (75 MHz, $CDCl_3$) δ 23.5, 33.9, 50.5, 110.7, 121.3, 125.6, 128.8, 132.6, 135.9, 139.5, 140.5, 153.5, 163.7.

   methyl(Z)-2-(2-(4-methoxyphenyl)hydrazineylidene)-2-(p-tolyl)acetate (4a) yellow solid, (30%), mp 84 ^{0}C, ^{1}H NMR (300 MHz, Chloroform-d) δ 2.21 (s, 3H), 3.83 (s, 3H), 3.90 (s, 3H), 6.92 (d, *J* = 8.9 Hz, 2H), 7.27 (d, *J* = 8.9 Hz, 2H), 7.45 (d, *J* = 8.4 H, 2H), 7.63 (d, *J* = 8.4 Hz, 2H), 12.48 (s, 1H), ^{13}C NMR (75 MHz, $CDCl_3$) δ31.4, 34.6, 51.6, 112.7, 117.4, 124.9, 128.3, 126.8, 133.8, 136.1, 150.4, 155.5, 162.4.

   methyl(E)-2-(2-(4-methoxyphenyl)hydrazineylidene)-2-(p-tolyl)acetate (4b) yellow solid, (21%), mp 126 ^{0}C, ^{1}H NMR (300 MHz, Chloroform-d) δ 2.18 (s, 3H), 3.82 (s, 3H), 3.89 (s, 3H), 6.90 (d, *J* = 8.2 Hz, 2H), 7.31 (d, *J* = 8.7 Hz, 2H), 7.48 (d, *J* = 8.2 Hz, 2H), 7.65 (d, *J* = 8.2 Hz, 2H), 8.79 (s, 1H), ^{13}C NMR (75 MHz, $CDCl_3$) δ 27.4, 31.2, 51.4, 114.6, 115.3, 124.7, 128.5, 128.6, 137.7, 153.4, 155.7, 157.6, 162.8.

5. **methyl (Z)-2-(2-(4-chlorophenyl)hydrazineylidene)-2-(p-tolyl)acetate (5a))** yellow solid, (30%), mp 89 ^{0}C, ^{1}H NMR (300 MHz, Chloroform-d) δ 2.76 (s, 3H), 3.86 (s, 3H), 6.91 (d, *J* = 7.8 Hz, 2H), 7.25 (d, *J* = 7.4 Hz, 2H), 7.68 (d, *J* = 8.4 Hz, 2H), 8.51 (d, *J* = 8.2 Hz, 2H), 12.24 (s, 1H), ^{13}C NMR (75 MHz, $CDCl_3$) δ 34.6, 51.6, 112.7, 118.4, 122.6, 123.6, 125.5, 137.2, 138.5, 153.4, 154.5, 165.4.

   methyl (E)-2-(2-(4-chlorophenyl)hydrazineylidene)-2-(p-tolyl)acetate (5b) yellow solid, (23%), mp 119 ^{0}C, ^{1}H NMR (300 MHz, Chloroform-d) δ 2.35 (s, 3H), 3.86 (s, 3H), 6.91 (d, *J* = 7.8 Hz, 2H), 7.25 (d, *J* = 7.4 Hz, 2H), 7.43 (d, *J* = 8.4 Hz, 2H), 7.53 (d, *J* = 8.2 Hz, 2H), 8.48 (s, 1H), ^{13}C NMR (75 MHz, $CDCl_3$) δ 32.8, 54.6, 117.7, 123.4, 126.6, 128.6, 134.5, 140.2, 142.8, 154.9, 152.7,162.4.

6. **methyl (Z)-2-(2-(4-bromophenyl)hydrazineylidene)-2-(p-tolyl)acetate (6a)** yellow solid, (35%), mp 66 ^{0}C, ^{1}H NMR (300 MHz, Chloroform-d) δ 2.76 (s, 3H), 3.86 (s, 3H), 6.91 (d, *J* = 7.8 Hz, 2H), 7.25 (d, *J* = 7.4 Hz, 2H), 7.68 (d, *J* = 8.4 Hz, 2H), 8.51 (d, *J* = 8.2 Hz, 2H), 12.24 (s, 1H), ^{13}C NMR (75 MHz, $CDCl_3$) δ 34.6, 51.6, 112.7, 118.4, 122.6, 123.6, 125.5, 137.2, 138.5, 153.4, 154.5, 165.4.

   methyl (E)-2-(2-(4-bromophenyl)hydrazineylidene)-2-(p-tolyl)acetate (6b) yellow solid, (30%), mp 100 ^{0}C, ^{1}H NMR (300 MHz, Chloroform-d) δ 2.45 (s, 3H), 3.83 (s, 3H), 6.84 (d, *J* = 7.8 Hz, 2H), 7.18 (d, *J* = 7.4 Hz, 2H), 7.89 (d, *J* = 8.4 Hz, 2H), 8.72 (d, *J* = 8.2 Hz, 2H), 8.48 (s, 1H), ^{13}C NMR (75 MHz, $CDCl_3$) δ 32.6, 50.6, 110.8, 115.4, 120.3, 121.7, 124.3, 133.7, 139.9, 155.4, 157.9, 166.5.

7. **methyl (Z)-2-(2-(4-nitrophenyl)hydrazineylidene)-2-(p-tolyl)acetate (7a)** yellow solid, (35%), mp 73 ^{0}C, ^{1}H NMR (300 MHz, Chloroform-d) δ 2.24 (s, 3H), 3.78 (s, 3H), 7.42 (m, 2H), 7.57 – 7.47 (m, 2H), 7.64 (d, *J* = 7.5 Hz, 2 H), 8.19 (d, *J* = 7.5 Hz, 2 H), 12.89 (s, 1H). ^{13}C NMR (75 MHz, $CDCl_3$) δ 32.4, 50.6, 110.52, 115.15, 126.40, 127.37, 133.48, 133.98, 135.51, 145.84, 145.58, 157.8, 159.8,

   methyl (E)-2-(2-(4-nitrophenyl)hydrazineylidene)-2-(p-tolyl)acetate (7b) yellow solid, (30%), mp 108 ^{0}C, ^{1}H NMR (300 MHz, Chloroform-d) δ 2.69 (s, 3H), 3.65 (s, 3H), 7.37 (m, 2H), 7.55 – 7.46 (m, 2H), 7.69 (d, *J* = 7.5 Hz, 2 H), 8.34 (d, *J* = 7.5 Hz, 2 H), 9.21 (s, 1H). ^{13}C NMR (75 MHz, $CDCl_3$) δ 35.6, 51.6, 110.2, 115.1, 124.4, 127.6, 133.4, 133.8, 135.5, 144.4, 145.6, 157.9, 159.4.

8. **methyl (Z)-2-(2-(4-cyanophenyl)hydrazineylidene)-2-(p-tolyl)acetate (8a)** yellow solid, (35%), mp 73 ^{0}C, ^{1}H NMR (300 MHz, Chloroform-d) δ 2.41 (s, 3H), 3.91 (s, 3H), 7.23-7.19 (m, 4H), 7.55-7.47 (m, 4H), 12.42 (s, 1H). 128.6, ^{13}C NMR (75 MHz, $CDCl_3$) δ 20.3, 52.6, 104.1, 114.1, 119.3, 128.8, 132.7, 133.1, 138.4, 146.6, 163.7, 169.6.

   methyl (E)-2-(2-(4-cyanophenyl)hydrazineylidene)-2-(p-tolyl)acetate (8b) yellow solid, (35%), mp 73 ^{0}C, ^{1}H NMR (300 MHz, Chloroform-d) δ 2.43 (s, 3H), 3.89 (s, 3H), 7.38-7.30 (m, 4H), 7.50-7.46 (m, 4 H), 8.28 (s, 1H). ^{13}C NMR (75 MHz, $CDCl_3$) δ 21.1, 50.4, 101.6, 113.3, 119.93, 127.1, 128.6, 129.7, 130.1, 137.8, 145.4, 163.5, 168.4.

9. **methyl(Z)-2-(2-(3,4-dimethylphenyl)hydrazineylidene)-2-(p-tolyl)acetate (9a)** yellow solid (40%), mp 100 ^{o}C. ^{1}H NMR (300 MHz, Chloroform-d) δ 2.31 (s, 3H), 2.35 (s, 3H), 2.47 (s, 3H), 3.93 (s, 3H), 7.18 – 7.09 (m, 3H), 7.29 (d, *J* = 8.0 Hz, 2H), 7.63 (d, *J* = 8.1 Hz, 2H), 12.46 (s, 1H),

^{13}C NMR (75 MHz, $CDCl_3$) δ 19.2, 20.1, 21.3, 51.6, 111.4, 116.5, 125.8, 129.7, 130.5, 131.5, 134.8, 137.4, 138.7, 142.3, 162.3.

methyl(E)-2-(2-(3,4-dimethylphenyl)hydrazineylidene)-2-(p-tolyl)acetate(9b) yellow solid (32%), mp 82 °C. ^{1}H NMR (300 MHz, Chloroform-d) δ 2.26 (s, 3H), 2.30 (s, 3H), 2.42 (s, 3H), 3.89 (s, 3H), 7.08 (dd, *J* = 20.2, 8.8 Hz, 3H), 7.24 (d, *J* = 7.9 Hz, 2H), 7.57 (d, *J* = 8.1 Hz, 2H), 8.12 (s, 1H), 12.39 (s, 1H). ^{13}C NMR (75 MHz, $CDCl_3$) δ 19.1, 20.1, 21.3, 51.6, 111.7, 115.5, 126.8, 128.6, 130.3, 130.7, 133.8, 137.4, 137.7, 141.2, 164.3.

REFERENCES

1. Eftekhari-Sis B, Zirak M. Chemistry of α-oxoesters: a powerful tool for the synthesis of heterocycles. Chemical reviews. 2015 Jan 14;115(1):151-264.
2. Elsebai MF, Kehraus S, Lindequist U, Sasse F, Shaaban S, Gütschow M, Josten M, Sahl HG, König GM. Antimicrobial phenalenone derivatives from the marine-derived fungus Coniothyrium cereale. Organic & Biomolecular Chemistry. 2011;9(3):802-8.
3. Kovács L. Methods for the synthesis of α-keto esters. Recueil des Travaux Chimiques des Pays-Bas. 1993;112(9):471-96.
4. Nazir M, El Maddah F, Kehraus S, Egereva E, Piel J, Brachmann AO, König GM. Phenalenones: insight into the biosynthesis of polyketides from the marine alga-derived fungus Coniothyrium cereale. Organic & biomolecular chemistry. 2015;13(29):8071-9.
5. Nie Y, Xiao R, Xu Y, Montelione GT. Novel anti-Prelog stereospecific carbonyl reductases from Candida parapsilosis for asymmetric reduction of prochiral ketones. Organic & biomolecular chemistry. 2011;9(11):4070-8.
6. Ocain TD, Rich DH. alpha. -Keto amide inhibitors of aminopeptidases. Journal of medicinal chemistry. 1992 Feb;35(3):451-6.
7. Babudri F, Fiandanese V, Marchese G, Punzi A. A General and Straightforward Approach to α, ω-Ketoesters. Tetrahedron. 1996 Oct 14;52(42):13513-20.
8. Javed E, Guthrie JD, Neu J, Chirayath GS, Huo S. Introducing an α-Keto Ester Functional Group through Pt-Catalyzed Direct C–H Acylation with Ethyl Chlorooxoacetate. ACS omega. 2020 Apr 3;5(14):8393-402.
9. Allen CL, Williams JM. Ruthenium-Catalyzed Alkene Synthesis by the Decarbonylative Coupling of Aldehydes with Alkynes. Angewandte Chemie International Edition. 2010 Feb 22;10(49):1724-5.
10. Correa A, Cornella J, Martin R. Nickel-Catalyzed Decarbonylative C◎ H Coupling Reactions: A Strategy for Preparing Bis (heteroaryl) Backbones. Angewandte Chemie International Edition. 2013 Feb 11;52(7).
11. Malapit CA, Ichiishi N, Sanford MS. Pd-catalyzed decarbonylative cross-couplings of aroyl chlorides. Organic letters. 2017 Aug 4;19(15):4142-5.
12. Wang S, Yang Z, Liu J, Xie K, Wang A, Chen X, Tan Z. Efficient synthesis of anthranilic esters via Pd-catalyzed dehydrogenative/decarbonylative coupling of anilides and glyoxylates. Chemical Communications. 2012;48(79):9924-6.
13. Wu XF. Acylation of (Hetero) Arenes through C◎ H Activation with Aroyl Surrogates. Chemistry–A European Journal. 2015 Aug 24;21(35):12252-65.
14. Sprenger RD, Ruoff PM, Frazer AH. Citrinin Studies. Hydroxy-and Methoxy-phenylglyoxylic Acids1. Journal of the American Chemical Society. 1950 Jul;72(7):2874-6.
15. Wadhwa K, Yang C, West PR, Deming KC, Chemburkar SR, Reddy RE. Synthesis of arylglyoxylic acids and their collision-induced dissociation. Synthetic Communications. 2008 Nov 13;38(24):4434-44.
16. Xiang JM, Li BL. Solvent-free synthesis of some ethyl arylglyoxylates. Chinese Chemical Letters. 2009 Jan 1;20(1):55-7.
17. Maharramov AM, Shikhaliyev NQ, Suleymanova GT, Gurbanov AV, Babayeva GV, Mammadova GZ, Zubkov FI, Nenajdenko VG, Mahmudov KT, Pombeiro AJ. Pnicogen, halogen and hydrogen bonds in (E)-1-(2, 2-dichloro-1-(2-nitrophenyl) vinyl)-2-(para-substituted phenyl)-diazenes. Dyes and Pigments. 2018 Dec 1;159:135-41.
18. Nenajdenko VG, Shikhaliyev NG, Maharramov AM, Bagirova KN, Suleymanova GT, Novikov AS, Khrustalev VN, Tskhovrebov AG. Halogenated diazabutadiene dyes: Synthesis, structures, supramolecular features, and theoretical studies. Molecules. 2020 Oct 29;25(21):5013.
19. Shikhaliyev NG, Maharramov AM, Bagirova KN, Suleymanova GT, Tsyrenova BD, Nenajdenko VG, Novikov AS, Khrustalev VN, Tskhovrebov AG. Supramolecular organic frameworks derived from bromoaryl-substituted dichlorodiazabutadienes via Cl··· Br halogen bonding. Mendeleev Communications. 2021 Mar 1;31(2):191-3.
20. Shikhaliyev NQ, Çelikesir ST, Akkurt M, Bagirova KN, Suleymanova GT, Toze FA. Crystal structure and Hirshfeld surface analysis of (E)-1-(4-chlorophenyl)-2-[2, 2-dichloro-1-(4-fluorophenyl) ethenyl] diazene. Acta Crystallographica Section E: Crystallographic Communications. 2019 Apr 1;75(4):465-9.

21. Akkurt M, Shikhaliyev NQ, Suleymanova GT, Babayeva GV, Mammadova GZ, Niyazova AA, Shikhaliyeva IM, Toze FA. Crystal structures and Hirshfeld surface analyses of the two isotypic compounds (E)-1-(4-bromophenyl)-2-[2, 2-dichloro-1-(4-nitrophenyl) ethenyl] diazene and (E)-1-(4-chlorophenyl)-2-[2, 2-dichloro-1-(4-nitrophenyl) ethenyl] diazene. Acta Crystallographica Section E: Crystallographic Communications. 2019 Aug 1;75(8):1199-204.

22. Çelikesir ST, Akkurt M, Shikhaliyev NQ, Mammadova NA, Suleymanova GT, Khrustalev VN, Bhattarai A. Crystal structure and Hirshfeld surface analysis of (E)-1-[2, 2-dibromo-1-(2-nitrophenyl) ethenyl]-2-(4-fluorophenyl) diazene. Acta Crystallographica Section E: Crystallographic Communications. 2022 Apr 1;78(4):404-8.

23. Akkurt M, Shikhaliyev NQ, Suleymanova GT, Babayeva GV, Mammadova GZ, Niyazova AA, Shikhaliyeva IM, Toze FA. Crystal structures and Hirshfeld surface analyses of the two isotypic compounds (E)-1-(4-bromophenyl)-2-[2, 2-dichloro-1-(4-nitrophenyl) ethenyl] diazene and (E)-1-(4-chlorophenyl)-2-[2, 2-dichloro-1-(4-nitrophenyl) ethenyl] diazene. Acta Crystallographica Section E: Crystallographic Communications. 2019 Aug 1;75(8):1199-204.

24. Shikhaliyev NG, Maharramov AM, Suleymanova GT, Babayeva GV, Mammadova GZ, Shikhaliyeva IM, Babazade AA, Nenajdenko VG. Halogen-bonding in 3-nitrobenzaldehyde-derived dichlorodiazadienes. Organic Chemistry. 2021 Jan 1(part iii):0-.

25. Nenajdenko VG, Shikhaliyev NG, Maharramov AM, Atakishiyeva GT, Niyazova AA, Mammadova NA, Novikov AS, Buslov IV, Khrustalev VN, Tskhovrebov AG. Structural Organization of Dibromodiazadienes in the Crystal and Identification of Br··· O Halogen Bonding Involving the Nitro Group. Molecules. 2022 Aug 11;27(16):5110.

26. Shikhaliyev NG, Maharramov AM, Suleymanova GT, Babazade AA, Nenajdenko VG, Khrustalev VN, Novikov AS, Tskhovrebov AG. Arylhydrazones of α-keto esters via methanolysis of dichlorodiazabutadienes: Synthesis and structural study. Mendeleev Communications. 2021 Sep 1;31(5):677-9.

27. Süleymanova G.T. Antimikrob xassələrinin tədqiqi. Journal of Baku Engineering University.:120.

28. Shikhaliyev N.G, Suleymanova G.T, İsrayilova A.A, Ganbarov K.G, Babayeva G.V, Garazadeh Kh.A, Mammadova GZ, Nenajdenko V.G. Synthesis, characterization and antibacterial studies of dichlorodiazadienes. Organic Chemistry. 2019(part vi):64-75

INSTRUCTIONS FOR AUTHORS

1. "The Baku Engineering University Journal-Chemistry and Biology" accepts original unpublished articles and reviews in the research field of the author.
2. Articles are accepted in English.
3. File format should be compatible with **Microsoft Word** and must be sent to the electronic mail (**journal@beu.edu.az**) of the Journal. The submitted article should follow the following format:

- Article title, author's name and surname
- The name of workplace
- Mail address
- Abstract and key words

4. The title of the article should be in each of the three languages of the abstract and should be centred on the page and in bold capitals before each summary.
5. **The abstract** should be written in **9 point** type size, between **100** and **150** words. The abstract should be written in the language of the text and in two more languages given above. The abstracts of the article written in each of the three languages should correspond to one another. The keywords should be written in two more languages besides the language of the article and should be at least three words.
6. . **UDC** and **PACS** index should be used in the article.
7. The article must consist of the followings:

- Introduction
- Research method and research
- Discussion of research method and its results
- In case the reference is in Russian it must be given in the Latin alphabet with the original language shown in brackets.

8. **Figures, pictures, graphics and tables** must be of publishing quality and inside the text. Figures, pictures and graphics should be captioned underneath, tables should be captioned above.
9. **References** should be given in square brackets in the text and listed according to the order inside the text at the end of the article. In order to cite the same reference twice or more, the appropriate pages should be given while keeping the numerical order. For example: [7, p.15].

Information about each of the given references should be full, clear and accurate. The bibliographic description of the reference should be cited according to its type (monograph, textbook, scientific research paper and etc.) While citing to scientific research articles, materials of symposiums, conferences and other popular scientific events, the name of the article, lecture or paper should be given.

Samples:

a) ***Article:*** Demukhamedova S.D., Aliyeva İ.N., Godjayev N.M.. *Spatial and electronic structure af monomerrik and dimeric conapeetes of carnosine üith zinc,* Journal of structural Chemistry, Vol.51, No.5, p.824-832, 2010

b) ***Book:*** Christie ohn Geankoplis. *Transport Processes and Separation Process Principles*. Fourth Edition, Prentice Hall, p.386-398, 2002

c) ***Conference paper:*** Sadychov F.S., Aydın C., Ahmedov A.İ.. Appligation of Information – Commu-nication Technologies in Science and education. II International Conference."*Higher Twist Effects In Photon- Proton Collisions", Bakı, 01-03 Noyabr, 2007, ss 384-391*

References should be in 9-point type size.

10. The margins sizes of the page: - Top 2.8 cm. bottom 2.8 cm. left 2.5 cm, right 2.5 cm. The article main text should be written in Palatino Linotype 11 point type size single-spaced. Paragraph spacing should be 6 point.
11. The maximum number of pages for an article should not exceed 15 pages
12. The decision to publish a given article is made through the following procedures:

- The article is sent to at least to experts.
- The article is sent back to the author to make amendments upon the recommendations of referees.
- After author makes amendments upon the recommendations of referees the article can be sent for the publication by the Editorial Board of the journal.

YAZI VƏ NƏŞR QAYDALARI

1. "Journal of Baku Engineering University-Kimya və Biologiya"- əvvəllər nəşr olunmamış orijinal əsərləri və müəllifin tədqiqat sahəsi üzrə yazılmış icmal məqalələri qəbul edir.
2. Məqalələr İngilis dilində qəbul edilir.
3. Yazılar **Microsoft Word** yazı proqramında, (**journal@beu.edu.az**) ünvanına göndərilməlidir. Göndərilən məqalələrdə aşağıdakılara nəzərə alınmalıdır:

- Məqalənin başlığı, müəllifin adı, soyadı,
- İş yeri,
- Elektron ünvanı,
- Xülasə və açar sözlər.

4. **Məqalədə başlıq hər xülasədən əvvəl** ortada, qara və böyük hərflə xülasələrin yazıldığı hər üç dildə olmalıdır.
5. **Xülasə** 100-150 söz aralığında olmaqla, 9 punto yazı tipi böyüklüyündə, məqalənin yazıldığı dildə və bundan əlavə yuxarıda göstərilən iki dildə olmalıdır. Məqalənin hər üç dildə yazılmış xülasəsi bir-birinin eyni olmalıdır. Açar sözlər uyğun xülasələrin sonunda onun yazıldığı dildə verilməklə ən azı üç sözdən ibarət olmalıdır.
6. Məqalədə UOT və PACS kodları göstərilməlidir.
7. Məqalə aşağıdakılardan ibarət olmalıdır:

- Giriş,
- Tədqiqat metodu
- Tədqiqat işinin müzakirəsi və onun nəticələri,
- İstinad ədəbiyyatı rus dilində olduğu halda orjinal dili mötərzə içərisində göstərməklə yalnız Latın əlifbası ilə verilməlidir.

8. **Şəkil**, **rəsm**, **grafik** və **cədvəllər** çapda düzgün, aydın çıxacaq vəziyyətdə və mətn içərisində olmalıdır. Şəkil, rəsm və grafiklərin yazıları onların altında yazılmalıdır. Cədvəllərdə başlıq cədvəlin üstündə yazılmalıdır.
9. **Mənbələr** mətn içərisində kvadrat mötərizə daxilində göstərilməklə məqalənin sonunda mətn daxilindəki sıra ilə düzülməlidir. Eyni mənbəyə iki və daha cox istinad edildikdə əvvəlki sıra sayı saxlanmaqla müvafiq səhifələr göstərilməlidir. Məsələn: [7,səh.15].

Ədəbiyyat siyahısında verilən hər bir istinad haqqında məlumat tam və dəqiq olmalıdır. İstinad olunan mənbənin biblioqrafik təsviri onun növündən (monoqrafiya, dərslik, elmi məqalə və s.) asılı olaraq verilməlidir. Elmi məqalələrə, simpozium, konfrans, və digər nüfuzlu elmi tədbirlərin materiallarına və ya tezislərinə istinad edərkən məqalənin, məruzənin və ya tezisin adı göstərilməlidir.

Nümunələr:

a) ***Məqalə:*** Demukhamedova S.D., Aliyeva İ.N., Godjayev N.M.. *Spatial and electronic structure af monomeric and dimeric complexes of carnosine with zinc,* Journal of structural Chemistry, Vol.51, No.5, p.824-832, 2010

b) ***Kitab:*** Christie ohn Geankoplis. *Transport Processes and Separation Process Principles*. Fourth Edition, Prentice Hall, 2002

c) ***Konfrans:*** Sadychov F.S., Aydın C., Ahmedov A.İ.. Appligation of Information-Communication Technologies in Science and education. II International Conference. "*Higher Twist Effects In Photon- Proton Collisions", Bakı, 01-03 Noyabr, 2007, ss 384-391*

Mənbələr 9 punto yazı tipi böyüklüyündə olmalıdır.

10. **Səhifə ölçüləri:** üstdən 2.8 sm, altdan 2.8 sm, soldan 2.5 sm və sağdan 2.5 sm olmalıdır. Mətn 11 punto yazı tipi böyüklüyündə, **Palatino Linotype** yazı tipi ilə və tək simvol aralığında yazılmalıdır. Paraqraflar arasında 6 punto yazı tipi aralığında məsafə olmalıdır.
11. Orijinal tədqiqat əsərlərinin tam mətni bir qayda olaraq 15 səhifədən artıq olmamalıdır.
12. Məqalənin nəşrə təqdimi aşağıdakı qaydada aparılır:

- Hər məqallə ən azı iki ekspertə göndərilir.
- Ekspertlərin tövsiyələrini nəzərə almaq üçün məqalə müəllifə göndərilir.
- Məqalə, ekspertlərin tənqidi qeydləri müəllif tərəfindən nəzərə alındıqdan sonra Jurnalın Redaksiya Heyəti tərəfindən çapa təqdim oluna bilər.

YAZIM KURALLARI

1. "Journal of Baku Engineering University- Kimya ve Bioloji" önceler yayımlanmamış orijinal çalışmaları ve yazarın kendi araştırma alanın-da yazılmış derleme makaleleri kabul etmektedir.
2. Makaleler İngilizce kabul edilir.
3. Makaleler Microsoft Word yazı programında, (**journal@beu.edu.az**) adresine gönderilmelidir. Gönderilen makalelerde şunlar dikkate alınmalıdır:

- Makalenin başlığı, yazarın adı, soyadı,
- İş yeri,
- E-posta adresi,
- Özet ve anahtar kelimeler.

4. **Özet** 100-150 kelime arasında olup 9 font büyüklüğünde, makalenin yazıldığı dilde ve yukarıda belirtilen iki dilde olmalıdır. Makalenin her üç dilde yazılmış özeti birbirinin aynı olmalıdır. Anahtar kelimeler uygun özetin sonunda onun yazıldığı dilde verilmekle en az üç sözcükten oluşmalıdır.
5. Makalede UOT ve PACS tipli kodlar gösterilmelidir.
6. Makale şunlardan oluşmalıdır:

- Giriş,
- Araştırma yöntemi
- Araştırma
- Tartışma ve sonuçlar,
- İstinat Edebiyatı Rusça olduğu halde orjinal dili parantez içerisinde göstermekle yalnız Latin alfabesi ile verilmelidir.

7. **Şekil, Resim, Grafik** ve **Tablolar** baskıda düzgün çıkacak nitelikte ve metin içerisinde olmalıdır. Şekil, Resim ve grafiklerin yazıları onların alt kısımda yer almalıdır. Tablolarda ise başlık, tablonun üst kısmında bulunmalıdır.
8. **Kullanılan kaynaklar**, metin dâhilinde köşeli parantez içerisinde numaralandırılmalı, aynı sırayla metin sonunda gösterilmelidir. Aynı kaynaklara tekrar başvurulduğunda sıra muhafaza edilmelidir. Örneğin: [7,seh.15].

Referans verilen her bir kaynağın künyesi tam ve kesin olmalıdır. Referans gösterilen kaynağın türü de eserin türüne (monografi, derslik, ilmî makale vs.) uygun olarak verilmelidir. İlmi makalelere, sempozyum, ve konferanslara müracaat ederken makalenin, bildirinin veya bildiri özetlerinin adı da gösterilmelidir.

Örnekler:

a) ***Makale:*** Demukhamedova S.D., Aliyeva İ.N., Godjayev N.M.. *Spatial and Electronic Structure of Monomerik and Dimeric Conapeetes of Carnosine Üith Zinc,* Journal of Structural Chemistry, Vol.51, No.5, p.824-832, 2010

b) ***Kitap:*** Christie ohn Geankoplis. *Transport Processes and Separation Process Principles.* Fourth Edition, Prentice Hall, p.386-398, 2002

c) ***Kongre:*** Sadychov F.S., Aydın C., Ahmedov A.İ. Appligation of Information-Communication Technologies in Science and education. II International Conference. "*Higher Twist Effects In Photon- Proton Collisions", Bakı, 01-03 Noyabr, 2007, ss 384-391*

Kaynakların büyüklüğü 9 punto olmalıdır.

9. **Sayfa ölçüleri**; üst: 2.8 cm, alt: 2.8 cm, sol: 2.5 cm, sağ: 2.5 cm şeklinde olmalıdır. Metin 11 punto büyüklükte **Palatino Linotype** fontu ile ve tek aralıkta yazılmalıdır. Paragraflar arasında 6 puntoluk yazı mesafesinde olmalıdır.
10. Orijinal araştırma eserlerinin tam metni 15 sayfadan fazla olmamalıdır.
11. Makaleler dergi editör kurulunun kararı ile yayımlanır. Editörler makaleyi düzeltme için yazara geri gönderilebilir.
12. Makalenin yayına sunuşu aşağıdaki şekilde yapılır:

- Her makale en az iki uzmana gönderilir.
- Uzmanların tavsiyelerini dikkate almak için makale yazara gönderilir.
- Makale, uzmanların eleştirel notları yazar tarafından dikkate alındıktan sonra Derginin Yayın Kurulu tarafından yayına sunulabilir.

13. Azerbaycan dışından gönderilen ve yayımlanacak olan makaleler için,(derginin kendilerine gonderilmesi zamani posta karşılığı) 30 ABD Doları veya karşılığı TL, T.C. Ziraat Bankası/Üsküdar-İstanbul 0403 0050 5917 No'lu hesaba yatırılmalı ve makbuzu üniversitemize fakslanmalıdır.

ПРАВИЛА ДЛЯ АВТОРОВ

1. «Journal of Baku Engineering University» - Химии и биологии публикует оригинальные, научные статьи из области исследования автора и ранее не опубликованные.
2. Статьи принимаются на английском языке.
3. Рукописи должны быть набраны согласно программы **Microsoft Word** и отправлены на электронный адрес **(journal@beu.edu.az)**. Отправляемые статьи должны учитывать следующие правила:

- Название статьи, имя и фамилия авторов
- Место работы
- Электронный адрес
- Аннотация и ключевые слова

4. **Заглавие статьи** пишется для каждой аннотации заглавными буквами, жирными буквами и располагается по центру. Заглавие и аннотации должны быть представлены на трех языках.
5. **Аннотация**, написанная на языке представленной статьи, должна содержать 100-150 слов, набранных шрифтом 9 punto. Кроме того, представляются аннотации на двух других выше указанных языках, перевод которых соответствует содержанию оригинала. Ключевые слова должны быть представлены после каждой аннотации на его языке и содержать не менее 3-х слов.
6. В статье должны быть указаны коды UOT и PACS.
7. Представленные статьи должны содержать:

- Введение
- Метод исследования
- Обсуждение результатов исследования и выводов.
- Если ссылаются на работу на русском языке, тогда оригинальный язык указывается в скобках, а ссылка дается только на латинском алфавите.

8. **Рисунки, картинки, графики и таблицы** должны быть четко выполнены и размещены внутри статьи. Подписи к рисункам размещаются под рисунком, картинкой или графиком. Название таблицы пишется над таблицей.
9. **Ссылки** на источники даются в тексте цифрой в квадратных скобках и располагаются в конце статьи в порядке цитирования в тексте. Если на один и тот же источник ссылаются два и более раз, необходимо указать соответствующую страницу, сохраняя порядковый номер цитирования. Например: [7, стр.15]. Библиографическое описание ссылаемой литературы должно быть проведено с учетом типа источника (монография, учебник, научная статья и др.). При ссылке на научную статью, материалы симпозиума, конференции или других значимых научных мероприятий должны быть указаны название статьи, доклада или тезиса.

Например:

a) ***Статья:*** Demukhamedova S.D., Aliyeva I.N., Godjayev N.M. *Spatial and electronic structure of monomeric and dimeric complexes of carnosine with zinc,* Journal of Structural Chemistry, Vol.51, No.5, p.824-832, 2010

b) ***Книга:*** Christie on Geankoplis. *Transport Processes and Separation Process Principles.* Fourth Edition, Prentice Hall, 2002

c) ***Конференция:*** Sadychov F.S, Fydin C,Ahmedov A.I. Appligation of Information-Communication Nechnologies in Science and education. II International Conference. *"Higher Twist Effects In Photon-Proton Collision",* Bakı,01-03 Noyabr, 2007, ss.384-391

Список цитированной литературы набирается шрифтом 9 punto.

10. **Размеры страницы:** сверху 2.8 см, снизу 2.8 см, слева 2.5 и справа 2.5. Текст печатается шрифтом **Palatino Linotype**, размер шрифта 11 punto, интервал-одинарный. Параграфы должны быть разделены расстоянием, соответствующим интервалу 6 punto.
11. Полный объем оригинальной статьи, как правило, не должен превышать 15 страниц.
12. Представление статьи к печати производится в ниже указанном порядке:

- Каждая статья посылается не менее двум экспертам.
- Статья посылается автору для учета замечаний экспертов.
- Статья, после того, как автор учел замечания экспертов, редакционной коллегией журнала может быть рекомендована к печати.